THE UNIVERSITY OF MICHIGAN

DEPARTMENT OF CIVIL ENGINEERING

Adsorption of Strong Acids, Phenol, and 4-Nitrophenol

From Aqueous Solution by Active Carbon

In Agitated Non-Flow Systems

Vernon L. Snoeyink

and

Walter J. Weber, Jr.

TABLE OF CONTENTS

LIST OF TABLES

LIST OF ILLUSTRATIONS

LIST OF APPENDICES

I. INTRODUCTION

Essentially complete removal of biologically-resistent organic pollutants is becoming more and more important in water purification and waste treatment operations as the frequency of water reuse increases. In light of projected rates of population growth, it can be expected that expansion of the water reuse practice will continue in order to meet water supply demands in the future. It is the primary task of engineers and scientists to provide the processes and techniques which will make such reuse completely safe and aesthetically acceptable, at the lowest possible cost.

One means for removal of organic materials from aqueous solution is by adsorption on active carbon. Active carbon has been used for some time in the water purification industry for taste and odor reduction, but its use in this regard has been rather inefficient, primarily because of the lack of fundamental information regarding the nature of the sorption process and optimum conditions for operation. Recently, however, much research has been done on definition of the nature of adsorption by active carbon (38, 68, 69, 70, 71) and on development of better methods for contacting carbon with the solutions to be treated (3, 15, 40, 67).

However, there is yet a definite need to know more about the basic mechanisms of adsorption on carbon. Specifically, very little research has been done on the effect of

1

inorganic constituents on the adsorption of organic substances from aqueous solution. Weber and Morris (70) have found that the rate of uptake of alkylbenzenesulfonates increases with decreasing pH, while Gould (25) has noted that high pH has a significant effect on the rate of adsorption of substituted phenols. The author has been motivated by a desire to extend this previous research on the effect of pH to a more extensive study of the effects of inorganic constituents in general on the adsorption process. It has been hoped also that a study of this type would reveal useful information about the "active sites" at which adsorption on carbon takes place.

PLAN OF RESEARCH

It was decided to approach the problem of determining the effect of selected inorganic substances on the adsorption process by first studying the direct reaction between such inorganic species and carbon. The adsorption of organic molecules then could be investigated in the absence and presence of these inorganic species, and the results obtained in the former systems used for interpretation of those obtained in the latter systems.

Preliminary studies showed that, for the active carbons used, the reaction of strong acids with the carbon surface was quite significant and, therefore, hydronium ion concentration was selected as a major variable. In an attempt to completely elucidate the hydronium ion-carbon reaction, it was studied as a function of pH, type of acid, salt concentration, temperature, ash content of the carbon and quantity of anion

removed from solution during the reaction. These variables were examined with respect to rate and extent of the reaction.

Once the information for the hydronium ion-active carbon reaction was obtained, the inorganic species could then be studied with respect to their effect on the adsorption of selected organic substances. For this purpose, phenol and 4-nitrophenol were chosen as sorbates. Phenol was selected primarily because it is a common pollutant and presents considerable problems in waste treatment (49). Also, it is stable in solutions over long periods of time and its concentration is easily analyzed. In addition, it can be studied as both neutral and anionic species, a factor which is useful for interpretation of sorptive behavior under different conditions. Nitrophenol was selected because it is structurally similar to phenol. It is a common pesticide which persists in the natural aquatic environment because of its resistance to biological break down (68). Furthermore, it too is chemically stable in aqueous solution, can be easily analyzed, and can be studied as both the neutral and negative species. It was thought that studies on both of these solutes would be complementary. Investigations of the kinetics and equilibria of adsorption of these two solutes were performed as a function of pH, type of acid, temperature, salt concentration and ash content of the carbon.

It is hoped that the results of this research will be useful in the further development and refinement of the process of adsorption on active carbon as a method for water purification and waste water treatment.

II. STRUCTURAL PROPERTIES AND SURFACE

CHEMISTRY OF ACTIVE CARBON

Before proceeding with discussion of the effect of in-

organic substances on the adsorption of organic molecules, it

is important to carefully examine what is known about the struc-

ture and surface chemistry of active carbon in order to estab-

lish a basis for interpreting experimental results. It is of

interest, for example, to examine how the extensive surfaces

of carbons having the same surface areas can have totally dif-

ferent adsorptive properties. Part of such differences in

adsorptive behavior can be explained in terms of relative pore

size distributions, but part must also be attributed to differ-

ences between the respective surface properties of the carbons.

The surface of any active carbon is comprised in part of resi-

dual electron- and ion-exchange functional groups, connected

by electron-conducting bond systems (22). The nature of these

functional groups is determined to a large extent by the method

of activation as well as by the type of raw material from which

the carbon is prepared. With the existence of electron- and

ion-exchange groups at the surface of carbon, it is reasonable

to expect that electrolytes in solution may interact with the

carbon to influence its behavior as an adsorbent. Indeed, such

interactions could markedly affect the over-all adsorption

process under certain conditions, possibly effecting changes

in the process which may be put to good advantage to achieve

higher efficiency or enhanced effectiveness of removal of pol-
lutants. Weber and Morris (70), for example, have shown that
the hydrogen ion activity of a solution affects both rate and
capacity for adsorption of negatively charged species of sul-
fonated alkylbenzene from aqueous solution by carbon. These
authors have interpreted their results as indicating that
decreasing pH leads to an increasing association of the posi-
tively charged hydrated proton with negatively charged func-
tional groups on the active carbon surface, thus neutralizing
electrostatic repulsive force to allow the charged organic
species to migrate more easily through the pore spaces and be
adsorbed at inner surface sites. Garten and Weiss (22) have
interpreted changes in hydrogen ion activity observed upon
addition of active carbon to acidic or basic solutions in
terms of interaction between the acid or base and a basic or
acidic heterocyclic surface structure, respectively. It is
highly probable that this interaction has a significant effect
on the sorptive properties of active carbon

Other inorganic species also seem to be important in
their effects on the manner in which active carbon functions
in aqueous solution as a sorbent for organic substances. Joyce
and Sukenik (39) have observed a 50% increase in ash content
(from 6 to 9% and from 12 to 18%) to be accompanied by a 50%
decrease in the capacity of an active carbon after 10 cycles
of sorption from a solution of the calcium salt of a sulfonated
alkylbenzene followed by thermal regeneration. Because the
ash was soluble in acid solution, but insoluble in near neutral

solution, these authors suggest that acid treatment in conjunction with thermal regeneration may prove feasible as a means for restoring active carbon to near original capacity. Before such treatment is effected however, one should know how the acid may affect the active carbon surface, and therefore, how it may influence the adsorption process.

Various chemical oxidizing agents can also interact with active carbon in aqueous solution to increase the amount of chemisorbed oxygen at the carbon surface (53). Once more, however, the effect of the presence of this oxygen on the sorptive properties of active carbon has not yet been sufficiently defined.

Many things are known, though, about the structure and surface properties which are invaluable, and this information will be used to develop a relatively unified concept or model of carbon which can be used as a basis for further research.

PREPARATION OF ACTIVE CARBON

The term active carbon actually implies a rather broad family of substances, with individual species being characterized by sorptive and catalytic properties rather than by definite structure or specific chemical composition (32). Particular properties may be imparted to an active carbon either by starting with different raw materials or by utilizing different preparative procedures.

Substances from which active carbons are manufactured are carbonaceous in nature, usually carbohydrates; wood, coal,

sugar, nut shells, and vegetable matter are examples of typical raw materials. Differences in active carbons may exist as a result of the particular characteristics of the starting material, but many of the differences commonly ascribed to dissimilar starting materials may be due in fact to noncarbonaceous impurities. In addition, preparative conditions may be varied and selected additives employed to produce a particular active carbon of desired structure and surface properties.

The production of active carbon involves first the formation of a char from the raw material. The starting material is heated--usually in the absence of air--to a temperature sufficient to effect drying and to drive off the volatile fraction. Carbonization is then accomplished by elevating the temperature, producing a carbonaceous char (32, 38). In this process the temperature is increased slowly to allow time for each step to be completed before the next begins. The entire process is usually carried out below 600° C., although exceptions do exist. Additives such as calcium chloride, magnesium chloride, zinc chloride, or any one of a number of similar materials may be used to catalyze the process and to impart certain characteristic properties to the finished product (32).

The char developed in the carbonization process has relatively little internal surface area, and because a large surface is required for most adsorption applications, the char is generally "activated" by treatment with oxidizing gases under carefully controlled conditions. The oxidizing gases--commonly carbon dioxide, steam, and air--attack the more readily

oxidizable portions of the char, resulting in the development of a porous structure and an extensive internal surface. The temperature of activation is a critical factor in the process, as will be discussed in more detail shortly. Treatment of the char with reagents such as chlorine, dolomite sulfates, and several other substances to develop special properties in the finished product and to catalyze the action of the oxidizing gas is often effected prior to the activation process (32). According to Johnson et al. (38), carbonization and activation can sometimes be carried out in one step, rather than as separate operations. The total surface area of a carbon, by far the greatest percentage of which is internal, can be as great as 2,500 square meters per gram after activation.

STRUCTURE AND STRUCTURAL DEVELOPMENT

The molecular and crystalline structure of active carbon is an important determinant of the types of functional groups which can exist on the surface and is, therefore, an important consideration in any discussion of the surface chemistry of this material. Although there is little direct information available on the structure of active carbon, much can be derived from existing data on the structure of carbon black. Very little chemical difference exists between these two substances, and the only apparent physical difference is that the carbon black has much less internal surface area (22).

As a basis for discussion of the active carbon structure, it is appropriate to consider first the structure of

ideal graphite in that it is closely approximated in the basic

structural unit of both active carbon and carbon black (33, 63,

74).

The structure of ideal graphite is given in Figure II-1.

According to Walker (6?), this structure is composed of a sys-

tem of infinite layers of fused hexagons. Within each layer

the carbon-carbon bond distance is 1.415 A. indicating a one-

third double bond character. Three of carbon's four electrons

are engaged in forming regular covalent bonds with neighboring

atoms and are localized, while the fourth resonates between

several valence-bond structures, giving each carbon-carbon bond

a one-third double bond character. Relatively weak van der

Waals forces act between the parallel layers to hold the dis-

tance of separation to approximately 3.35 A. The carbon layers

form an a-b-a-b-a-b stacking sequence in which one-half of the

carbon atoms in any one plane lie above the center of the hex-

agons in the layer immediately below it. The carbon atoms

are directly superimposed in alternate layers. X-ray diffrac-

tion spectra obtained for most natural graphites indicate that

this structural configuration is in fact predominant (63).

During the carbonization of the raw material in the pre-

paration of active carbon, small aromatic nuclei, interpreted

from x-ray spectrographs as microcrystallites consisting of

places of fused hexagonal rings of carbon atoms having a struc-

ture similar to that of graphite, are formed (33, 74). The

diameters of the planes making up the microcrystallite have
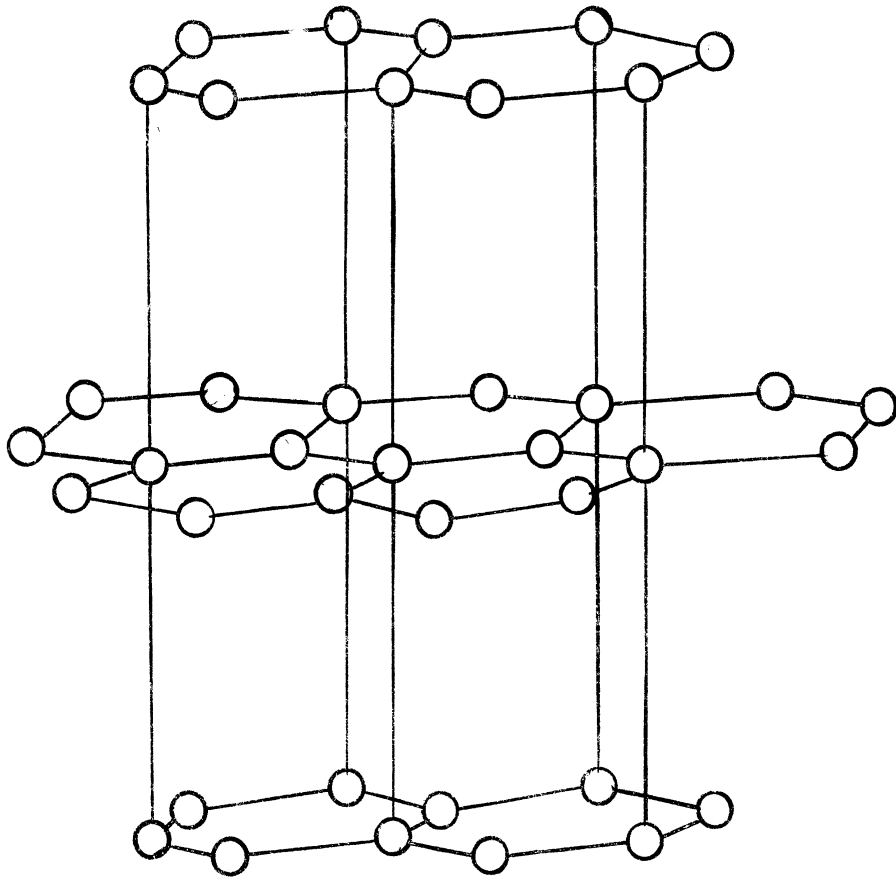
Figure II-1 The Arrangement of Carbon
Atoms in the Graphite
Crystal (63)

been estimated as 20 to 50 A. (33). The height of stacking is also in the range of 20 to 50 A., indicating that each microcrystallite consists of 5 to 15 layers of aromatic planes.

Although the structure of the microcrystallite is similar to that of graphite, it differs in many ways. During the formation of the microcrystallite, impurities should be expelled from its interior. However, Walker (63) states that interior vacancies exist in the microcrystallite and that their formation depends on the method of preparation. Possibly these vacancies contain some of the impurities; the presence of impurities may, in fact, influence the formation of such a vacancy. Sometimes there is a considerable content of disorganized, tetrahedrally bonded carbon, often cross-linking different layers (56). In addition, the ringed structures at the edges of the planes making up the microcrystallite are often heterocyclic owing to the nature of either the starting material or of the preparation process used (22). Heterocyclic groups would tend to affect both the distance of separation of adjacent planes and the sorptive properties of the carbon. The heteroatoms incorporated into the planes and the termination of the planes at the edges of the microcrystallite produce "free" valences which are very reactive (56). Usually these valences do not remain free for any length of time, but form compounds with any suitable element present. Needless to say, the "free" valences and the compounds formed as a result of them affect the nature of the carbon surface greatly. Also, orientation

between adjacent planes in the microcrystallite varies from that found in ideal graphitic structure to that of complete random orientation found in turbostratic carbons (63). The definite a-b-a-b-a-b stacking order, therefore, does not exist in most active carbons. Functional groups terminating the microcrystallite planes interconnect the microcrystallites, and are at least partially responsible for the turbostratic character in that they prevent orientation of the planes with respect to each other. Because of its special properties and the many differences between it and graphite, Garten and Weiss (22) have chosen to compare active carbon with a complex organic polymer rather than with a graphitic type particle.

The structure of the char particle is developed further by treatment with oxidizing gases at high temperature during the activation process. Dubinin et al. (17), have noticed two stages of oxidation in the activation of carbonized sucrose. First, macropores were formed by the burnout of microcrystallite planes. Once a plane is attacked by an oxidizing gas, oxidation of that plane continues in preference to another area until a stable structure is developed (74). Snow et al. (56) have reported that a higher ash content causes faster pore development during activation. Apparently, inorganic matter causes stress localizations on the surface of the microcrystallite at which point, oxidation is initiated more easily. The diameter of the macropore is generally taken to be in the range 5,000 to 20,000 A., while micropore diameters are usually

assumed to be less than 30 A. (16). The macropores and micro-pores are connected by transitional pores. The surface area of the interior walls of the macropores is less than 2 square meters per gram while the surface area for transitional pores can vary from 20 to 450 square meters per gram (16). However, the majority of surface area for carbons is usually found in the micropore. Transitional pores are often not well developed for carbons which are used for gas adsorption since these molecules can be adsorbed in micropores. But large molecules can not enter the micropores; thus carbons used to adsorb large molecules usually have well-developed transitional pores.

Carbonization and activation temperatures are signifi-cant considerations in the structural development of active carbons. Riley (19) has demonstrated that the size of the microcrystallites of carbons prepared from carbohydrates in-creases with increasing temperature of carbonization. In addition, the mechanical strength and electrical conductivity of a carbon increase when prepared at temperatures above 700° C. The temperature at which activation is effected is important also because carbonization continues during this process via the mechanisms of actual removal, cracking, or cyclization of functional groups present at the edges of the microcrystallite (74).

CHEMICAL NATURE OF THE ACTIVE CARBON SURFACE

If we proceed on the basis of the structure outlined above, and neglect for the moment the effects of noncarbonaceous impurities, two major types of surfaces can be postulated for

active carbon: the basal planes of the microcrystallites and the edges of the carbon planes making up the sides of the microcrystallite.

The basal planes are probably relatively uniform in nature. No attached functional groups should be present because the electrons of the carbon atoms are involved in covalent bonding with neighboring carbon atoms. Studies by Boehm (6), for example, showed that oxygen could only be chemisorbed on the periphery of the crystallite and not on the basal planes. Because oxidation occurs much more readily at the edge of the carbon plane than on the surface of the plane (35), few vacancies owing to oxidation during the activation process are expected in the basal plane. The majority of the sorptive processes occurring on this surface would be due then to the relatively weak van der Waals forces, although electrons are available for π-bonding if the sorbate is capable of entering into such a bond (24). Because most of the surface area of a carbon particle is found in the micropores, and because micropores are formed by the "eating out" of microcrystallite planes (74), the larger percentage of the total surface area is probably of the basal plane type.

The sides of the microcrystallites are more heterogeneous than the basal planes, and are characterized by various types of functional groups and vacancies owing to the action of oxidizing gases. Corners or raised positions on the surface have the greatest tendency to participate in the electron-sharing reactions which characterize chemisorption (75).

Sorption in depressions is probably physical in nature, but the bonds formed in this case should be much stronger than the bonds formed in physical sorption on the basal planes of the microcrystallite.

Although surfaces of the preceding types can be expected for a very pure active carbon, many carbons have large percentages of oxygen, hydrogen, and inorganic ash. The concept of the type of surface available for sorption must be modified somewhat when such substances are present. The presence of hydrogen on the surface of active carbon, for example, lends quite definite properties to that surface. Certain sorption reactions are known to be more or less specific for surfaces comprised of hydrogen sites. Kipling and Shooter (42) reported that iodine vapor adsorption on Spheron 6 can be interpreted in terms of adsorption, on that part of the surface covered with hydrogen sites, to the exclusion of those portions of the surface covered with oxygen-containing functional groups. Hydrogen presumably exists either in the form of terminal groups on the fused aromatic planes of the microcrystallite or as part of the hydrocarbon functional groups attached to these planes (74). Wolff (73) reported that hydrogen is present in amounts ranging from eight to 19 times that of oxygen, on a molar basis, for carbons containing 0.94 to 2.25% oxygen by weight.

Inorganic matter is present in most commercial active carbons to a very significant extent, and its presence has

many noticeable effects (32, 73). The total amount present
consists of those inorganic constituents originally present
in the starting material as well as various inorganic salts
added to catalyze the carbonization and activation processes
or to impart special sorptive properties such as selectivity
to the active carbon. The fact that strong acid will remove
almost all of the ash content of active carbon suggests that
the inorganic matter exists primarily on the microcrystallite
surfaces (5, 73). The special properties which the inorganic
salts develop possibly are due to their effect on the active
carbon surface and to their interactions with the sorbate or
other solution constituents. Sorption on a surface covered
with tightly held inorganic species would very likely differ
in nature from sorption on an active carbon surface free of
such species. Pore structure would also be affected differ-
ently by different types of salts used to catalyze the act-
ivation process. Possible interactions between the inor-
ganic salts on the active carbon surface and the sorbate or
other solution constituents include complex formation, ion-
pair formation, precipitation reactions, and oxidation-re-
duction reactions. Basic studies of the sorptive properties
of active carbon should include a careful study of the effect
of the active carbon's inorganic constituents.

Electron spin resonance studies of active carbon have
suggested free radical structures or structures with unpaired
electrons in the microcrystallite (30). According to Ingram
(37), large number of unpaired electrons are trapped during

17

the carbonization period owing to bond breakage at the edges

of the planar structures. These electrons are undoubtedly

the "free" valences to which Boehm (6) refers and which are

very reactive. Studies by Harker et al. (30) have indicated

that oxygen interacts with these electrons to form oxygen

complexes on the surface. The only means by which this oxy-

gen can be removed is as oxides of carbon by degassing at

high temperature.

Oxygen, one of the major noncarbon constituents of

active carbon, constitutes 2 to 25% by weight of this mater-

ial, the exact amount present depending upon the temperature

and method of activation (74). The temperature of activation

ranges from 400° to 1200° C., and the oxygen content decreases

with increasing temperature of activation (20). Heating carbon

at a temperature of 1000° to 1200° C., in a high vacuum removes

nearly all of the oxygen from the carbon surface, usually as

oxides of carbon. For this reason oxygen is thought to exist

in structures on the surface of the microcrystallite or be-

tween carbon planes near the surface of the microcrystallite

(19).

The presence of oxygen complexes on the surface of the

carbon affects the sorptive properties of this material in

that they tend to increase the polarity of the surface (4). In

aqueous solution, therefore, a stronger solvent-active carbon

bond must be broken before sorption of the sorbate can occur

if oxygen complexes exist at the carbon surface. Excluding

any specific oxygen complex-sorbate interaction, increased

polarity decreases the quantity of nonpolar sorbate removed

from solution by the carbon. For a polar sorbate, the oxygen

complex-sorbate interaction usually is stronger, compensating,

at least in part, for the added energy required to desorb

water. Kipling (41) discovered that oxygen on the surface of

carbon affects the specificity of sorption from an organic,

binary liquid solution. As indicated previously, Kipling

and Shooter (42) reported that iodine apparently does not

absorb on that portion of the active carbon surface covered

with oxygen sites, but does absorb on the part of the surface

covered with hydrogen sites. These authors also indicate

that the normally strong lateral interactions of absorbed

iodine molecules appear to be lessened in the presence of

the oxygen, thus preventing attainment of the extent of

uptake realized in the absence of surface oxygen. An

additional consideration is that sorbates which have a

natural tendency to combine with oxygen probably sorb more

easily on oxygenated surfaces than they do on non-oxygenated

surfaces.

Oxygen can be added to an active carbon in one or more

of three principal ways. If the starting material contains

oxygen, this may become incorporated into the microcrystallite

surface structure during the manufacture of the carbon (19).

If the starting material is a carbohydrate, for example, heat-

ing will cause condensation and cyclization of the carbohydrate

with the inclusion of an oxygen atom in the ringed structure

as an ether oxygen. As a second possibility, oxygen can be
sorbed on active carbon at room temperature. Part of the
oxygen added in this manner can be evacuated at room temp-
erature--this phenomenon being known as "the reversible effect"--
while another part requires evacuation at temperatures in
excess of 1000° C. (30). The latter phenomenon, which has
been studied by electron spin resonance methods, is known
as "the surface oxide effect." Thirdly, oxygen can be chemi-
sorbed on the surface of the active carbon during treatment
with oxidizing agents. As previously indicated, the principal
oxidizing gases in the activation process are air, steam, and
carbon dioxide. These three gases form oxygen complexes at
the surface of the carbon which can be removed--as carbon mon-
oxide, carbon dioxide, and water vapor--only by degassing at
very high temperatures (32, 54). Treatment of active carbon
with chemical oxidizing agents in aqueous solution also leads
to the chemisorption of oxygen on the surface of the carbon
(32, 52, 54).

CHARACTERIZATION OF OXYGEN SURFACE STRUCTURES

Because of their numbers and their probable effects on
the sorption process, oxygen complexes on the surface of carbon
merit careful consideration. An excellent review of this topic
has been given by Boehm (6); anyone contemplating further work
in this area should consult this review.

One of the principal methods for study of the nature
of oxygen structures on carbon has been by simple

acidimetric-alkalimetric titrations, and major interest has focused on the very important variable of temperature of activation (22, 56). Garten and Weiss (22) have provided an excellent review on the findings of such research, and these may be summarized briefly as follows:

Carbon activated at 400° C. (L-carbon) will sorb base but not acid from aqueous solution while carbon activated at 800° to 1000° C. (H-carbon) will sorb acid but not base.

Carbon activated at intermediate temperatures will sorb both acid and base.

Capacities for both acid and base are usually in the milli-equivalent per gram range, but this value depends on the substances added to the carbon during the activation process.

Similar to ion exchange resins with basic and acidic functional groups, respectively, H-carbons produce a basic pH while L-carbons yield an acidic solution pH (22). Since no acid or base can be extracted from the solution after contact with the carbon, the conclusion is made that surface structures are responsible for this phenomenon. Electrokinetic studies have indicated that H-carbons exhibit a positive surface potential, as opposed to a negative surface potential for L-carbons. However, unless care is taken to cool H-carbons in an inert atmosphere after activation, formation of structures which change the potential from positive to negative does occur. The presence of inorganic constituents at the surface may also affect the potential to the point of reversing its sign from that which might be expected on the basis of the activation temperature.

A negative potential for L-carbons is consistent with
the presence of surface acids, while the existence of a posi-
tive potential for H-carbons requires further consideration.
Garten and Weiss (20, 22), using various techniques for the
study of L-carbons, have concluded that surface acids re-
sponsible for the sorption of alkali from aqueous solution
consist of at least three fundamental types: phenol; n-lactone;
and f-lactone--the type present in fluorescein and phthalein
dyestuffs (23). The relative proportions of these three
groups vary with the method of preparation of the active
carbon.

In determining the total number of acidic groups pre-
sent on L-carbons by alkalimetric titrations, Garten et al.
(23) noted that the titration curves closely resembled the
type obtained for weak acids and were comparable with that
for titration of a phenolic functional group ion exchange
resin. These observations point to the possibility of pheno-
lic surface structures, as illustrated in Figure II-2. By
way of additional evidence, a certain proportion of the
acidic groups have resisted methylation with diazomethane,
but the methoxyl group thus introduced resists hydrolysis when
treated with boiling dilute acid. This behavior is charac-
teristic of the phenolic structure (23, 53). Conversely, a
portion of the total number of acidic groups have resisted
methylation with diazomethane, while supplementary infrared
spectroscopy studies have produced data consistent with the
postulation that these groups are of the n-lactone type given
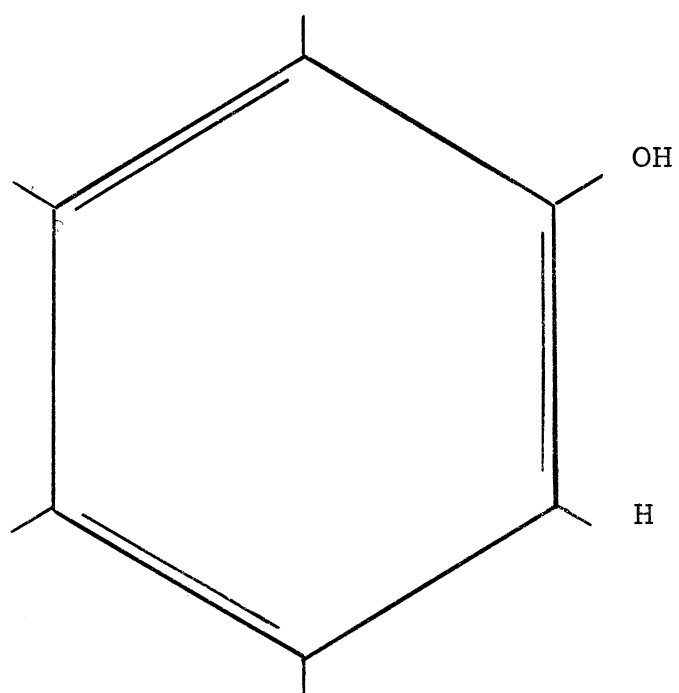
Figure II-2. A Phenolic Surface
Structure (23)

in Figure II-3, with an absorption band at 1710 cm.$^{-1}$

A third fraction of the acidic groups on L-carbons was methylated with diazomethane, but with the methoxyl group thus formed being hydrolyzable in dilute boiling acide (23). Carbon compounds which have phenolic groups in association with lactone groups, as in fluorescein or phthalein dyestuffs, act similarly. Figure II-4 gives illustration of the structure of such lactones, called f-lactones, as well as some of the reactions of this group (23). The infrared data referred to previously have also revealed an absorption peak at 1750 cm.$^{-1}$, consistent with the presence of f-lactones.

While simple alkalimetric titration has been used rather extensively for measurement of the total number of acid groups present on carbon, some questions have been raised as to the quantitativeness of this procedure. For example, Studebaker (62), using sodium aminoethoxide in ethylene diamine as a titrant and comparing his results with those obtained by NaOH-titration of active carbon in aqueous solution, has discovered that alkalimetric titration determines only about 68% of the total acidity as measured by the aminoethoxide titration.

Quinone groups are also known to be present on the surface of active carbon (21, 22, 62). An H-carbon cooled in nitrogen gas after activation does not sorb base, but reduction of the H-carbon with sodium borohydride develops base properties (22, 62). This observation can be explained in terms of quinone reduction to hydroquinone. Hallum and Drushel (26) also found polarographic evidence for quinones. Reduced quinones,
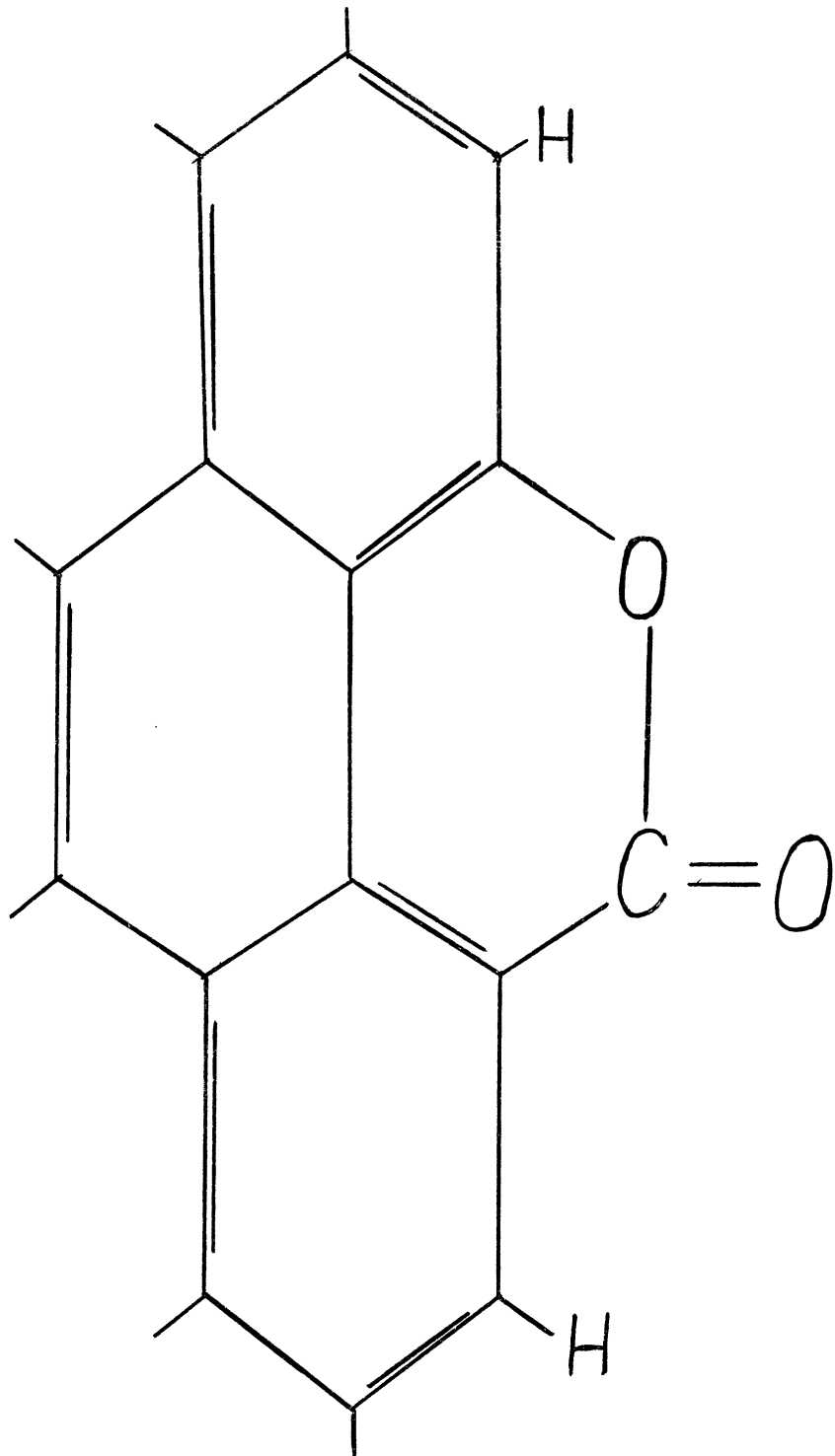
Figure II-3. A n-Lactone Surface Structure (23)
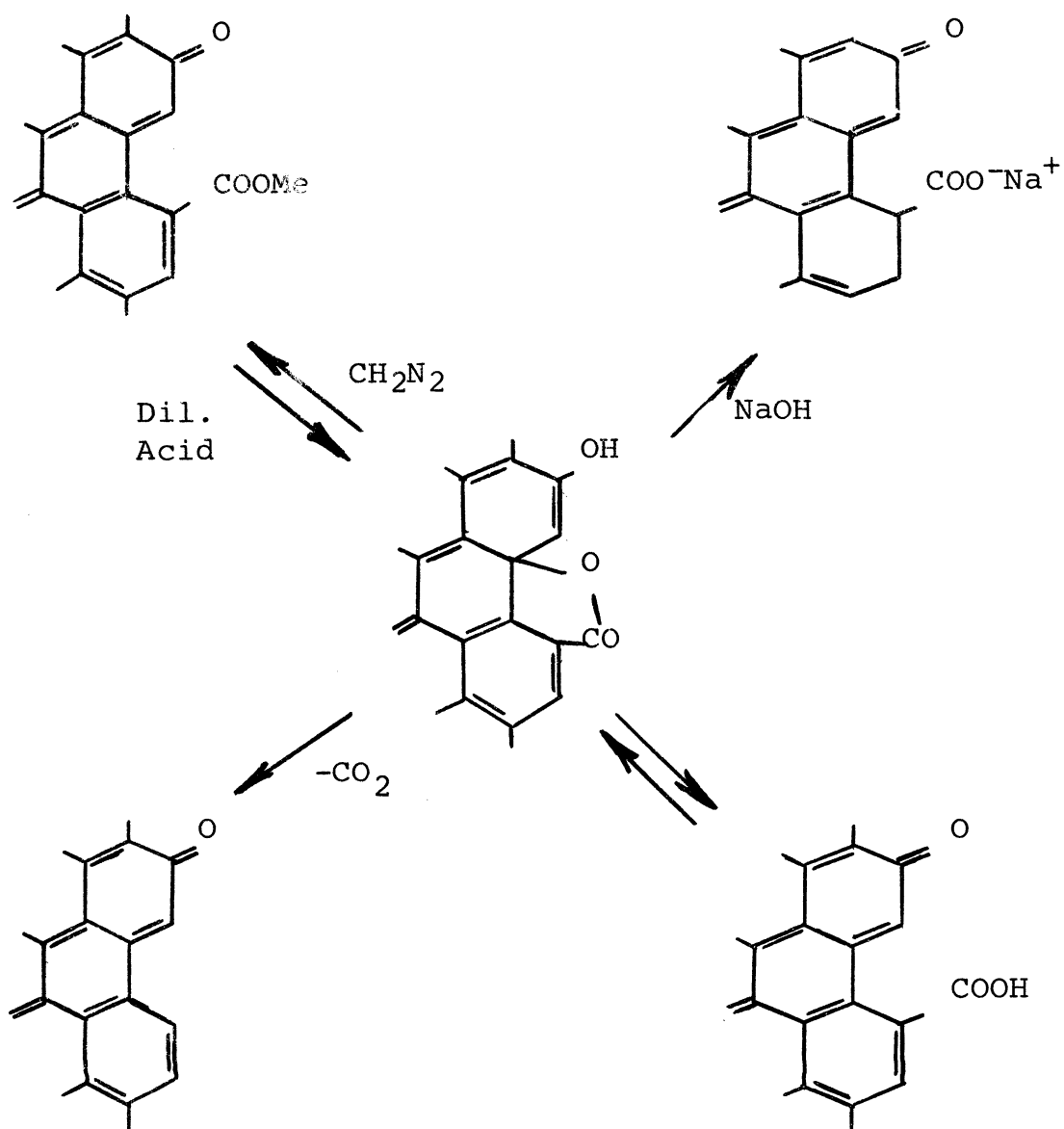
Figure II-4. Some Reactions of Fluorescein-Type Lactones (23)

or hydroquinones, might be expected to behave as phenols when treated with diazomethane and thus would be included in the phenolic fraction given by the method of analysis used by Garten and Weiss.

Although a carbon activated at a temperature of 800° to 1000° C. will sorb acid, evacuation at the temperature of activation followed by cooling in an inert atmosphere will so affect the carbon that it will not sorb acid from a deaerated solution until oxygen is admitted (20). Indeed, an exponential relationship exists between the acid sorbed and oxygen partial pressure for the range of 0 to 20 mm of Hg. Kolthoff (44) discovered that hydrogen peroxide is released by carbon to a solution from which acid is adsorbed (21). Garten and Weiss (20), on the basis of this phenomenon, propose the presence of chromene (benzpyran) groups on the H-carbon surface. As illustrated in Figure II-5, this structure contains an activated $>CH_2$ or $>CHR$ group which can react with a strong acid and oxygen (65). There is much difficulty in establishing the stoichiometry of this reaction, however, because active carbon also catalyzes the breakdown of the hydrogen peroxide (20).

The carbonium ion formed by acid reaction with the chromene group, as shown in Figure II-5, will hydrolyze readily in water to form the chromenol group illustrated in Figure II-6, a weakly basic group having a dissociation constant of 10^{-11} (58). The fact that the carbonium ion tends to associate so strongly with a negative ion could account for the fact that sorbed acid is very difficult to wash from carbon (20). Boehm (6)
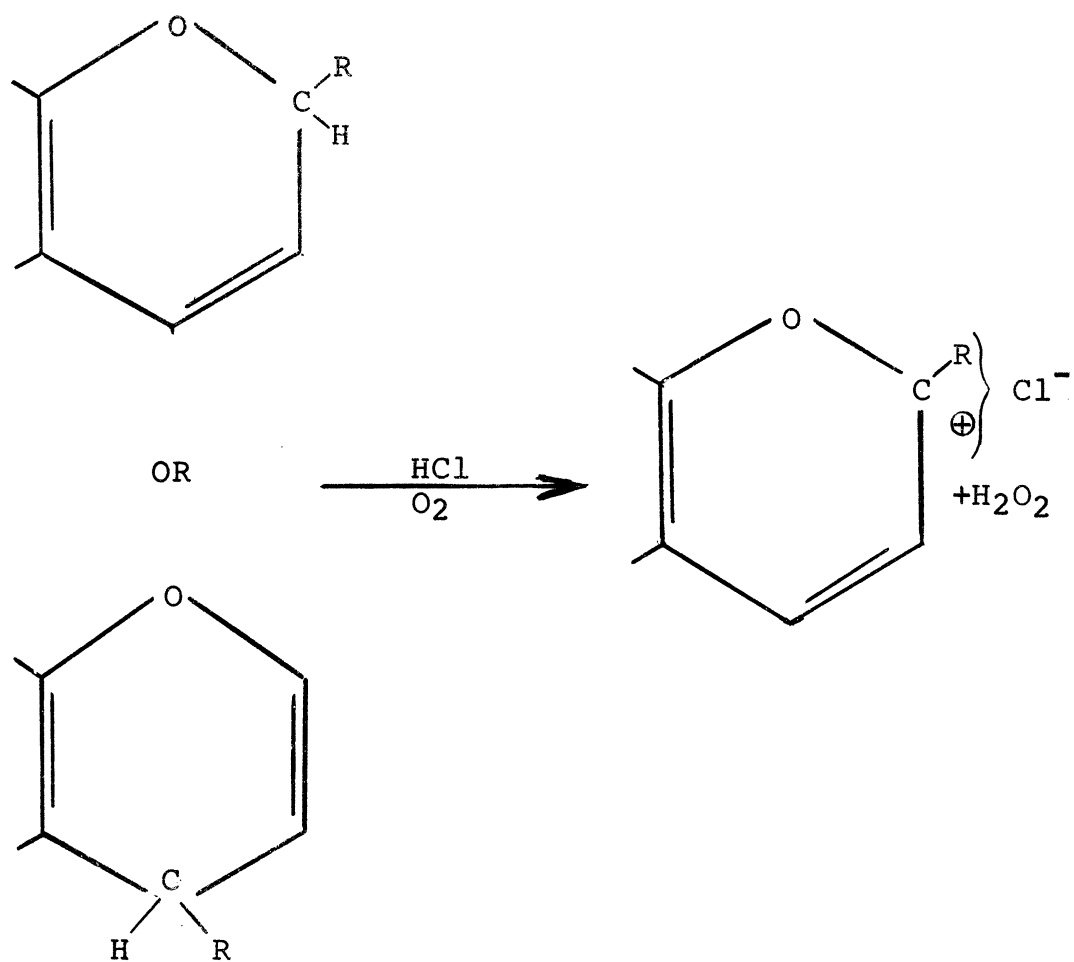
Figure II-5. The Chromene Acid Reaction (20)
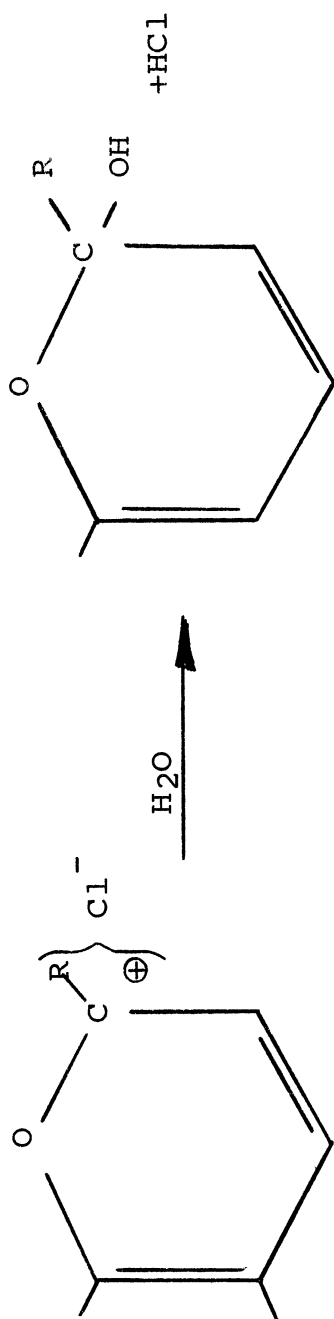
Figure II-6. Hydrolysis of the Carbonium Ion (20)

states that although the chromene reaction hypothesis explains
many phenomena related to basic oxides on carbon, the evidence
for it is rather circumstantial, and a more direct proof would
be desirable.

In addition to the evidence for chemisorption and the
chromene groups, there is also strong evidence that some physi-
cal sorption of acid takes place. Garten and Weiss (22) have
shown that a portion of the sorbed acid on an acid-saturated
carbon can be displaced by strongly adsorbed organic molecules.
The assumption is made that the physically sorbed acid can be
displaced and the chemisorbed acid can not. By this means,
an approximation can be made of the number of chromene groups
present on the carbon surface. The relative proportion of
the quantity of acid physically sorbed to that chemically
sorbed again depends on the methods of preparation, especially
the length of time the carbon is activated.

DISCUSSION

Pore surfaces of active carbon appear to consist princ-
ipally of either the basal or the edge surfaces of the micro-
crystallite. The planar surfaces are relatively homogeneous,
but the edge surfaces are heterogeneous, quite probably covered
with oxygen- and hydrogen-containing functional groups. Some
of the oxygen complexes appear to be highly reactive with
certain inorganic species in aqueous solution, particularly
acids and bases. This interaction can be especially signifi-
cant for active carbons having appreciable quantities of

surface oxygen, since it probably results in changes in the nature of the pore surface.

Ash content, which is appreciable for most commercial carbons, might also be expected to affect markedly the nature of the active carbon surface if the inorganic species are distributed over the internal surface of the pores. If the ash is localized in specific vacancies rather than distributed over the pore interior, however, the sorptive properties are likely to be affected very little.

The purpose of this review of structure and surface chemistry of carbon has been to set forth some of the more significant interfacial factors and mechanisms to be considered in interpretation of sorption phenomena associated with active carbon in aqueous solutions and to provide a basis for further research aimed at more thorough delineation of sorption processes. It will be used to this end in the following chapters.

III.   REACTION OF THE HYDRATED PROTON

WITH ACTIVE CARBON

EXPERIMENTAL

CARBONS

The active carbon used for the majority of the experiments in this study was Columbia Activated Carbon, LC Grade, obtained from the National Carbon Company (13). This carbon is a coconut-shell carbon and was obtained in a size range which included particles passing a U. S. Standard Sieve No. 20 and being retained on a No. 40 sieve. These particles were mechanically ground to a smaller size and were then carefully sieved to a size range which included particles passing a No. 50 sieve and being retained on a No. 60 sieve; the mean particle diameter for this size range is 273 microns. After sieving, the carbon was washed thoroughly with distilled water to remove dust and fines, and was then dried to a constant weight at 105° C.,

The inorganic content was 0.7% which is low for commercial carbons. Primary reasons for choosing this carbon included its low ash content, its resistance to attrition in rapidly-stirred experimental reactors and the fact that several previous investigations to which the work relates were carried out using this same carbon (68, 69, 70, 71).

A coal-base carbon, Pittsburgh Activated Carbon obtained

from the Pittsburg Coke and Chemical Company (41), which was prepared in the same fashion and of the same mean particle size was also employed in several experiments. The maximum ash content for this material, as reported by the manufacturer, was 8%. This carbon, too, has been used in related previous investigations (39, 40, 67).

A pore size distribution was not available for the coconut-shell carbon, but, again, according to the manufacturer, approximately 55% of the intraparticle volume of the coal-base carbon was comprised of diameters between 15 and 20 A., and 33% between 20 and 500 A. (51). The coal-base carbon is designed primarily for adsorption from solution, and thus probably has a more highly developed transitional-pore surface area than does the coconut-shell carbon, which is intended primarily for application in gaseous systems (13, 51).

EXPERIMENTAL SYSTEMS

Rate-of-reaction studies for the hydronium ion-active carbon reaction were carried out utilizing both finite and infinite bath techniques. Test solutions were prepared at the desired ionic strength, temperature, and initial pH. These solutions were stirred rapidly with a motor-driven polythylene stirring blade. For each test, a carefully measured quantity of carbon was added in the dry form. The finite bath technique consisted of allowing the pH to vary and recording pH values as a function of time after carbon addition. All finite bath pH measurements were made with a Corning Model 12,

expanded-scale pH meter. The infinite bath technique consisted of maintaining a constant pH throughout the reaction with a Sargent recording pH Stat. As the reaction proceeded, the pH Stat continuously added and recorded the quantity of standard acid (0.1 $\underline{N}$ in this case) needed to maintain a constant pH. Stirring speeds in all cases were in excess of the minimum required to keep the carbon in suspension; separate experiments indicated independence of sorption rate on stirring speeds greater than this minimum which was about 500 RPM. Except where specified, carbon dosages for all finite bath studies were 1.5 grams per liter.

Equilibrium studies were performed to determine the extent of the hydronium ion-active carbon reaction. These studies were carried out in reaction vessels containing 1.5 liters of distilled water adjusted to the desired pH and ionic strength. Temperature control was provided by immersing the reactor in a water bath, except for tests at room temperature ($25 \pm 3^{\circ}C$). At the start of each experiment a known quantity of carbon was added to the test solution. Stirring was again accomplished with a motor-driven polyethylene stirring blade at speed sufficient to keep the carbon in suspension at all times. After 2 to 3 days (experimentally determined as the time required for the system to come to equilibrium) the pH was measured and recorded, and an additional quantity of standard acid was added; 2 to 3 days later the equilibrium pH was again measured and another quantity of acid was added. This procedure was

repeated several times, usually over a period of from 2 to 4 weeks, to provide a series of adsorption capacities with increasing equilibrium H_3O^+ activity. Distilled water was added to the solutions periodically to correct the volume for evaporation. When evaporation was small, it was necessary to correct the data for increased volume owing to addition of acid. The data obtained could then be reduced to moles of acid reacted per gram of carbon at a given hydronium-ion activity, using the Extended DeBye-Huckel Law for calculating activity coefficients. The activity coefficient for the 1 $\underline{M}$ NaCl solution, $\gamma = 0.75$, was obtained from Harned and Owen (31). Freundlich parameters were obtained from log-log plots of the experimental data. Except when otherwise specified, the data reported in this paper have been obtained from experiments at $25^{\circ}C$.

ASH CONTENT ANALYSIS

The ash content of an active carbon is an important consideration in adsorption studies. Blackburn and Kipling (5) have demonstrated some of the effects of ash contest in the adsorption process. To assess the effects of ash on the interaction of strong acid with active carbon, separate quantities of the experimental coconut carbon were washed with 1+1 hydrochloric acid and with 1+1 glacial acetic acid to reduce the ash content of the carbon. Thirty- to forty-gram samples of carbon were shaken with the acids for about 5 days. The carbons were then washed continuously with distilled water for a

period of 3 months until the carbon could be contacted with distilled water for a few days without significantly reducing the pH. The carbons were then dried at 105° C to a constant weight. The ash content was measured by burning a known weight of the carbon at 700° C and weighing the residue. The ash content of the carbon washed with acetic acid was reduced from 0.7% to 0.6%, while that washed with hydrochloric acid was reduced from 0.7% to 0.3%. Adsorption studies could then be carried out on the treated and untreated carbon for purposes of comparison.

STOICHIOMETRY STUDIES

The HCl-NaCl system was studied to determine if Cl^- ion was removed stoichiometrically with H_3O^+ as the reaction occurred. Two 1-liter solutions were prepared at $pC_H+ = 3.00$ and 10^{-3} $\underline{M}$ NaCl; two 1-liter solutions at $pC_H+ = 3.00$ and 2×10^{-3} $\underline{M}$ NaCl; and two 1-liter solutions at $pC_H+ = 2.70$ and 10^{-3} $\underline{M}$ NaCl. A five-gram quantity of coconut-shell carbon was added to each of the $pC_H+ = 3.00$ solutions, and a ten-gram quantity to each of the $pC_H+ = 2.70$ solutions. After one day of stirring, the residual H_3O^+ concentration was measured using a pH meter and correcting for activity, and the residual Cl^- ion concentration was determined by means of the Mercuric Nitrate Method (59). The percent stoichiometry was then calculated from the data obtained.

RESULTS AND DISCUSSION

RATE-CONTROLLING STEP

The rate-limiting step for the hydronium ion-active carbon reaction appears to be intraparticle transport. From a phenomenological point of view, both the hydronium ion and the conjugate anion of the acid added are removed stoichimetrically. The studies made on the HCl-NaCl systems described above show that the ration of Cl^- ion removed from solution to H_3O^+ ion removed is in the range of 0.93:1 to 1:1. This corresponds to similar findings by Carr et al. (11) and Miller (16, 47). The data indicates that the electroneutrality requirement for sorption is satisfied in this reaction. Since the hydronium ion and anion are removed from solution stoichiometrically, it seems reasonable to expect that they would also diffuse through the pore in pairs with the anion limiting the rate of diffusion. The diffusion coefficients for different acids, calculated assuming intraparticle transport as rate-limited, are on the order of those expected for the anion, thus giving support to the assumption. Additionally, the anion would probably be rate limiting because the aqueous solution conductivity is much less for an anion than for the hydronium ion. Helfferich (34) states that film diffusion, the other likely possibility for being the rate-limiting step, will control only under extreme conditions. A study of sorption rate vs. stirring speed showed no increase in rate for stirring speeds above that required to keep the carbon in suspension. Other evidence in

support of intraparticle transport as the rate controlling
mechanism is the fact that the experimental data are described
well by a diffusion model, as will be illustrated shortly.
An activation engery of -1.8 to -2.5 kcal/mole $-^{O}K$, also dis-
cussed in more detail in a later section of this paper, falls
in the range expected for a diffusion-controlled process (64).

DIFFUSION MODEL

Assuming that pore diffusion is rate limiting, a dif-
fusion model based on Fick's second law can be utilized for
calculation of diffusion coefficients from the experimental
data. The model must take account of the simultaneous diffu-
sion-reaction process. If the sorption reaction is not taken
into account, the calculated diffusion coefficients will de-
viate considerably from the actual values. Such a model has
been developed by Crank (14)--and utilized later by Weber and
Rumer (71)--by modifying Fick's second law to include a term
which accounts for non-linear sorption. The general form is

$$\frac{\partial X}{\partial t} = \frac{1}{r^2} \frac{\partial}{\partial r} \left(r^2 D \frac{\partial X}{\partial r} \right) - \frac{\partial S}{\partial t} \qquad \text{III-1}$$

Equation III-1 is given in spherical coordinates, thus assuming
a spherical shape for the carbon particle, an assumption which
accords reasonably well with microscopic observations of the
geometry of particles of the experimental carbon. In Equation
III-1, X represents the H_3O^+ activity in solution; t, time; r,
the radial distance from the particle center; D, the diffusion
coefficient; and S, the H_3O^+ concentration at the surface of
the carbon. For the present experiments, the equilibrium

relationship between S and X is described in terms of

the Freundlich expression

$$S = FX^N \qquad N > 1.0 \qquad\qquad III-2$$

Equation 1 is subject to the boundary conditions

$$X = 0 \quad t = 0 \quad \text{for } 0 \leq r \leq a$$

and

$$\frac{A}{\overline{V}}(X_o - X_a) = 4\pi \int_0^a (\frac{X}{\overline{V}} + S) \; r^2 dr \qquad III-3$$

where A represents the volume of solution "served" by each par-

ticle; X_o, the initial H_3O^+ activity in bulk solution; X_a, the

H_3O^+ activity in bulk solution at any time; and a, the radius

of the spherical particle. Equation III-1 is a non-linear, par-

tial differential equation which can be solved by a finite dif-

ference technique after Crank (14). The solution is made easier

by expressing the equation in terms of the dimensionless para-

meters:

$$x = \frac{X}{X_o}, \qquad \tau = \frac{Dt}{a^2}, \qquad \rho = \frac{r}{a}, \qquad s = \frac{S}{X_o}$$

Before S can be divided by X_o to give the dimensionless quantity,

s, it must be converted from units of moles per gram to moles

per liter by multiplying by the specific weight of the carbon.

The specific weight for the 273-μ coal-base carbon is 0.750

grams per cc as given by the manufacturer (51), and that for

the coconut-shell carbon is assumed to be the same. The equa-

tion requiring solution, in dimensionless form, is then

$$\frac{\partial x}{\partial \tau} = \frac{1}{\rho^2} \frac{\partial}{\partial \rho} \left(\rho^2 \frac{\partial x}{\partial \rho} \right) - \frac{\partial s}{\partial \tau} \qquad\qquad III-4$$

with the boundary conditions,

$$x = 0 \quad T = 0 \quad \text{for } 0 \leq \rho \leq 1$$

and

$$\frac{A}{\gamma \pi a^3} \quad (1 - x_1) = 4 \int_0^1 (\frac{x}{\gamma} + s) \, \rho^2 d\rho \quad \text{III-5}$$

and

$$s = F' x^N \qquad \qquad \text{III-6}$$

where F', the dimensionless Freundlich parameter, is given by

$$F' = F \times sp. \; wt. \; of \; carbon \times X_o^{N-1}$$

Assuming a spherical particle and using the specific weight, the term A can be calculated for the finite-bath systems. For the 1.5 grams per liter dosage used in these studies, A = 0.00533 cm^3 for both the coconut-shell and the coal-base carbons.

An IBM 7090 digital computer was used to calculate all rate curves; the program is given in Appendix I. Calculated curves for the finite bath studies were printed out in the form X_a/X_o vs. T. These curves were then compared with the experimental X_a/X_o vs. t curves, and D was calculated by a trial and error procedure. This approach was modified slightly in order to calculate the rate curves for the infinite bath studies. The value for "A" taken for calculation purposes, in this case 1000 cm^3 was very much greater than the actual value, thus producing the effect of an essentially constant X_a with time. In this case, the integral value

$$4 \pi \int_{o}^{a} \frac{(X}{\gamma} + S) \quad r^2 dr \qquad\qquad III\text{-}7$$

which represents the total amount of solute in one carbon par-
ticle, was printed out as a function of the dimensionless time
parameter, T. This value, when multiplied by the total number
of particles present in the solution volume, represents the
number of moles of acid added to the solution to maintain a
constant pH. By comparing the calculated data to the experi-
mental curves for H_3O^+ added vs. time, the diffusion coefficient
could be calculated by a trial and error procedure. Carbon
dosages for the infinite bath experiments were 1.0 to 2.0 grams
per liter.

The basic assumptions made in developing the model should
be kept in mind when analyzing the results. Sorption is assumed
to be occurring at a rate much faster than pore diffusion, while
pore diffusion is taken to be slower than film diffusion. The
model assumes radial flux only, and a homogeneous particle.
Thus no differentiation is made between pore volume and solid
carbon. Also, the assumption of spherical geometry neglects
the fact that the particle surface is extremely irregular. The
diffusion coefficient, D, is also assumed constant with varying
acid concentration.

The inclusion of the non-linear isotherm effect requires
that the isotherm parameters be known in order to calculate
the rate curves. Thus, for each system analyzed, both rate
and equilibrium data were required.

EFFECT OF INITIAL HYDRONIUM-ION ACTIVITY

The isotherm shown in Figure III-1 was determined by the procedure described, for the coconut carbon in a 10^{-2} $\underline{M}$ NaCl system at 25°C. The data shown are a composite of several runs. The Freundlich equation, determined from a log-log plot of this data, is $S = 6.5 \times 10^{-4}X^{.127}$. The Freundlich equation was used because the log-log plot of the data was linear.

Finite and infinite bath rate data were collected for the same system for different initial hydronium ion activities. Figure III-2 presents the calculated and experimental rate curves for the finite bath experiments and Figure III-3 those obtained by the infinite bath method. Table III-1 is a summary of the results.

TABLE III-1

Diffusion Coefficients as a Function of Initial pH
For the HCl-NaCl System

10^{-2} $\underline{M}$ NaCl, 25°C, $S=6.5x10^{-4}X^{.127}$		
Initial pH (HCl)	Diffusion Coefficient, D, $(cm^2/sec)x10^7$ (Finite Bath)	Diffusion Coefficient, D, $(cm^2/sec)x10^7$ (Infinite Bath)
3.50	6.75	5.9
3.70	9.50	7.8
4.00	13.00	8.6

$S = 1.23 \times 10^{-3} \cdot x^{.14}$

$S = 6.5 \times 10^{-4} \cdot x^{.127}$

○ Coal-base carbon

△ Coconut-shell carbon

—— Calculated curve
    from Freundlich
    equation

X, H_3O^+ Activity, x 10^5

S (moles/gram) x10^4
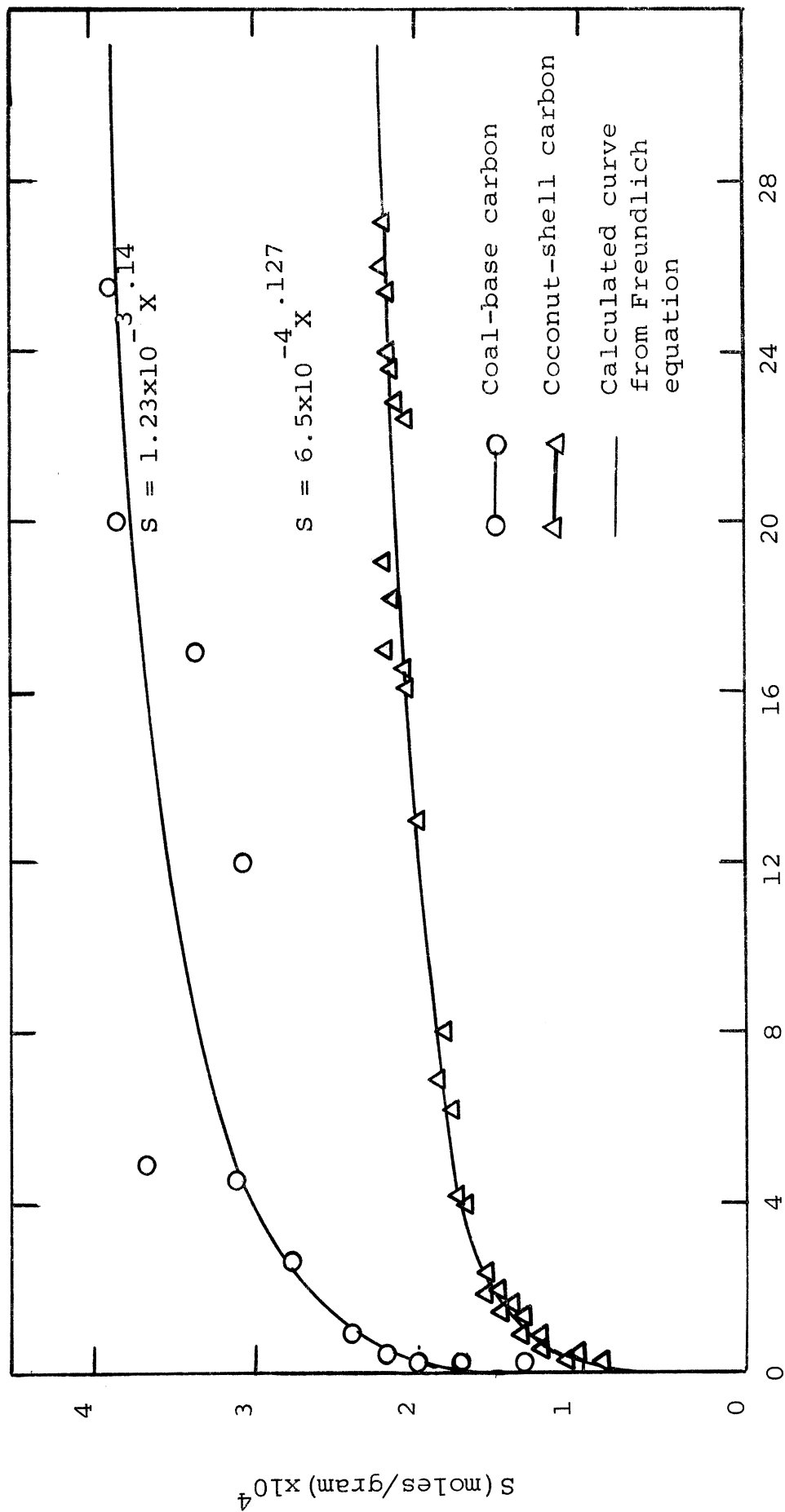
Figure III-1. Adsorption Isotherms for HCl
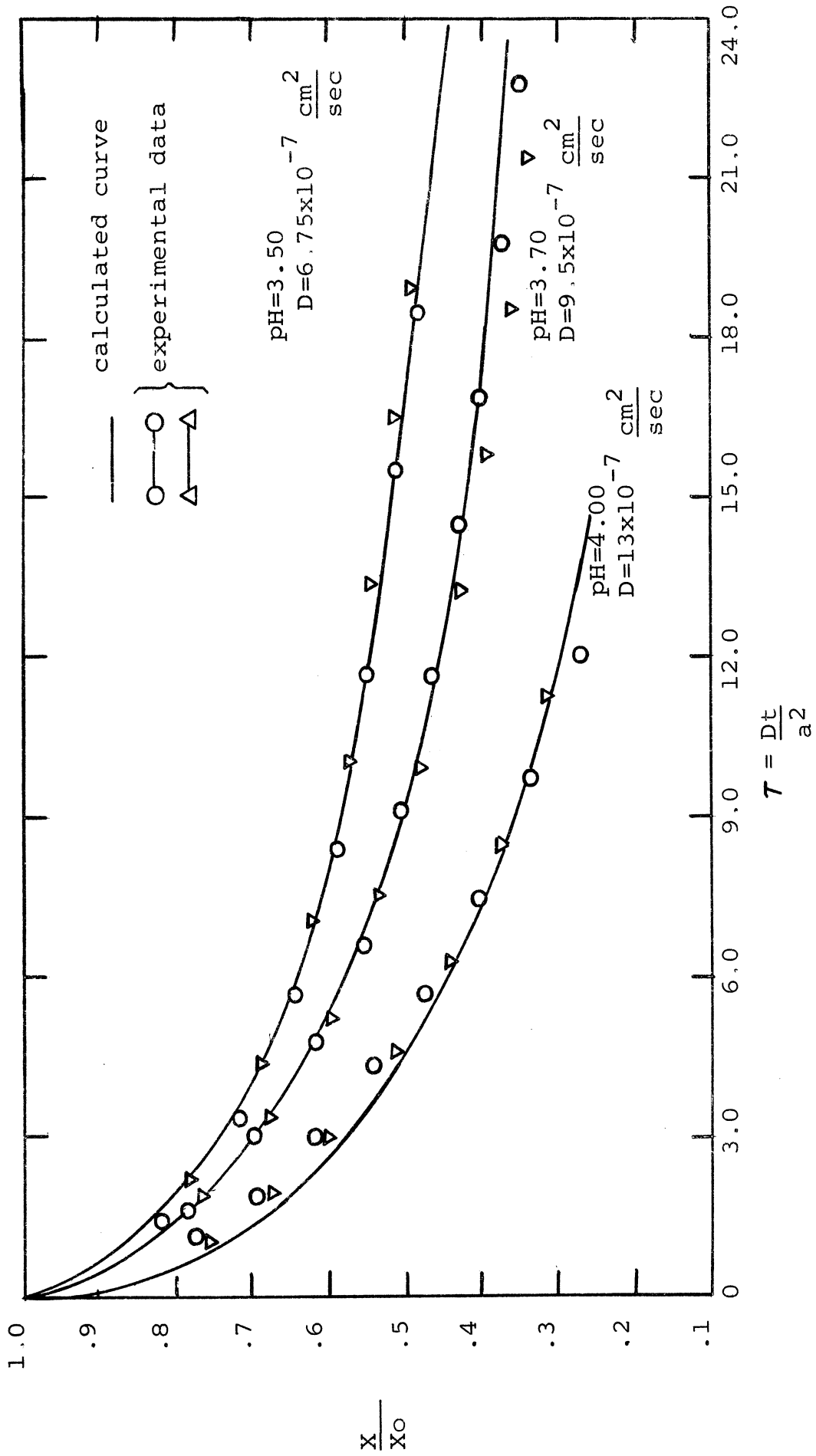
Figure III-2. Finite-Bath Rates of Adsorption for HCl
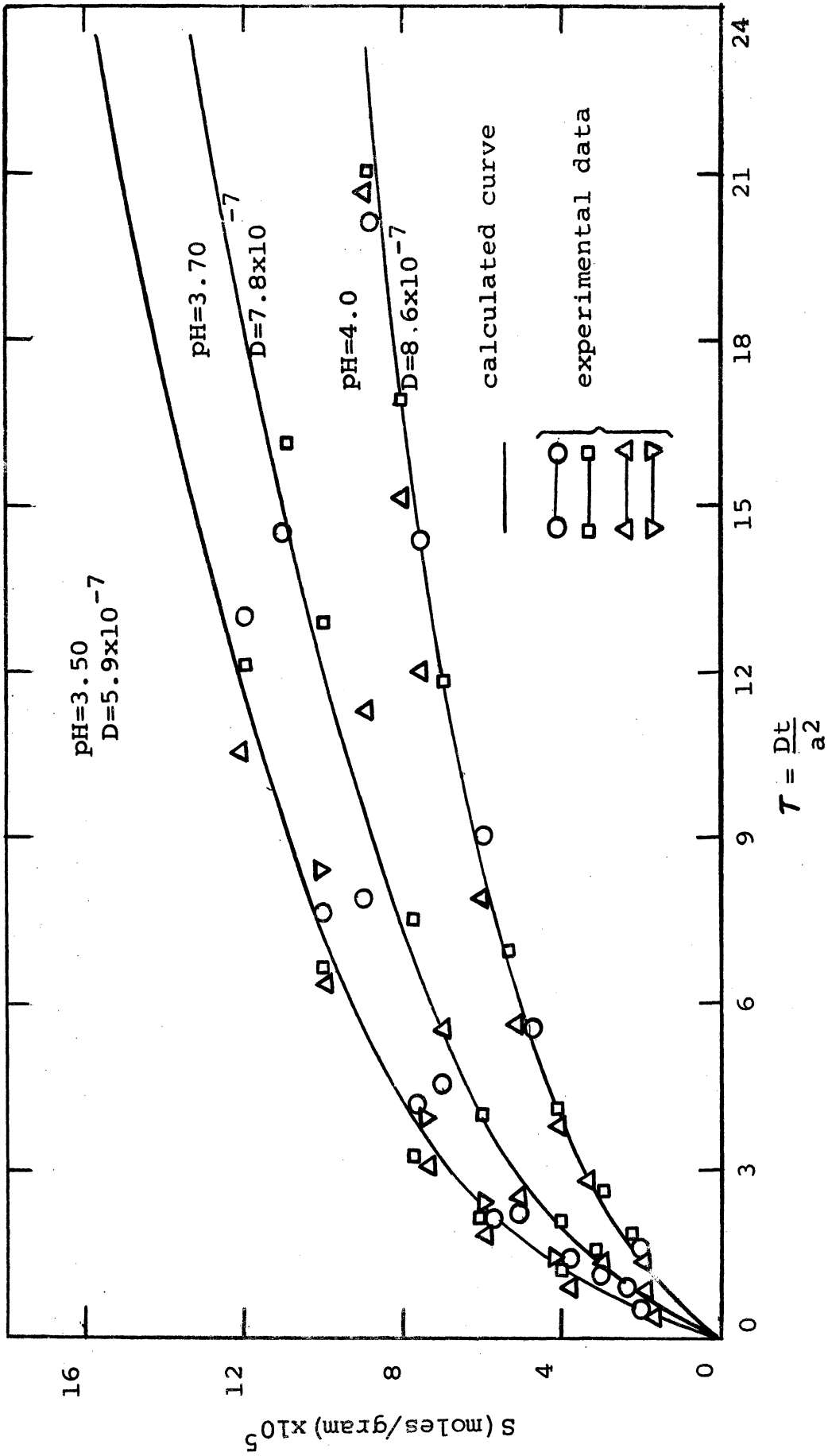
Figure III-3. Infinite-Bath Rates of Adsorption for HCl

The magnitude of the diffusion coefficients given in Table III-1 can be compared with a value of 3.3×10^{-5} cm^2/sec determined experimentally by Stokes (61) for HCl in bulk solution at infinite dilution. The pore diffusion coefficients listed in Table III-1 for HCl range from about 1/30 to 1/60 of that given by Stokes. McNeill and Weiss (45) have indicated that active carbon can be considered as a weak-base anion-exchange sorbent. According to Helfferich (34), diffusion coefficients in such resins can be several orders of magnitude less than the corresponding bulk solution coefficients. The Cl^- ion probably limits the rate of diffusion, since its mobility in aqueous solution is much less than that of the H_3O^+ ion. Further evidence to support this conclusion has been obtained in the present work from determinations of pore diffusion coefficients for several different strong acids; these will be discussed shortly (see Table III-4).

The large difference between the bulk solution coefficients and the pore coefficients may be attributable to one or more of a number of factors, the most likely of which is the size and geometry of the pores of the active carbon. The smaller the pore, the more likely is the diffusing ion to interact with internal surfaces, both physically and electrostatically (34). The relative effect of pore size is indicated by comparative studies carried out with 273-micron coal-base carbon. Although there was no pore size distribution data available for the coconut carbon, the average size of the

micropores of this carbon can be assumed to be considerably
smaller than that of the coal-base carbon, since the former
was designed for adsorption from gas phase while the latter
was designed for adsorption from solution. The solution used
for this equilibrium study had an initial pH of 3.50 (HCl),
was 10^{-2} $\underline{M}$ in NaCl, and contained 1.33 grams of the coal-
base carbon per liter; the study was made at $25^{\circ}C$. The iso-
therm for this system is shown in Figure III-1, along with
the isotherm for the coconut carbon. Kinetic measurements
were made on the same system using the finite-bath technique,
and the calculated and experimental rate curves are shown in Fig-
ure III-4. The corresponding rate curve for the coconut car-
bon with this system is included in Figure III-4. The calculated
diffusion coefficient for HCl in the coal-base carbon is 1.4
x 10^{-5} cm^2/sec, which is nearly equal to that for HCl in
bulk solution. Although many other factors might contribute
to the large difference between the two carbons, relative pore
size is probably a major one.

Other factors which may also be responsible to some
extent for the small coefficient obtained for the coconut car-
bon include the approximation of spherical particle geometry,
the assumption of an isotropic medium, and the assumption of
a radial diffusion path (34).

Specific chemical interaction between the chloride ion
and metal ions present at the pore surfaces has also been con-
sidered as a possible factor contributing to retardation of
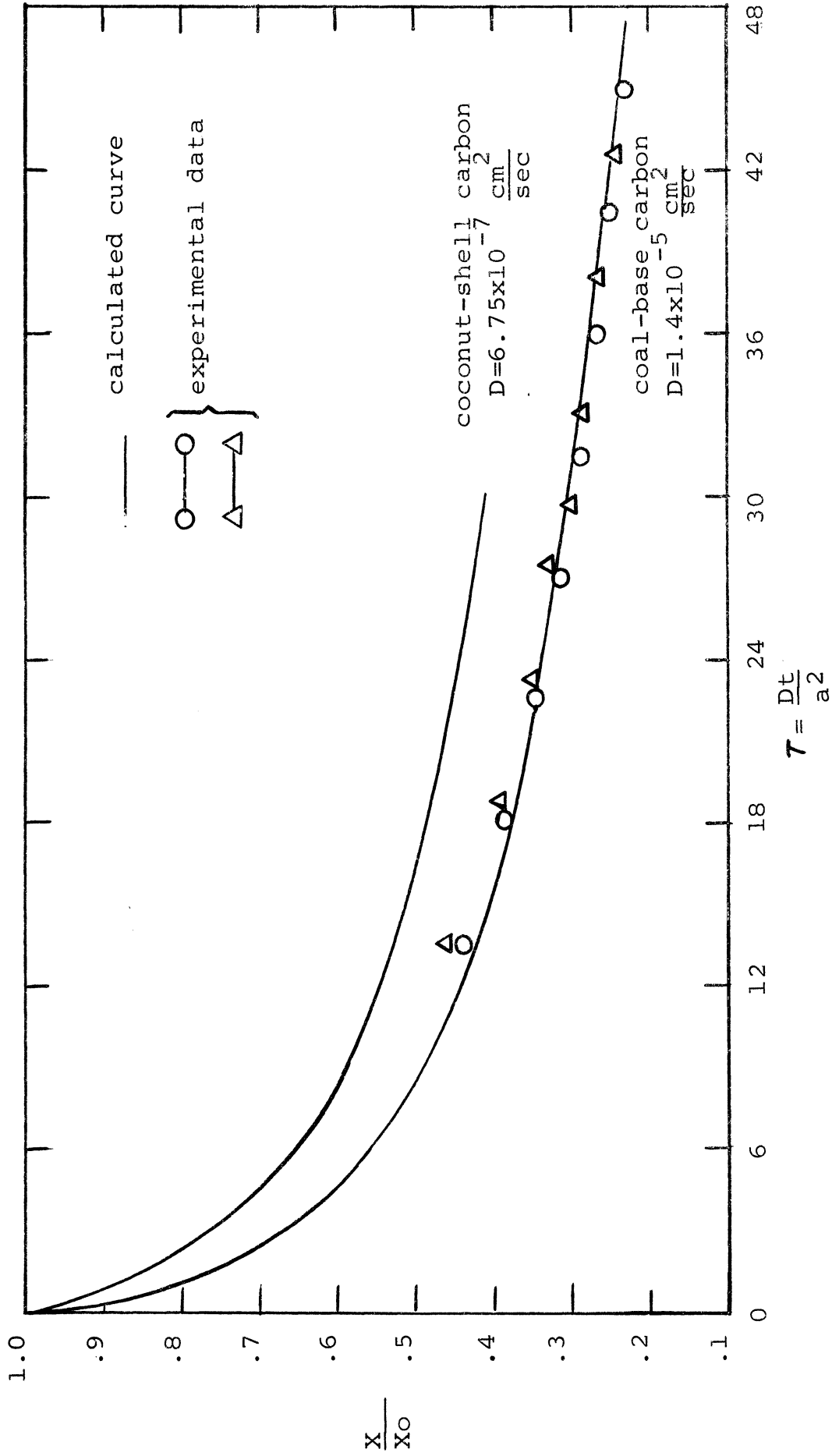
Figure III-4. Finite-Bath Rates of Adsorption for HCl on Different Carbons

HCl diffusion. To evaluate this possibility, one portion of
the coconut carbon was washed with acetic acid to reduce its
ash content from 0.7% to 0.6%, and another portion with hydro-
chloric acid to reduce its ash content from 0.7% to 0.3% The
finite bath technique was used to study these two carbons in
otherwise identical systems consisting of 10^{-2} $\underline{M}$ NaCl, 1.5
grams carbon per liter, an initial pH of 3.50 (HCl), at a
temperature of $25^{\circ}C$. The corresponding isotherms show no
significant difference between these carbons and the untreated
coconut carbon. The experimental rate data and calculated
curves for the two systems are plotted in Figure III-5. Be-
cause there was found to be no essential difference between
the calculated curves for the acid treated and the untreated
carbon, only one curve is shown. The experimental rate data
for the acetic-acid-treated carbon are not described as well
as are those for the hydrochloric-acid-treated carbon, nor as
well as those for the untreated carbon fitted by the calculated
curve shown in Figure III-1. The diffusion coefficient derived
from the curve of best fit for the acetic-acid washed carbon
is 9 x 10^{-7} cm^2/sec, and that for the hydrocholoric-acid-
washed carbon is 9.5 x 10^{-7} cm^2/sec; this compares with 6.75 x
10^{-7} cm^2/sec for the untreated carbon. The increase in the
diffusion coefficient for the treated carbon over that for the
untreated carbon indicates that interaction of the HCl with
the inorganic content of the carbon could be responsible to
some extent for retarding diffusion. Analysis has shown that
the ash is approximately 50% iron, which in ionic form tends
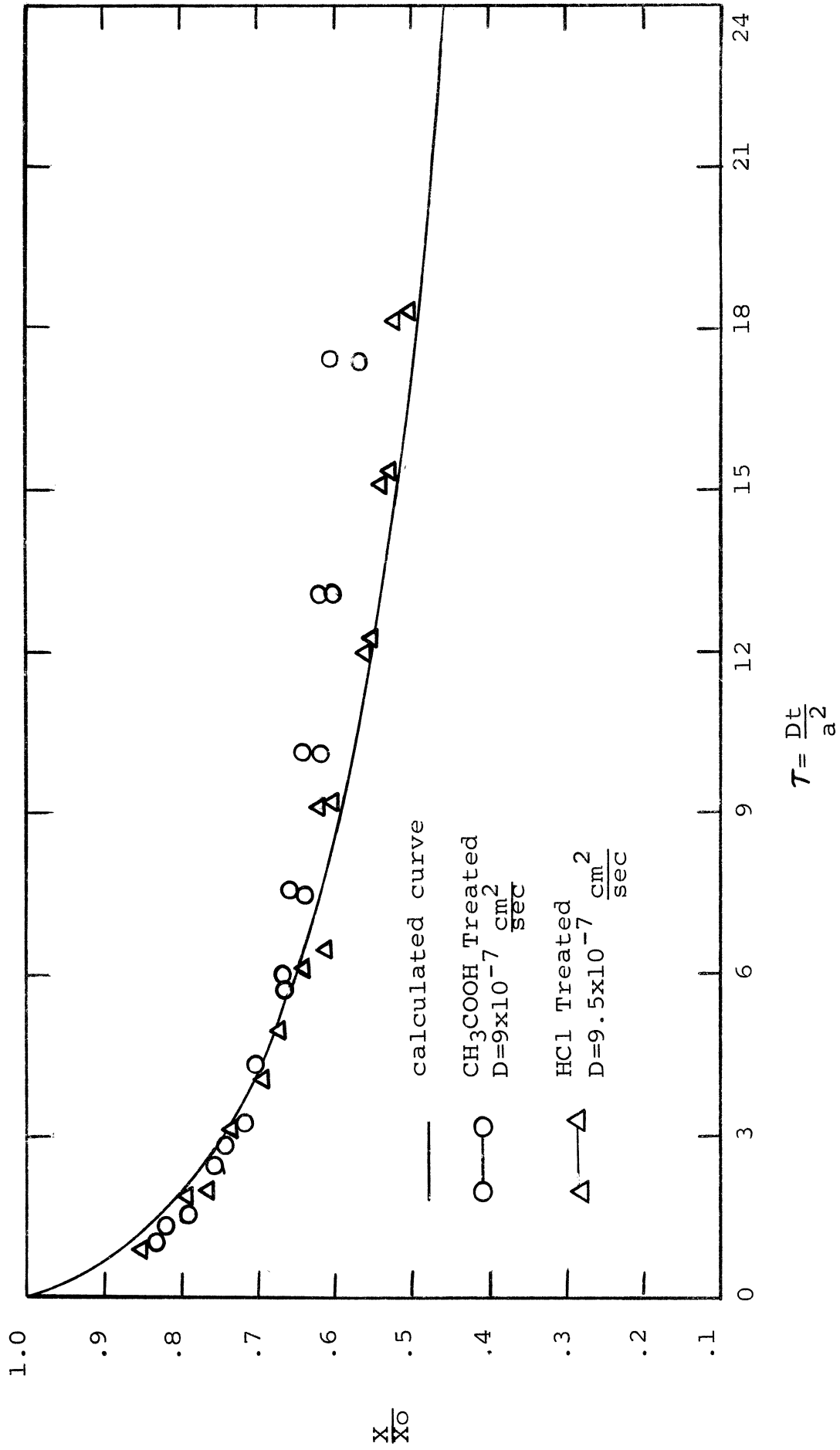
Figure III-5. The Effect of Ash Removal on Finite-Bath Adsorption Rate

to form complexes with the Cl⁻ ion.

Diffusion coefficients for different initial pH calculated from data obtained by the finite bath technique compare favorably with those determined by the infinite bath technique as can be seen in Table III-1. The calculated rate curves fit the experimental data very well for initial pH values of 3.50 and 3.70, but for initial pH of 4.00, finite bath case, the fit is not as good. For the latter case, the range of the diffusion coefficient is $6-14 \times 10^{-7}$ cm^2/sec for all of the experimental data to fall on the calculated curve. Another effect shown by the data is that the diffusion coefficient increases with increasing initial pH, indicating that the coefficient is a function of activity. This is contrary to the assumption of a constant diffusion coefficient built into the rate model. However, except for the case of an initial pH of 4.0, finite bath case, the effect is apparently not very great for the activity change occurring in a given rate study for those shown in Figure III-2; otherwise the experimental data would not be described as well by the calculated curves. The decrease in diffusion coefficient with increasing H_3O^+ activity is probably due to hydration effects. The increased number of hydrated H_3O^+ and Cl⁻ ions in the pore decreases the amount of free solvent available for diffusion of the ions, thus decreasing effective pore size and increasing retardation effects due to interaction of the diffusing species with the carbon framework. A decrease in the diffusion coefficient is thereby brought about (34).

SALT EFFECTS

The HCl-NaCl system has been studied further to deter-
mine the effect of NaCl concentration on the acid-carbon re-
action. The carbon dosage was varied from 0.33 to 2.0 grams
of 273-micron coconut carbon per liter for the equilibrium
studies, and the temperature was $25^\circ C$. NaCl concentration
was studied over a range from 5×10^{-3} to 1.0 $\underline{M}$. The effect of
salt concentration on the equilibrium position of the reaction
is shown in Figures III-6 and III-9. Typical rate data, along
with the corresponding calculated curve, are shown in Figure
III-7 for a 2×10^{-2} $\underline{M}$ concentration of NaCl. The finite bath
method was used for these rate studies. A summary of the
results is given in Table III-2. It should be noted that
the range of the Freundlich parameters used for the rate curve
calculations produced very slight changes in the shapes of
the resulting curves.

TABLE III-2

The Effect of NaCl Concentration
on Diffusion of HCl

Initial pH = 3.50,		Temperature = 25°	
Freundlich Parameters		NaCl Concentration, (moles/liter)$\times 10^2$	D, (cm^2/sec)$\times 10^7$
$F \times 10^4$	N		
5.6	0.125	0.5	4.00
6.5	0.127	1.0	6.75
6.9	0.133	2.0	7.50
7.1	0.120	10.0	15.10
7.6	0.105	100.0	68.00
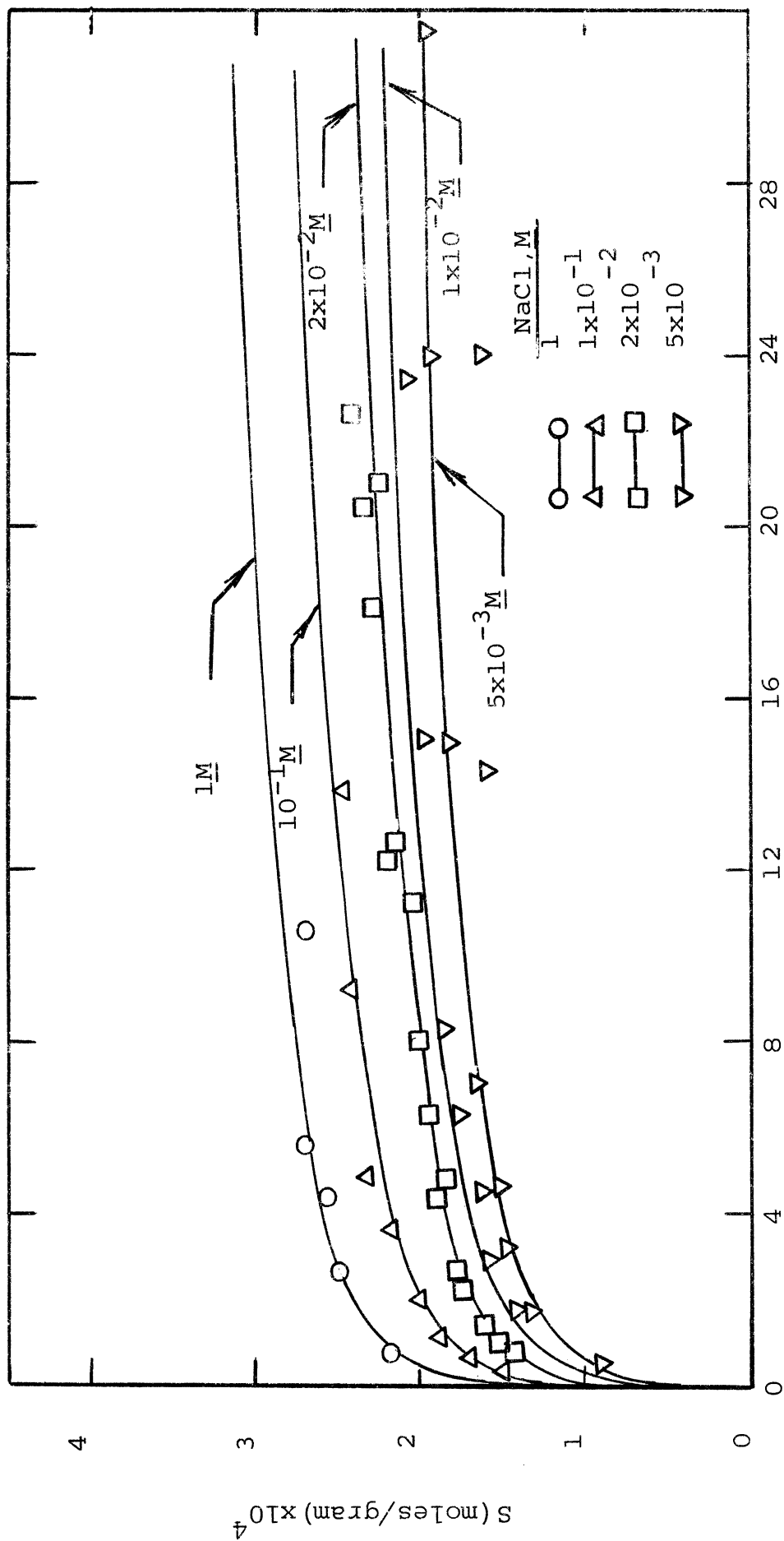
Figure III-6. The Effect of Salt Concentration on Adsorption Capacity for HCl
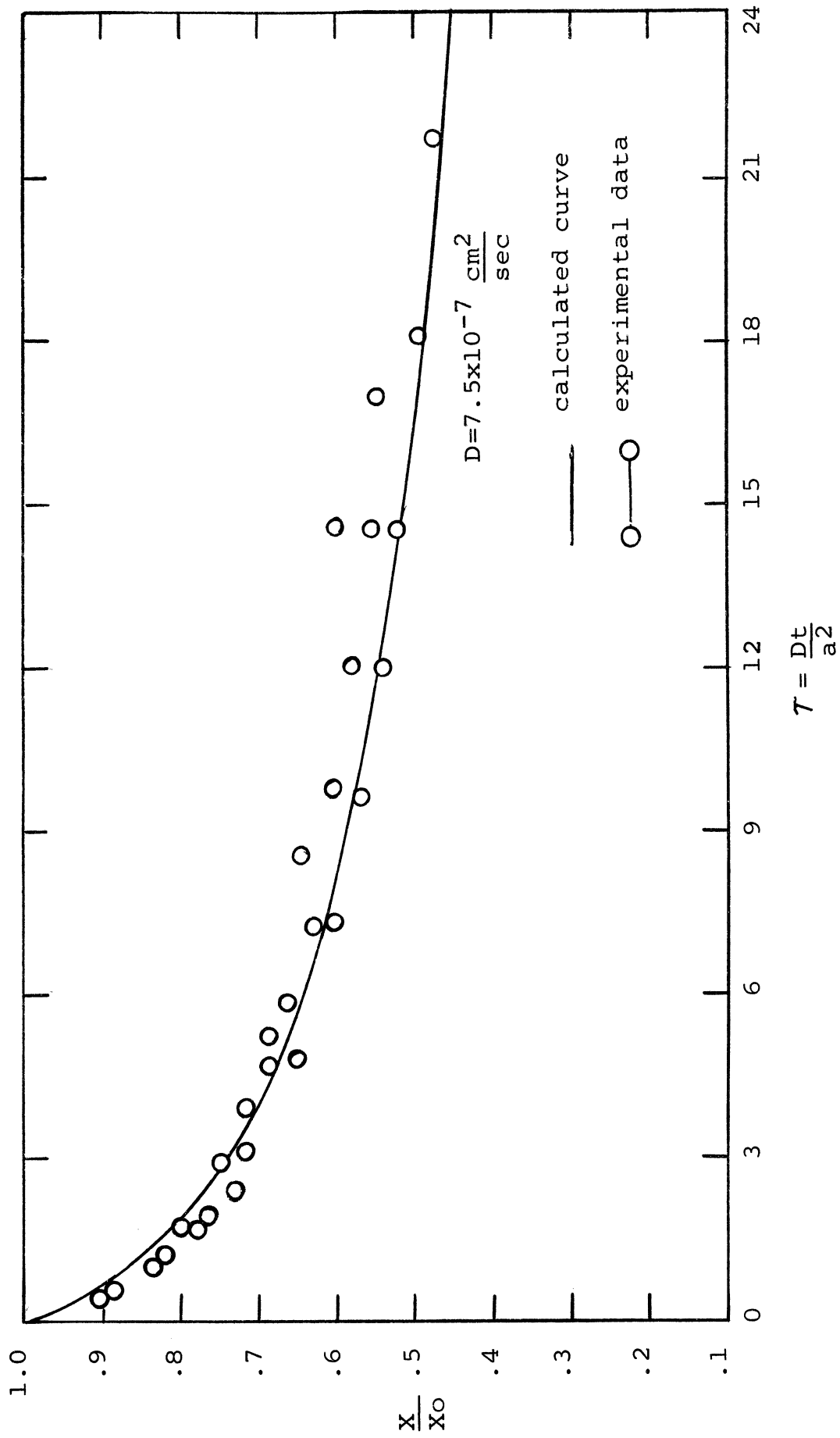
Figure III-7. Finite-Bath Rate of Adsorption for HCl at 0.02 $\underline{M}$ NaCl

Similar studies have been carried out on the $HClO_4$-$NaClO_4$ system. All conditions were the same as those for the HCl-NaCl tests, except that the carbon dosage was 1.33 grams per liter for the equilibrium study and the concentration of $NaClO_4$ ranged from 5×10^{-3} to 10^{-1} $\underline{M}$. The effect on the extent of reaction is shown in Figures III-8 and III-9, and typical rate data along with the corresponding calculated curve for a concentration of 10^{-2} $\underline{M}$ $NaClO_4$ are given in Figure III-10. The results are summarized in Table III-3.

TABLE III-3

The Effect of $NaClO_4$ Concentration
on Diffusion of $HClO_4$

Initial pH = 3.50,		Temperature = 25°	
Freundlich Parameters		$NaClO_4$ Concentration (moles/liter) $\times 10^2$	D, (cm²/sec) $\times 10^6$
$F, \times 10^4$	N		
7.6	0.1050	0.5	4.7
8.2	0.1030	1.0	5.3
8.4	0.1000	2.0	6.0
10.0	0.1065	10.0	10.0

The equilibrium studies were performed with only sodium salts. Rate studies, however, were performed with LiCl and KCl as well as with NaCl, and no significant difference was found.

There is a marked increase in the quantity of acid sorbed with increasing salt concentration for both the HCl-NaCl and
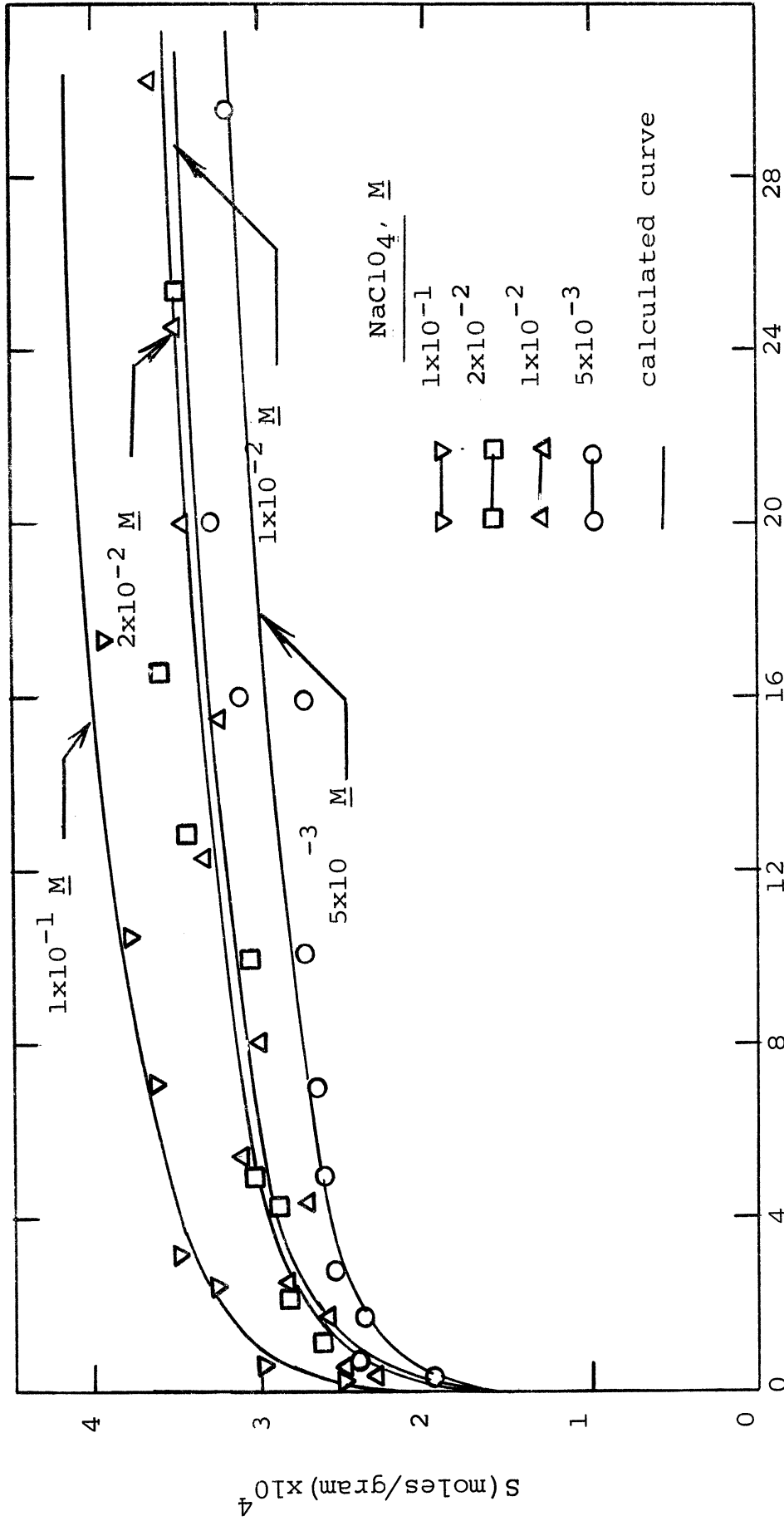
Figure III-8.   The Effect of Salt Concentration on Adsorption
Capacity for HClO$_4$
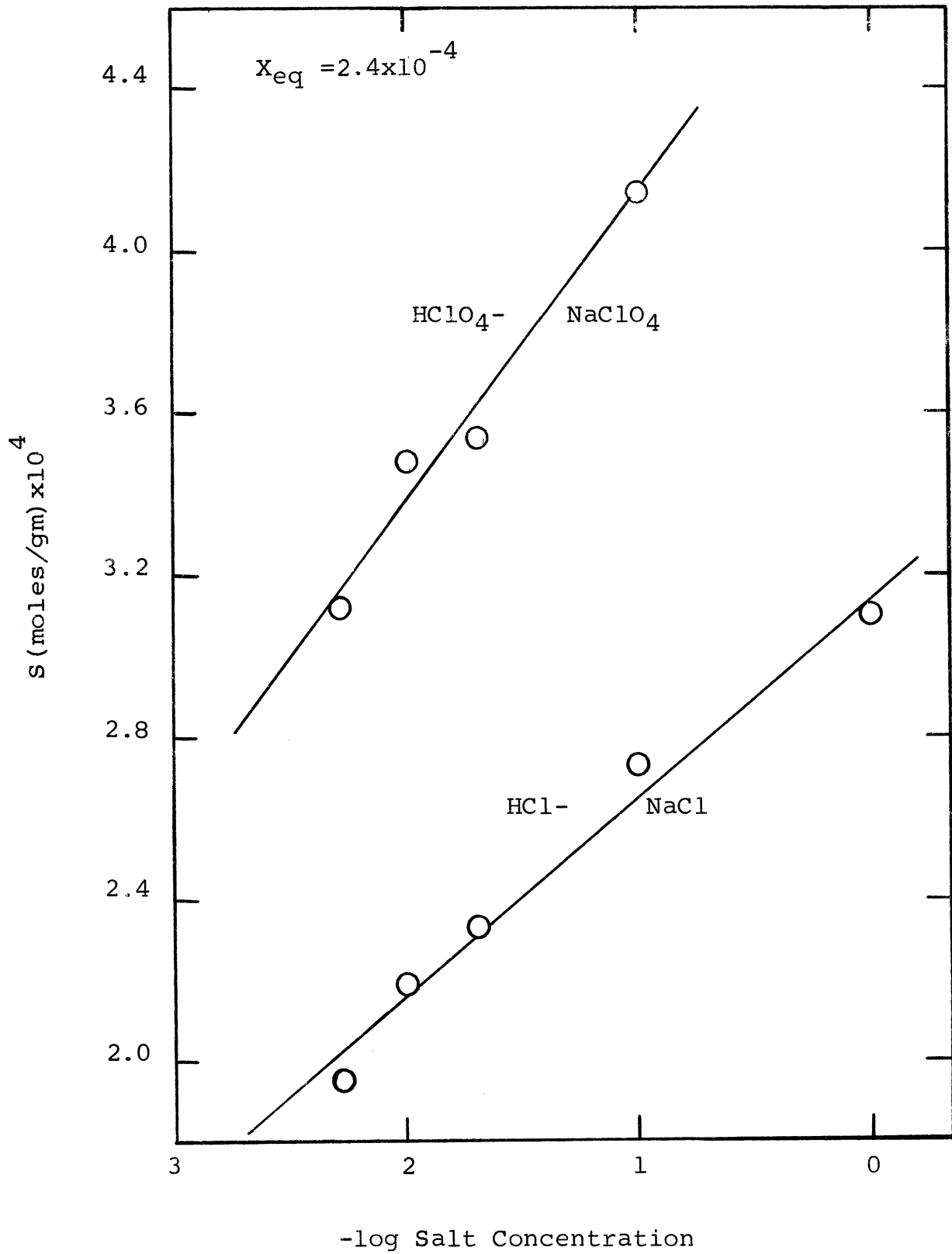
Figure III-9. The Effect of Salt Concentration
on Adsorption Capacity for Acid
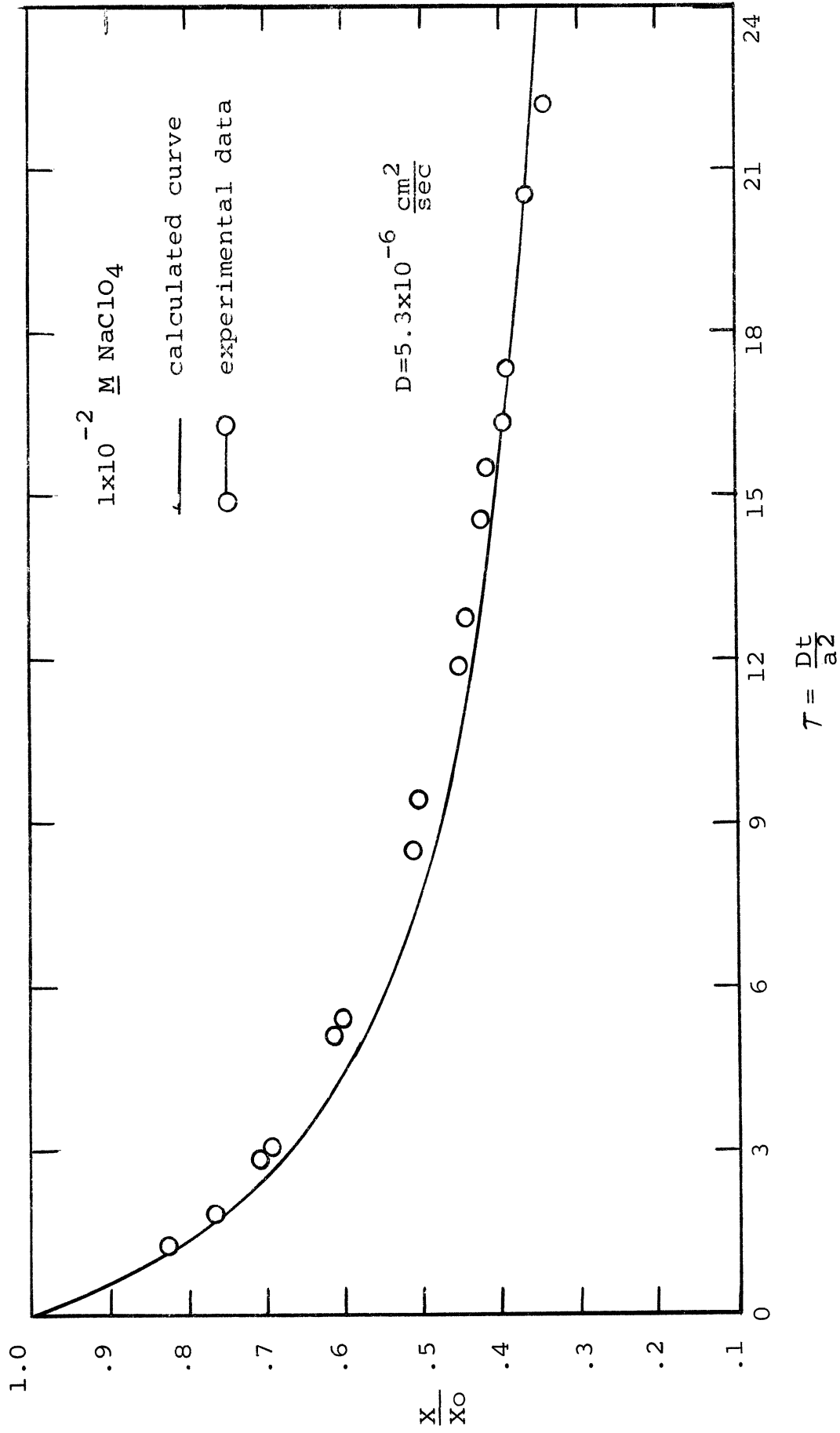
Figure III-10. Finite-Bath Rate of Adsorption for $HClO_4$

the $HClO_4$-$NaClO_4$ systems. A two-hundred-fold increase in NaCl concentration produces a 60% increase in HCl sorption at pH 3.40, while a twenty-fold increase in $NaClO_4$ concentration causes a 30% increase in $HClO_4$ sorption at the same pH. This observation is consistent with a physical sorption model. Electrophoretic mobility measurements have shown that the active carbon has a negative surface potential. It is possible, therefore, that the proton is primarily adsorbed while the anion is secondarily adsorbed in the double layer. If the proton is adsorbed readily but held back because the anion is not easily taken into the double layer, then an increase in salt concentration would have the effect of increasing the anion pressure, and more acid would tend to be adsorbed. The effect is consistent with that noted by Steenberg (22), and Parks and Bartlett (50). Indeed, Boehm (6) found evidence that physical sorption of acid took place on the basal planes of the microcrystallite. Other sorption mechanisms can not be ruled out, however, because reverisble chemisorption could show a similar effect within a given range of salt concentrations. Also, pores which might be inaccessable at low salt concentrations could become of importance at the higher anion pressures.

The increase in the diffusion coefficient for the HCl-NaCl system with increased chloride concentration is especially noteworthy. This effect best can be explained by the fact that the driving force for the rate-limiting Cl^- ion is increased, with a resulting increase in the HCl flux. Since the effect of anion concentration is not built into the mathematical

diffusion model, higher diffusion coefficients result. The reason for the effect being greater for the HCl-NaCl system than for the $HClO_4$-$NaClO_4$ system may be related to relative ionic size and to the fact that the diffusion coefficient for the HCl is much further from its bulk solution value than is that for $HClO_4$. Because of hydration effects, the Cl^- ion is larger in solution than is the ClO_4^- ion (12). As a result, there are probably many more retardation effects due to ionic size which can be overcome by the increased in Cl^- ion activity. The fact that the diffusion coefficient for $HClO_4$ is ten times as large as that for HCl could also be due to the relative sizes.

The much higher capacity of the active carbon for $HClO_4$ then for HCl has been observed by others for ion exchange resins (12). The observation is in keeping with the smaller hydrated radius of the ClO_4^- ion as noted above. Chu et al. (12) have claimed that an additional effect derives from the inability of the ClO_4^- ion to orient surrounding water molecules in bulk solution as effectively as does the Cl^- ion. The water molecules adjacent to the ClO_4^- ion are attracted more strongly to other water molecules than to the ClO_4^-; thus a disrupture zone is created in the structure of the bulk-solution water. Because the structure of the water in the resin (active carbon) is already highly disrupted by the charged internal surfaces, the bulk-phase water tends to "push" the ClO_4^- ion into the resin. The Cl^- ion, however, tends to be held back in bulk phase because its attraction for the water is stronger than

is that of the ClO^- ion.

EFFECTS OF THE TYPE OF ACID

Additional kinetic and equilibrium studies have been performed with HNO_3 and H_2SO_4. The results of the equilibrium studies are given in Figure III-11; comparable isotherms for HCl and $HClO_4$ are shown also for comparison. These studies were carried out at $2^{?}°C$ in 10^{-2} $\underline{N}$ solutions of the sodium salt of the conjugate base. Carbon dosages were again 1.33 grams of 273-micron coconut carbon per liter for the equilibrium studies. Typical rate data for HNO_3 in a 10^{-2} $\underline{N}$ $NaNO_3$ solution are shown in Figure III-12. Table III-4 is a tabulation of the results.

TABLE III-4

Diffusion Coefficients
for Different Strong Acids

Initial pH = 3.50 Sodium Salt Concentration = $10^{-2}\underline{N}$ Temperature = $25°C$			
	Freundlich Parameters		D
Acid	$F, \times 10^4$	N	$(cm^2/sec) \times 10^7$
H_2SO_4	14.5	.1970	2.00
HCl	6.5	.1270	6.75
HNO_3	6.6	.1065	24.50
$HClO_4$	8.2	.1030	53.00

The equilibrium curve for the HNO_3 falls between those for the HCl and $HClO_4$, as expected on the basis of the explanation given previously for the difference between HCl and $HClO_4$ capacities. The NO_3^- ion would be less hydrated than
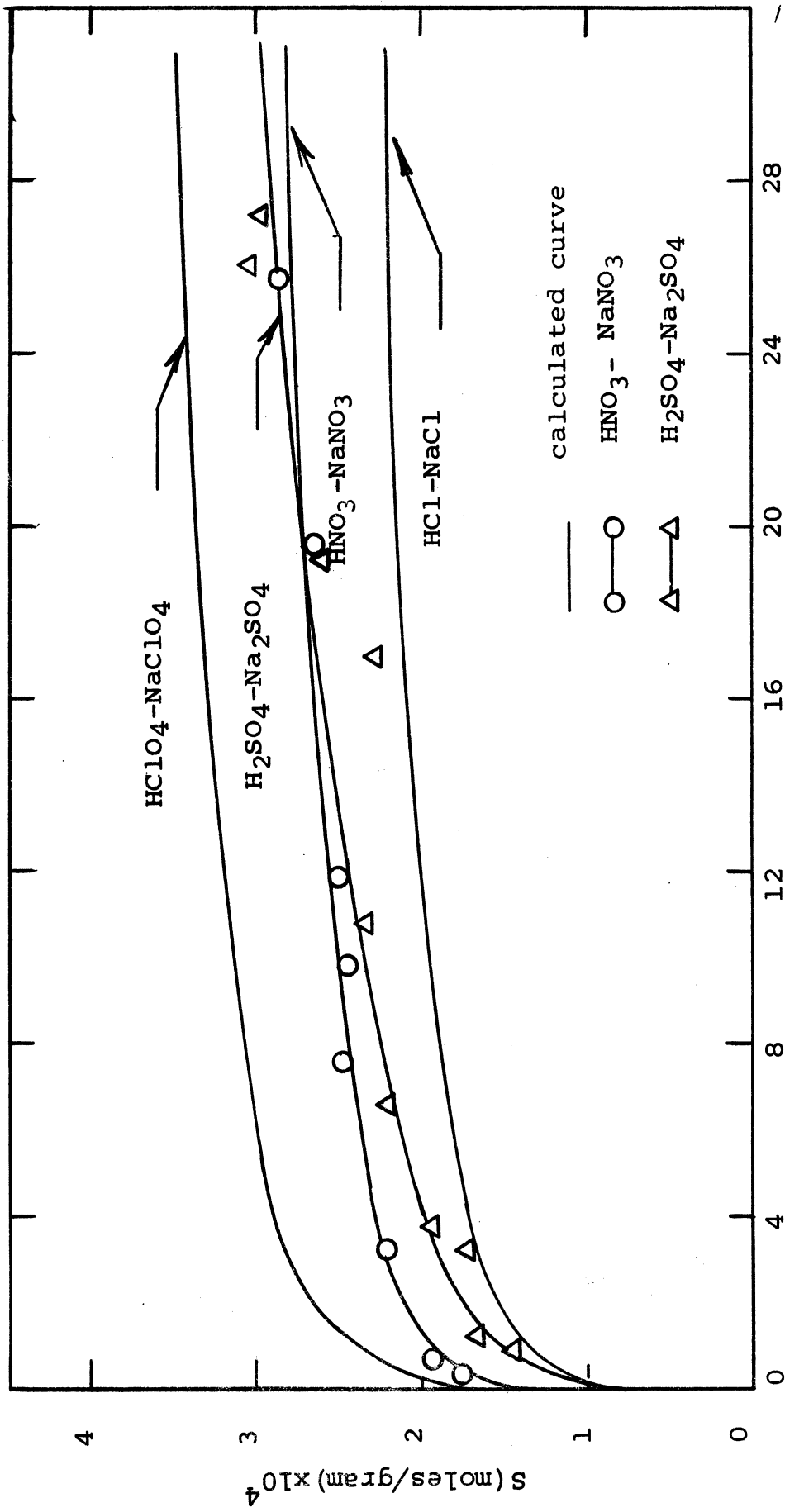
X, H_3O^+ Activity, $x10^5$

Figure III-11. Adsorption Isotherms for
Different Strong Acids
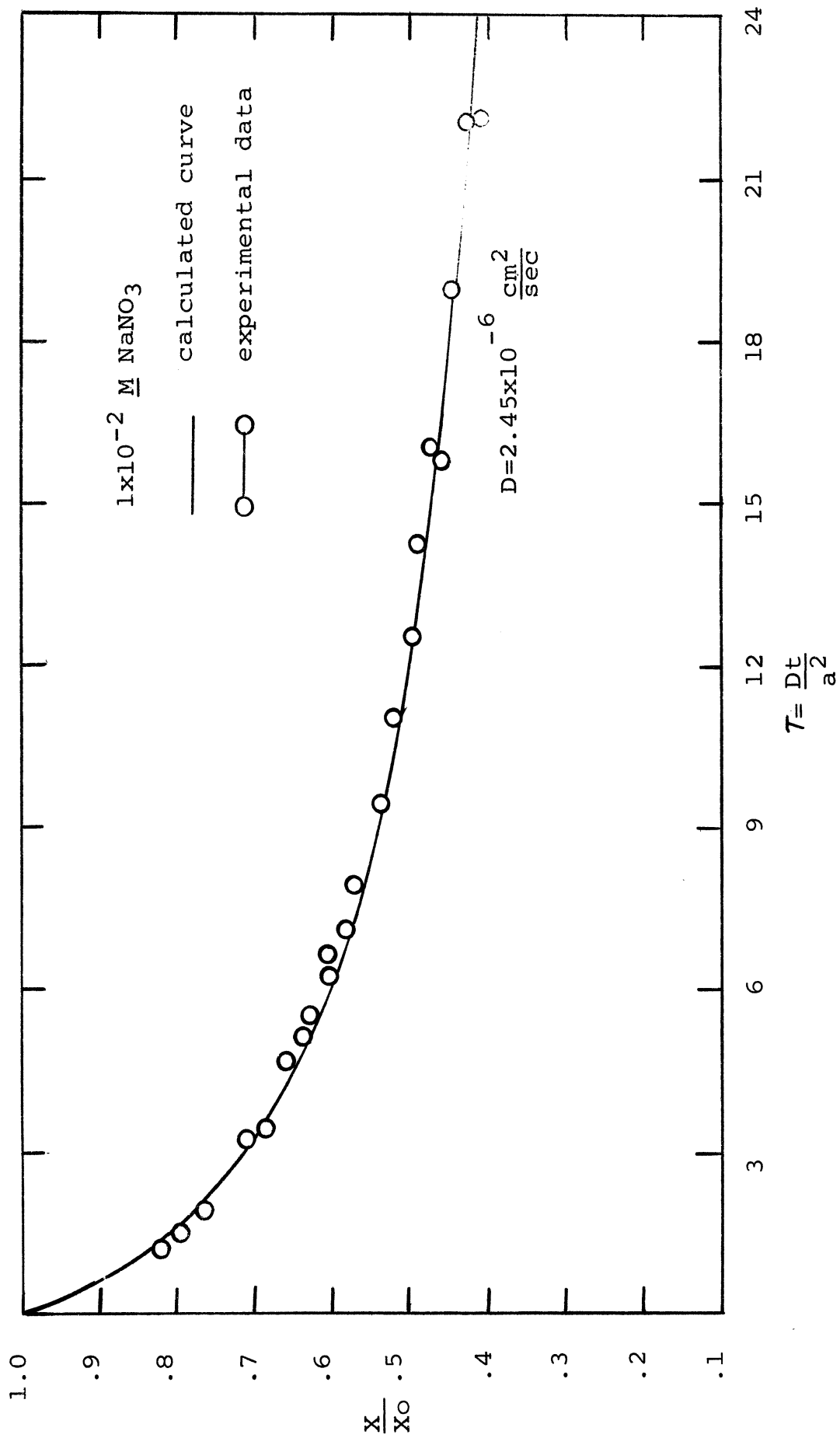
Figure III-12. Finite-Bath Rate of Adsorption for HNO_3

the Cl^- ion but more hydrated than the ClO_4^- ion. The disruptive effect on the bulk water structure would thus be expected to be intermediate, and the capacity sequence to be $HClO_4 > HNO_3 > HCl$, as observed. This corresponds to the affinity scale given by Kitchner for ion exchange resins (43). Because of the valence effect on the interaction of the SO_4^{2-} ion with the active carbon and on the relative extent of hydration, prediction of H_2SO_4 capacity relative to the monoprotonic acids is difficult. It is interesting to note that the active carbon has a higher capacity for $HClO_4$ than for H_2SO_4. Thus it is probably true that the more extensive hydration of the SO_4^{2-} prevents it from entering some of the smaller pores.

The diffusion coefficient for HNO_3 is intermediate between those for HCl and $HClO_4$, in keeping with the relative effects of hydration and disruption of water structure. The diffusion coefficient for H_2SO_4, however, is lower than those of the monoprotonic acids. According to Helfferich (34), the change in the magnitude of the diffusion coefficient between bulk solution and resin phase is much greater for divalent ions than for monovalent ions. This effect could be the result of a combination of increased electrostatic interaction with internal surfaces and of increased physical resistance attributable to the size of the hydrated ion. The sequence of the diffusion coefficients,

$$SO_4^{2-}(2x10^{-7}) < Cl^-(6.75x10^{-7}) < NO_3^-(24.5x10^{-7}) < ClO_4-(53x10^{-7}),$$

compares favorably with that found by Soldano and Boyd (57, 60),

the Cl$^-$ ion but more hydrated than the ClO$_4^-$ ion. The disruptive effect on the bulk water structure would thus be expected to be intermediate, and the capacity sequence to be HClO$_4$ > HNO$_3$ > HCl, as observed. This corresponds to the affinity scale given by Kitchner for ion exchange resins (43). Because of the valence effect on the interaction of the SO$_4^{2-}$ ion with the active carbon and on the relative extent of hydration, prediction of H$_2$SO$_4$ capacity relative to the monoprotonic acids is difficult. It is interesting to note that the active carbon has a higher capacity for HClO$_4$ than for H$_2$SO$_4$. Thus it is probably true that the more extensive hydration of the SO$_4^{2-}$ prevents it from entering some of the smaller pores.

The diffusion coefficient for HNO$_3$ is intermediate between those for HCl and HClO$_4$, in keeping with the relative effects of hydration and disruption of water structure. The diffusion coefficient for H$_2$SO$_4$, however, is lower than those of the monoprotonic acids. According to Helfferich (34), the change in the magnitude of the diffusion coefficient between bulk solution and resin phase is much greater for divalent ions than for monovalent ions. This effect could be the result of a combination of increased electrostatic interaction with internal surfaces and of increased physical resistance attributable to the size of the hydrated ion. The sequence of the diffusion coefficients,

$$SO_4^{2-}(2 \times 10^{-7}) < Cl^-(6.75 \times 10^{-7}) < NO_3^-(24.5 \times 10^{-7}) < ClO_4-(53 \times 10^{-7}),$$

compares favorably with that found by Soldano and Boyd (57, 60),

$$PO_4^{3-} (0.57 \times 10^{-7}) < WO_4^{2-} (1.80 \times 10^{-7}) < Cl^- (3.54 \times 10^{-7}) < BrO_3^- (4.56 \times 10^{-7}).$$
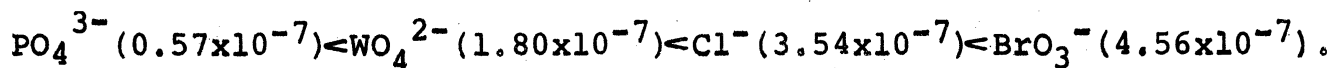
The hydrated radii probably follow the same sequence in each case. In addition, the diffusion coefficients for Cl^- are of nearly the same magnitude.

TEMPERATURE EFFECTS

Equilibrium studies have been performed on the HCl, 10^{-2} $\underline{M}$ NaCl system at temperatures at $2^{\circ}C$, 25°, and $50^{\circ}C$. The results are shown in Figure III-13 and the equilibrium parameters are tabulated in Table III-5. The results of rate studies on the same systems at the three different temperatures are shown in Figures III-14 and III-15 for $2^{\circ}C$ and $50^{\circ}C$, and in Figure III-2 for $25^{\circ}C$, while the results are tabulated in Table III-5.

TABLE III-5

Diffusion Coefficients for the HCl-NaCl
System at Different Temperatures

Initial pH = 3.50,			10^{-2} $\underline{M}$ NaCl
Temperature $^{\circ}C$	Freundlich Parameters		D $(cm^2/sec) \times 10^7$
	$F, \times 10^4$	N	
2	4.4	0.093	4.0
25	6.5	0.127	6.75
50	9.3	0.17	8.50

The diffusion coefficients, as expected, increased with increasing temperature. Variation of the diffusion coefficient as a function of temperature can be expressed in terms of the
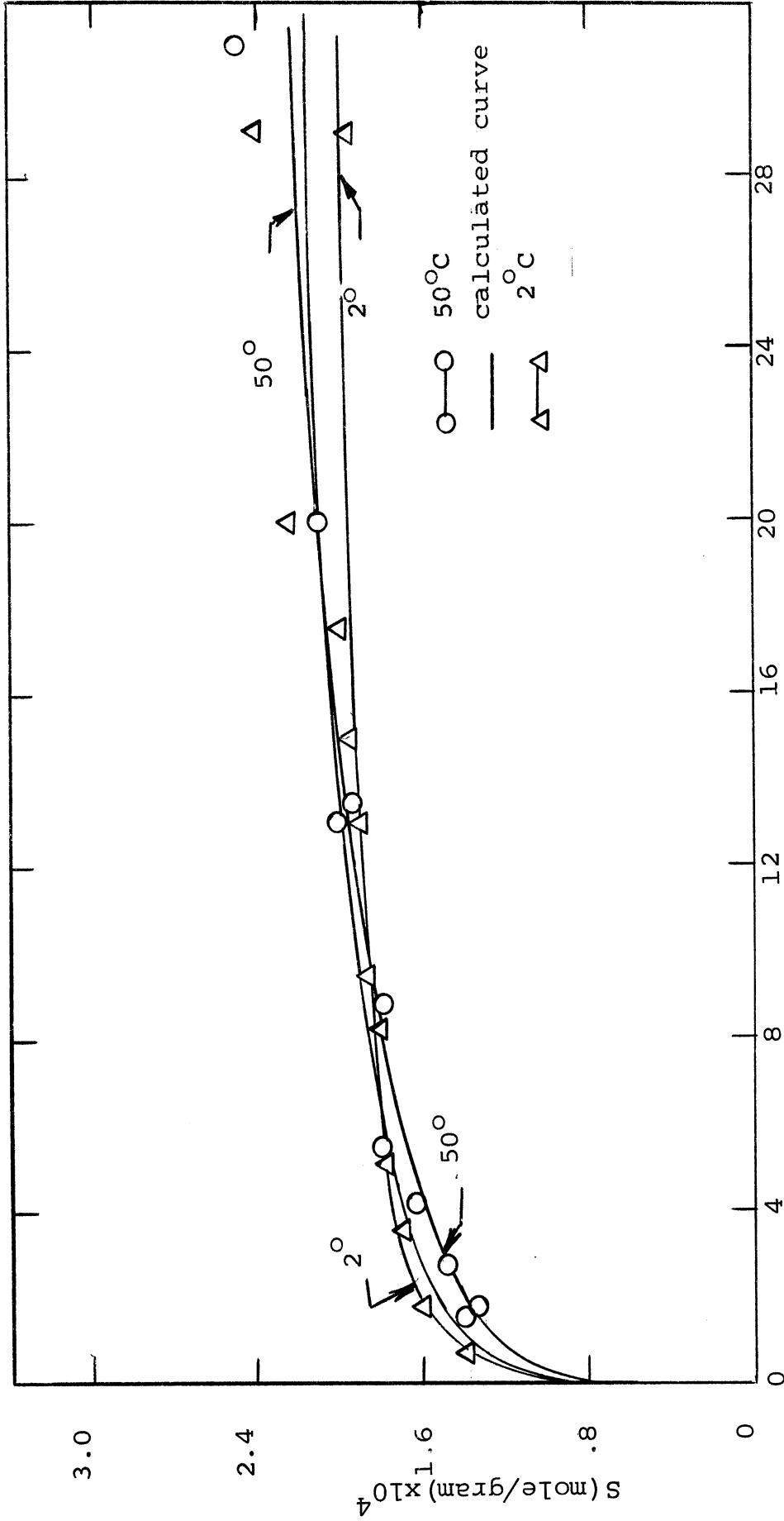
Figure III-13. The Effect of Temperature on
Adsorption Capacity for HCl
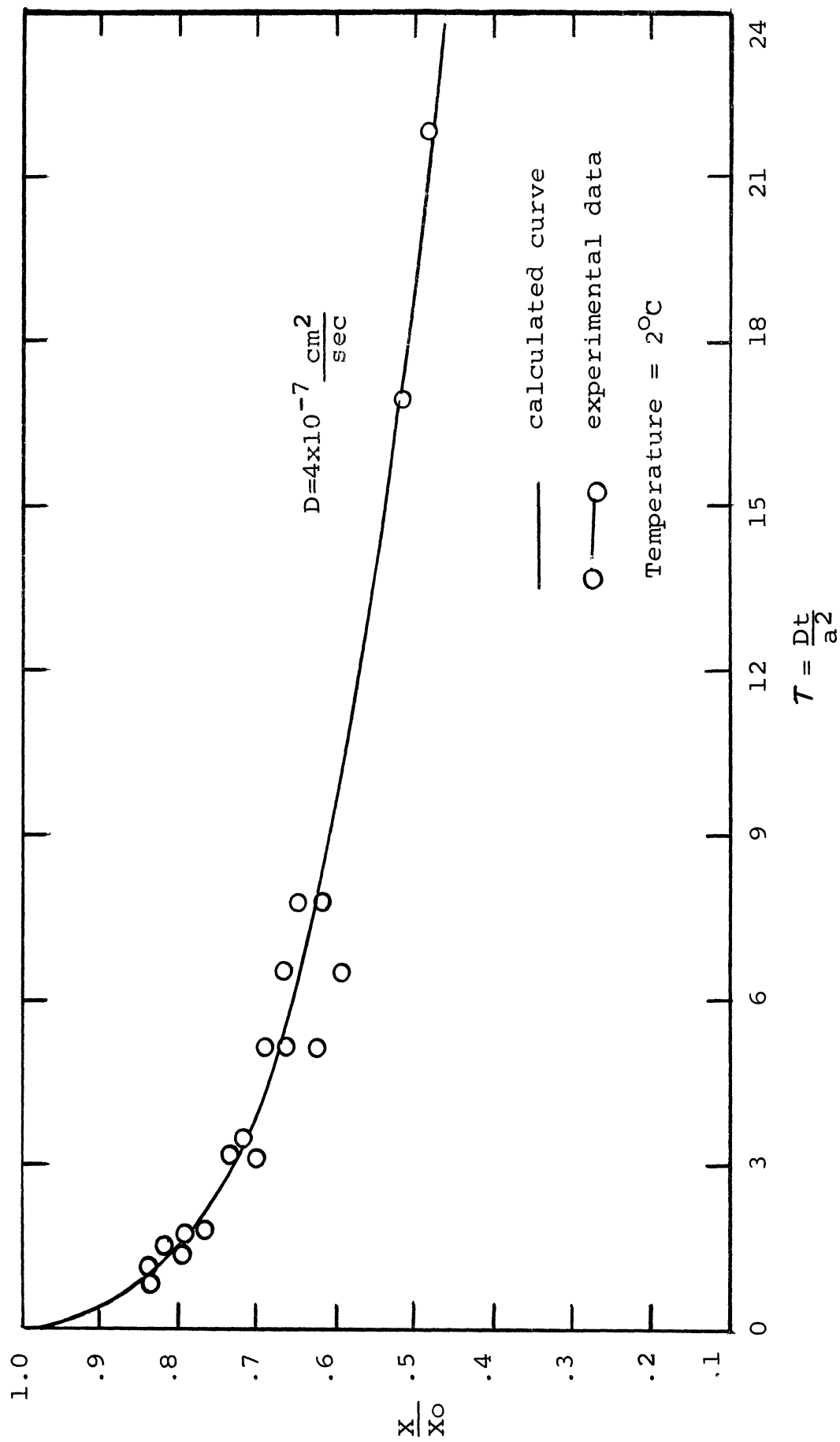
Figure III-14. Finite-Bath Rate of Adsorption for HCl at 2°C.
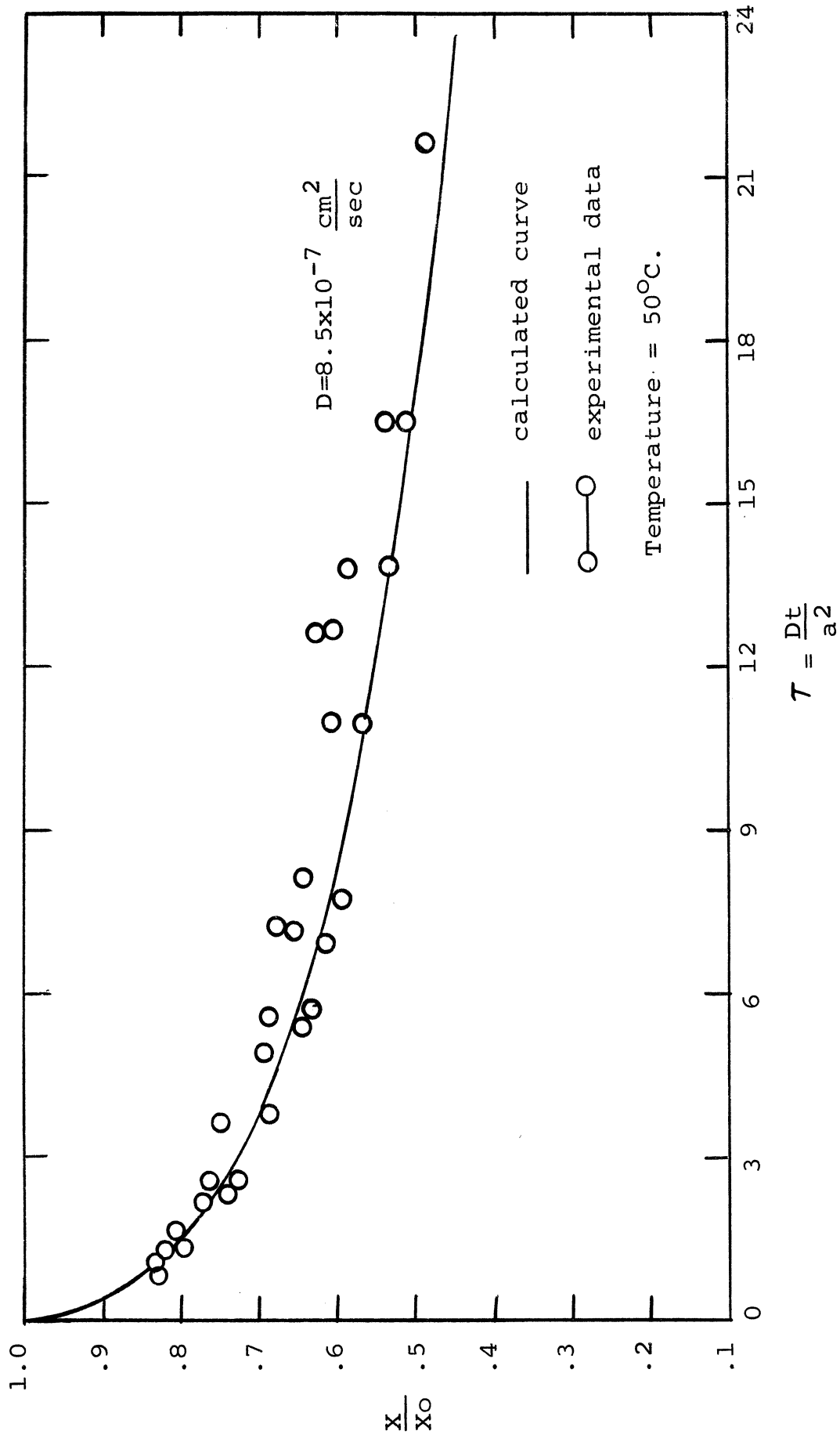
Figure III-15. Finite-Bath Rate of Adsorption for HCl at 50°C.

Arrhenius equation, which, in logarithmic form is

$$\log \frac{D_2}{D_1} = \frac{E_a}{2.303R} \frac{T_2 - T_1}{T_1 \quad T_2} \qquad \qquad III\text{-}8$$

In Equation III-8, D is the diffusion coefficient in cm^2/sec;
E_a is the activation energy in $cal/mole\text{-}^{\circ}K$; R is the ideal gas
constant ($1.987 \ cal/mole\text{-}^{\circ}K$); and, T is the temperature on the
Kelvin scale. A value of $E_a = -(1.8 \ to \ 2.5) \ kcal/mole\text{-}^{\circ}K$,
was calculated from the diffusion coefficients listed in Table
III-5, in line with values expected for electrolyte diffusion
(34).

The data shown in Figure III-13 for the equilibrium
studies suggest that the process goes from exothermic at low
equilibrium activities to endothermic at high equilibrium activ-
ities. The differences between isotherms is not very signifi-
cant and without further research to verify the suggested
trends, an elaborate explanation is not warranted. Zettlemoyer
and Narayan (76) have shown, though, that the heats of adsorp-
tion of electrical double layer formation are endothermic.
An endothermic reaction is indicated by the higher equilibrium
activity data, and this indication can be taken in support of
physical adsorption of acid on the carbon surface.

SUMMARY

Garten and Weiss (20) have postulated that strong acids
react with chromene functional groups on the active carbon sur-
face as shown in Figure II-5.

This reaction can be used to explain some of the

observations of the present work. The carbonium ion has a high affinity for the OH^- ion, as illustrated by a $pK_b = 11$ (58). The carbonium salt will thus hydrolyze readily as given in Figure II-6. This reaction would account for the fact that carbon which had been contacted with 1+1 HCl for five days could be washed continuously with distilled water over a period of three months to remove essentially all of the sorbed acid. This is illustrated by the fact that essentially the same isotherm was obtained for 1+1 HCl-treated carbon as for untreated carbon.

The possibility that diffusion of oxygen into the pore is rate limiting has been ruled out because solutions used were exposed to the atmosphere, and oxygen was found to be rate limiting only when the partial pressure is less than 20 mm Hg. (8).

It has been noticed also that only a small fraction of the total amount of sorbed acid could be removed by washing with water which contained the salt of the acid in the same concentration as was present in the solution with which the carbon was equilibrated originally. This observation suggests that the conjugate anion is tightly held, which is consistent with the findings of others (22, 48, 72).

It would appear, however, that not all of the acid is taken up by means of the chromene reaction, since 50% to 60% of the acid sorbed at an equilibrium pH of approximately 3.5 can be displaced by adding phenol to the solution in sufficient quantity to bring the phenol concentration to approximately

0.1 $\underline{M}$ at equilibrium. This percentage, at least, of the acid originally sorbed is evidently taken up as a displaceable entity. Garten and Weiss (22) have show that the amount of acid which can be displaced by a strongly adsorbing organic molecule is dependent upon the extent of oxidation' of the active carbon during manufacture. The nature of reactions at the surface therefore depends upon the method of preparation. It becomes difficult to make any generalized conclusions regarding the displaceable character of the sorbed acids. It should be noted that some of the sorbed acid may be in pores which are not readily accessible to the organic molecule, and thus are not displaced by the latter.

There is not sufficient evidence to conclusively prove or disprove one or two definite mechanisms for reaction of acid with active carbon. However, the chromene-acid reaction as herein described appears to be a logical and significant part of the overall reaction. Physical, electrostatic, or other mechanisms for acid sorption probably account for the remainer of the reaction.

Regardless of the actual mechanism, the rate and extent of the acid reaction with active carbon are important factors, and the information obtained about these factors should prove useful for interpreting sorption data of various kinds. In addition, systematic sorption studies should also lead ultimately to a better understanding of the nature of the acid-carbon reaction.

IV. ADSORPTION OF PHENOL AND 4-NITROPHENOL

EXPERIMENTAL

CARBON

The active carbon used for these studies was the 273-μ coconut-shell carbon, the same type as was used for the majority of the studies reported in Chapter III. The carbon was prepared in the same manner as described in Chapter III.

SOLUTE PROPERTIES AND ANALYSIS

The solutes used for these studies, phenol and 4-nitrophenol (PNP), were selected because they are typical pollutants which can be studied as both neutral and negative species, and can be easily analyzed in aqueous solution. Phenol is found in many wastes, especially steel mill wastes (49), and 4-nitrophenol is a typical pesticide (67). The phenol used was obtained as analytical reagent grade in the crystalline form. Solution concentration analyses were performed on a Beckman DU Spectrophotometer at the wave length of maximum adsorption, 270 mμ. The molar adsorptivity at this wave length was experimentally determined to be 1540 liter/mole-cm. Since the pK$_a$ for phenol is 9.9 (8), all concentrations were measured at a pH below 6, thereby assuring that only the neutral species was present. Glass-distilled water was used for all experiments and for preparation of all stock solutions.

71

The solubility limit of the neutral phenol species was determined to be about 0.8 $\underline{M}$. The anion solubility was not determined, but it is very soluble.

The 4-nitrophenol was obtained as reagent grade in powdered form. Spectrophotometric analyses for concentration were performed at a wave length of 226 mμ. The molar absorptivity at this wave length of peak absorbance is 6580 liters/mole-cm.. This molar adsorptivity applies only to the neutral species; thus all analyses were performed at a pH less than 4, assuring that essentially all species were present in the neutral form since the pK_a is 7.0 (8). The solubility of the neutral species is 0.1 $\underline{M}$ while that for the anionic species is 0.2 $\underline{M}$, as determined experimentally. Glass-distilled water was again used for all experiments.

EQUILIBRIA STUDIES

Equilibria studies were performed by first preparing 3 liters of solution at the desired pH, salt concentration, solute concentration and temperature. Then, 100 ml portions of this solution were pipeted into a 125-ml, French-Square, wide-mouth bottle which contained a carefully measured quantity of carbon. The usual procedure was to fill 20 bottles in this manner, along with 4 bottles which contained no carbon for use as blanks. The weights of carbon added to these bottles were carefully calculated to give as wide a range of equilibria concentrations as possible for a given initial concentration. The bottles were then shaken on either a

reciprocating or a tumbling shaker for a period of 3 to 4 weeks which was experimentally determined as the time required for equilibrium. After the shaking period, the concentration of each bottle was analyzed. The points in the isotherm could then be calculated from the equation,

$$S = \frac{(C_o - C_{eq})}{m} V \qquad \qquad IV-1$$

where C_o is the initial concentration in moles per liter and is taken to be the average concentration of the 4 blanks, C_{eq} is the equilibrium concentration in moles per liter for a given bottle, V is the volume of solution contained in the bottle in liters, m is the weight of carbon contained in the bottle, and S is the solute removed by the carbon in moles per gram. S could then be plotted against C_{eq} to yield what is called the adsorption isotherm. If the data showed too much scatter, the procedure was repeated. The final pH of each bottle was also measured and compared with the initial pH in order to determine if too large a pH change had occurred for the data to be valid. The data was discarded if a change greater than 0.2 of a pH unit occurred in the range of pH=4 to 10, and 0.1 of a unit for pH less than 4 and greater than 10.

KINETIC STUDIES

Rate studies were performed by preparing 3 liters of solution at the desired initial solute concentration, pH, salt concentration and temperature. Temperature control of the system was accomplished with a water bath except at room temperature. The system was stirred with a motor-driven,

polyethylene stirring blade. After carefully measuring the initial concentration of solute, C_o, a known quantity of carbon was added to the system. The solute concentration was then measured several times with respect to time after addition of the carbon. The stirring rate was such that the carbon was well-suspended at all times. The concentration of the system was analyzed by turning off the stirring motor to allow the carbon to settle just below the surface of the water, pipetting out the sample, diluting and making the necessary pH adjustment, and measuring the absorbance spectrophotometrically. The stirring motor was turned off for 15 to 20 seconds while each sample was being removed. A study was carried out to determine the effect of this shut-off time on the rate curve, and it was found that essentially identical rate curves resulted for 2 systems, one of which was analyzed more times than is necessary to determine a good rate curve. The pH of the system was analyzed after the test was over to determine if an excessive pH change had occurred during the run, and if it had, the data was discarded. The rate data taken in this manner was found to be very reproducible. The data was generally analyzed by means of a S_t vs. $t^{\frac{1}{2}}$ plot where S_t is given by Equation IV-1 with C_{eq} replaced by C_t, the concentration at time, t.

RESULTS AND DISCUSSION

PHENOL AND 4-NITROPHENOL ADSORPTION EQUILIBRIA

The first system studied in depth consisted of distilled

water, phenol and carbon. The initial pH of this system was 5.6 and the deviation from neutrality was probably due to atmospheric CO_2 dissolved in the distilled water. The results of this study are shown in a log-log plot in Figure IV-1.

An attempt was made to formulate these data in terms of the Brunauer-Emmett-Teller (BET) (10) and Langmuir (1) equilibrium adsorption equations. It was impossible, however, to get either of these equations to fit any appreciable range of these data, but approximations could be made to individual sections of these data. The problem seemed to be caused by a heterogeneous surface which resulted in a constantly changing heat of adsorption (2, 27, 28, 55). This was shown by an attempt to plot these data according to the linear relationship,

$$\frac{C}{S} = \frac{1}{S_m b} + \frac{C}{S} \qquad\qquad IV-2$$

derived from the Langmuir equation,

$$S = \frac{S_m b C}{1 + bC} \qquad\qquad IV-3$$

where C is the equilibrium concentration in moles per liter, S is the equilibrium concentration of the adsorbed phase in moles per gram, S_m is the maximum value which S can attain, and b is a constant in liters per mole indicative of the energy of adsorption. The constant, b, is defined by the equation,

$$b = b' e^{Q/RT} \qquad\qquad IV-4$$

where b is a constant and Q, the heat of adsorption, is constant. When equation IV-2 is used, a straight line plot of
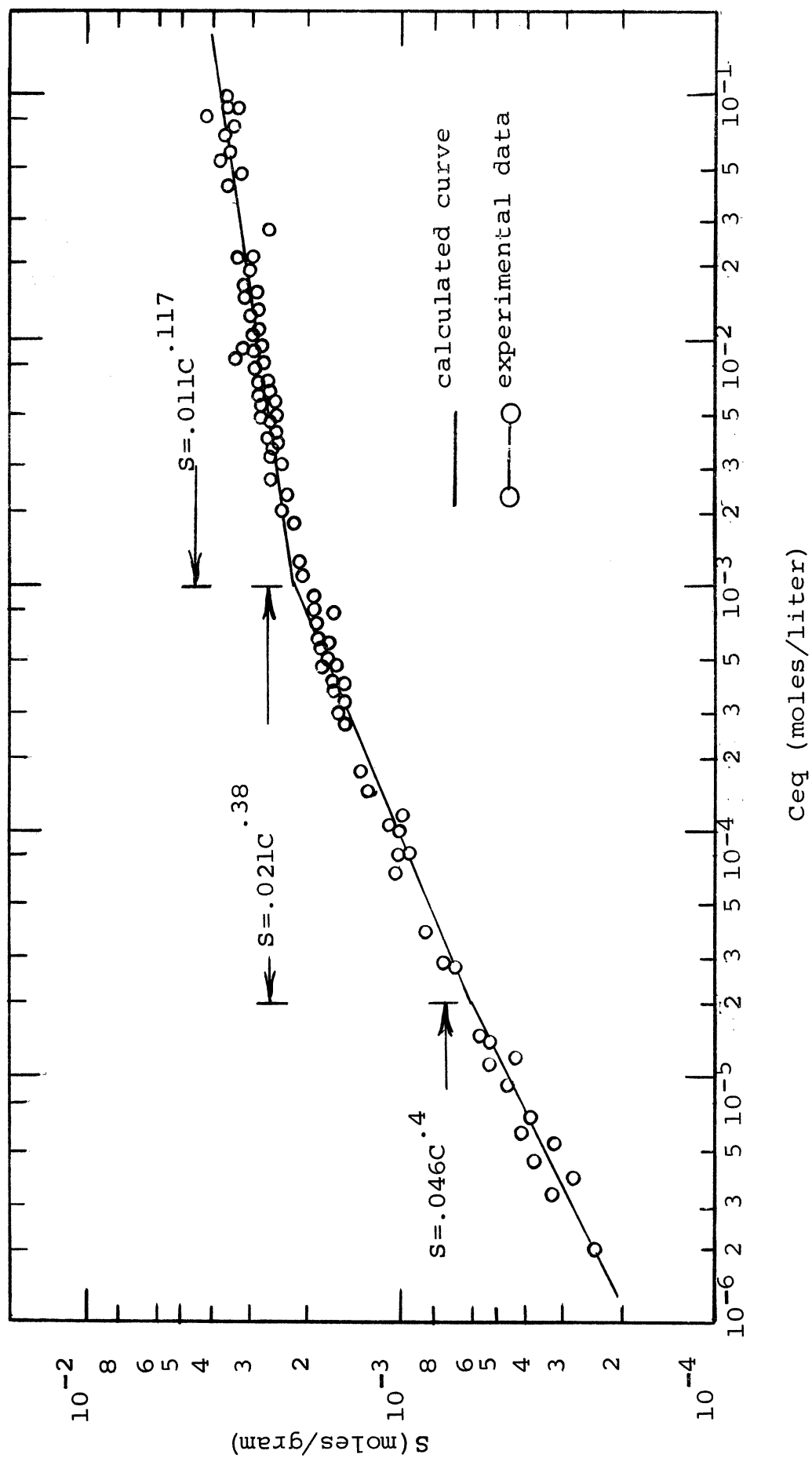
Figure IV-1. Phenol Equilibria with Freundlich Equations

the data does not result as it should if the assumptions of the model apply, but a curved line does indicating a changing value for b, and therefore for Q, and S_m.

It is possible, though, to fit major concentration ranges of the data with the empirical Freundlich equation,

$$S = FC^N \ , \ N < 1 \qquad \qquad \text{IV-5}$$

The constants F and N can be determined by log-log plots of the data. It is interesting to note that if an exponential distribution is assumed for the heat of adsorption,

$$f(Q) = \alpha e^{-Q/RT} \qquad \qquad \text{IV-6}$$

and if the variation in `b with surface coverage is attributed entirely to the variation in heat of adsorption, then

$$S(C,T) = \int_0^\infty S(b,C,T) \ f(b) \ db \qquad \qquad \text{IV-7}$$

where $S(C,T)$ is the adsorption function, $S(b,C,T)$ is the Langmuir equation and $f(b)$ is the distribution function for b, becomes

$$S(C,T) = FC^N \ , \ N < 1 \qquad \qquad \text{IV-8}$$

which is equation IV-5, the Freundlich equation (1). F in this case is given by

$$F = \alpha RT \ \frac{1}{N} \ b' \qquad \qquad \text{IV-9}$$

There is no assurance that the above derivation is unique. Therefore, that the surface is heterogeneous with respect to site energy is only suggested by the fact that experimental data conforms to the Freundlich equation, but is by no means proven (1).

One of the problems involved in using the Freundlich equation is that it does not predict an ultimate capacity for

the adsorbent. It is apparent upon examining Figure IV-1 that the slope approaches the horizontal, indicating that such an ultimate capacity, approximately 4×10^{-3} moles per gram in this case, does exist. A complicating factor which also could cause a changing slope is that the distribution function for the heat of adsorption is different than the exponential function postulated.

For purposes of comparison, the phenol equilibrium data was approximated with the Langmuir equation, Equation IV-3, for a "high" and a "low" concentration range. The constants for the Langmuir equation were determined with Equation IV-3. These equations are plotted together with the experimental data in Figure IV-2. The increase in S_m, 1.15×10^{-3} to 2.84×10^{-3} moles per gram, and decrease in b, 6.7×10^4 to 2.93×10^3 liters per mole, upon going from the low concentration to the high concentration approximation is especially noteworthy.

The equilibria data shown in Figure IV-3 are for the 4-nitrophenol-distilled water-carbon system. The pH of this system was lowered slightly to 4.0 with HCl in order to insure that essentially all solute species were present in the neutral form. This system is assumed to be comparable to the phenol system studied above. The two Freundlich equation approximations to the data are shown in Figure IV-3.

The Langmuir equation seemed to fit the 4-nitrophenol adsorption data much better than the phenol. This equation, as determined from Equation IV-2, is shown together with the experimental data in Figure IV-4. Evidently the heat of
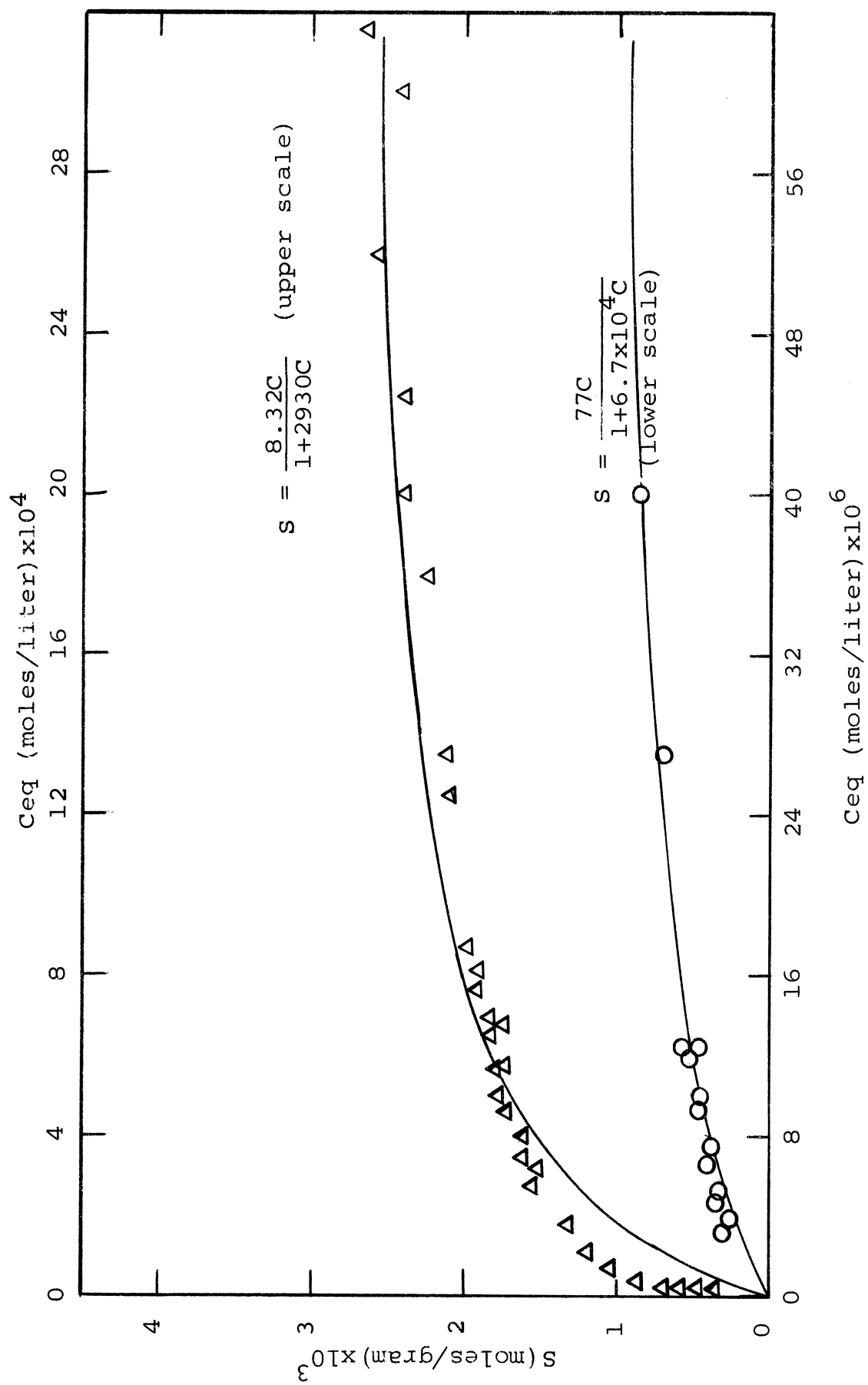
Figure IV-2. Phenol Equilibria with Langmuir Equations

Ceq (moles/liter)
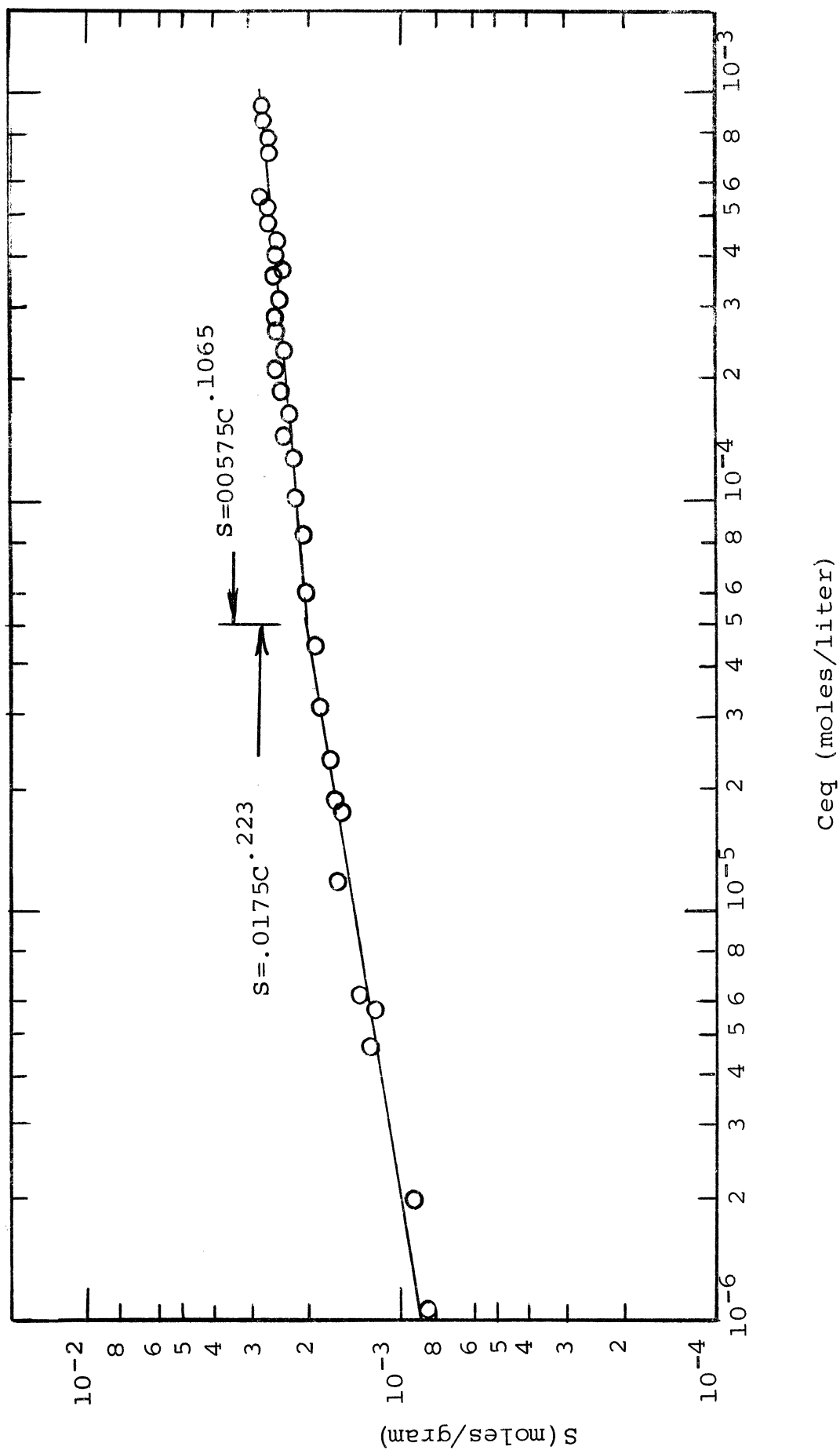
Figure IV-3. 4-Nitrophenol Equilibria with Freundlich Equations

$$s = \frac{71.4C}{1+24,700C}$$

Ceq (moles/liter) x10^4

S (moles/gram) x10^4
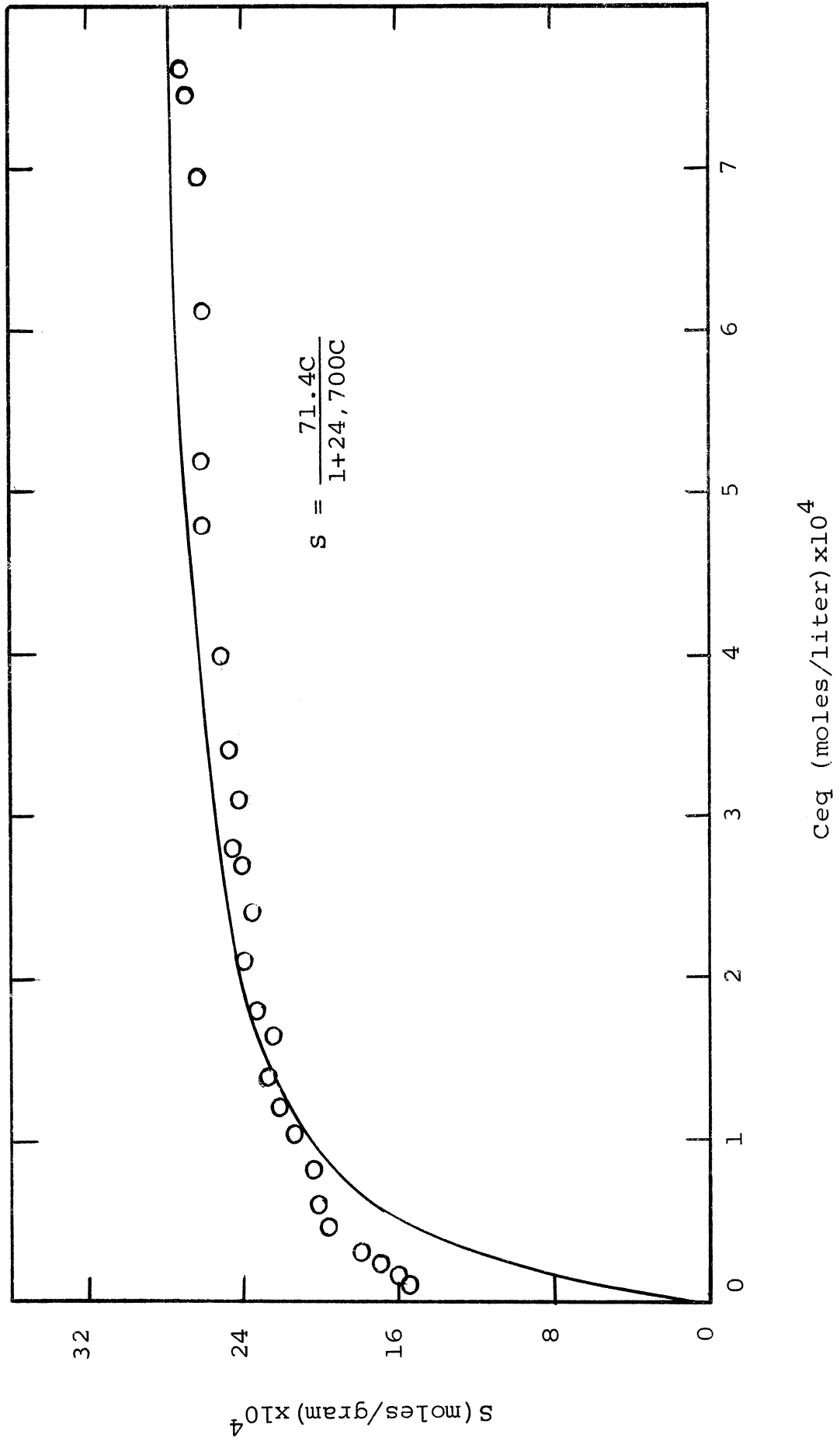
Figure IV-4.   4-Nitrophenol Equilibria with Langmuir Isotherms

adsorption does not change as much with surface coverage for 4-nitrophenol adsorption at this pH as it does for phenol. This could be due to the fact that 4-nitrophenol is adsorbed at different sites, sites of more uniform energy than phenol, or that the effects of an increasing heat of interaction between sorbate molecules with surface coverage is compensating for the effect of a decreasing heat of adsorption as described by Brunauer (9).

It is informative also to compare the adsorption isotherms of phenol and 4-nitrophenol on the same plot. This can best be done by plotting the moles of sorbate removed per gram of carbon, S, vs. the reduced equilibrium concentration, C/C_S, after Hansen and Craig (29). C_S is the maximum possible solution concentration as limited by solubility. This reduced concentration has the effect of eliminating differences in equilibrium adsorption characteristics due to solubility. Differences in equilibrium adsorption curves which are plotted in this manner should then be due to the nature of the adsorption bond formed, or to the fact that adsorption occurs at different types of sites on the adsorbent surface. The quantity of phenol and 4-nitrophenol is plotted as a function of C/C_S in Figure IV-5. The experimental data is not shown; rather, the normalized curves of the data shown in Figures IV-1 and IV-3 are used for this purpose. It can be seen from this plot that in the lower C/C_S range, more 4-nitrophenol is adsorbed than phenol. A determination of Langmuir "b" values for the same concentration range, 1×10^{-4} to 1×10^{-3} $\underline{M}$, revealed that b for
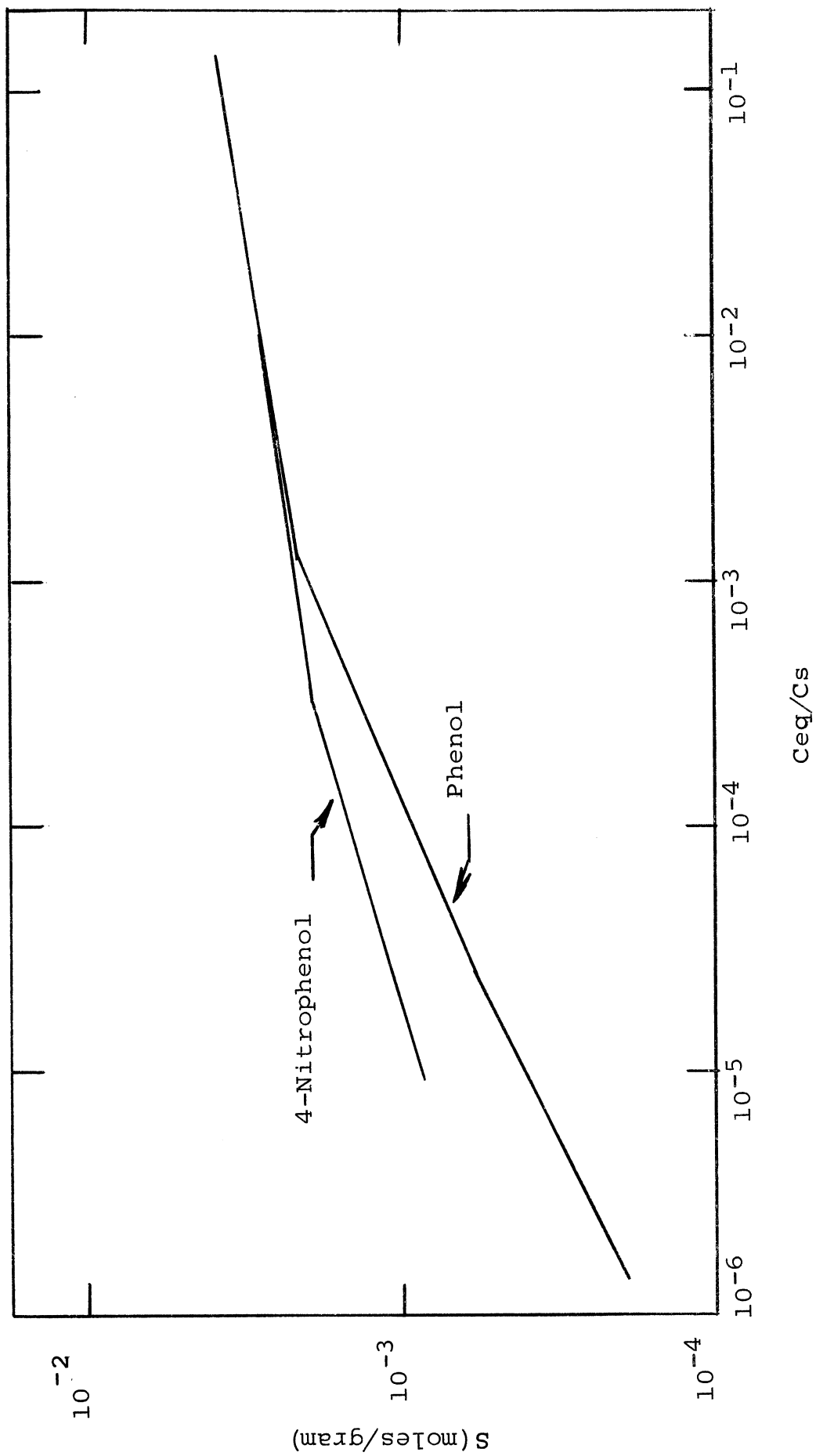
Figure IV-5. Phenol and 4-Nitrophenol Equilibria as a
Function of Reduced Concentration

phenol is 15,600 liters per mole while b for 4-nitrophenol is 24,700 liters per mole, indicating that phenol has a lower heat of adsorption. This higher heat of adsorption for 4-nitrophenol could possibly be due to adsorption taking place at sites where the nitro group can contribute significantly to the heat of adsorption. At high C/C_S, the curves show the same capacity for each solute; the solute molecules are evidently packed unto the surface in such a way that the nitro group cannot contribute to the energy of adsorption, and in such a way that the larger molecular volume of the nitrophenol does not affect the number of molecules adsorbed. Alternatively, the equilibrium concentration is high enough to cause adsorption at every site, regardless of the adsorption energy for the adsorbate.

PHENOL REVERSIBILITY

Reversibility studies were performed on the phenol system in order to characterize more fully the nature of adsorption by active carbon. In one 3-liter, distilled water-phenol system, 5 grams of carbon were brought to equilibrium at a phenol concentration of 5×10^{-3} $\underline{M}$. In another 3-liter, distilled water-phenol system, 1 gram of carbon was brought to equilibrium as a concentration of 4×10^{-3} $\underline{M}$. The carbon was kept in suspension at all times with a motor driven, polyethylene stirring blade. Every 3 to 5 days the carbon was allowed to settle to the bottom of the reaction vessel and 2.5 liters of the equilibrated solution was decanted and replaced with distilled water. Each time the new surface concentration could be calculated and plotted as a function of equilibrium concentration. This

procedure was repeated for a period of 5 months. The results are shown in Figure IV-6 with the normalized adsorption curve reproduced from Figure IV-1 for comparison.

Figure IV-6 shows the hysteresis effect which Adamson (1) describes as being due to "ink bottle" pores. These pores have a narrow entrance but a large interior. A high concentration of adsorbate is required to force phenol molecule into the pore, but once the pore is filled, the solute is "trapped" inside the pore as solution concentration is decreased in the manner described above. The difference between the two desorption curves can be interpreted as being due to the fact that the higher initial equilibrium concentration for the 5 gram system results in more of these types of pores being filled. In each case, only about 50% of the phenol can be desorbed from the carbon.

An alternative explanation is that the "ink bottle" pores are not entirely responsible for the hysteresis effect, but that the carbon surface catalyzes the breakdown of at least some of the phenol. After 5 months of performing the desorption experiment, the u.v. spectrum of the desorbed species was compared with that of a freshly prepared phenol solution and no significant differences were noted. It should be noted, though, that if the decomposition product was CO_2, it would not have been observed by this means. The small phenol heat of adsorption reported below does not support the decomposition hypothesis, however. There does not seem to be sufficient evidence to prove either explanation, but the former is more
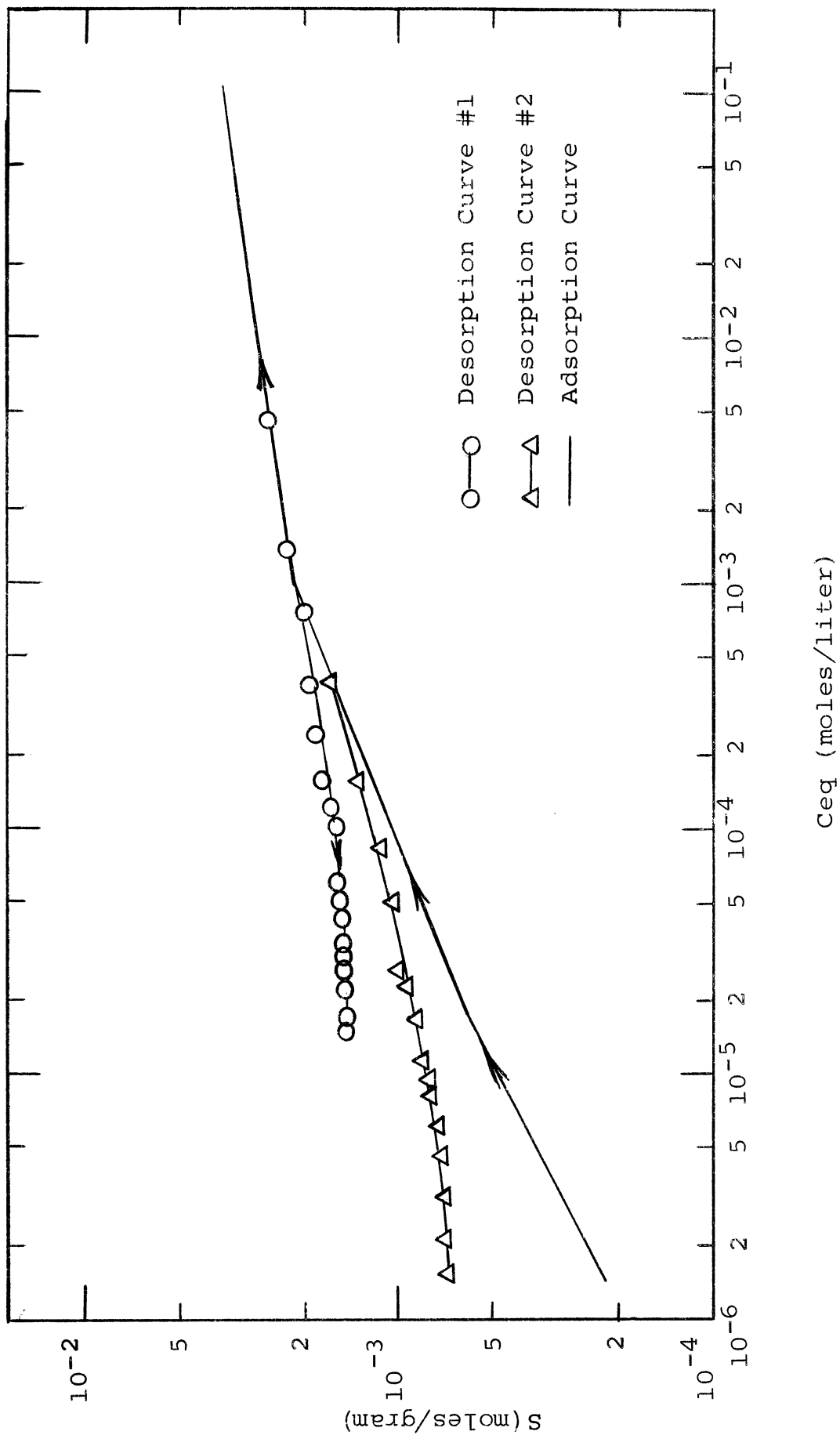
Figure IV-6. Phenol Desorption Isotherms

strongly indicated than the latter.

TEMPERATURE DEPENDENCE OF EQUILIBRIA

Equilibria studies were performed on the phenol-distilled water-carbon system, pH 5.6, at temperatures of 11° and 37° C., in addition to the room temperature studies at 25° C. already reported. The results are illustrated by means of a log-log plot in Figure IV-7. The isosteric heat of adsorption, q_{st}, and the heat of adsorption as given by the Langmuir adsorption model, Q, were both calculated from the data shown.

The isosteric heat of adsorption is defined (55) as,

$$q_{st} = RT^2 \left(\frac{\partial \ln C}{\partial T} \right)_s \qquad \text{IV-10}$$

The isosteric heat is actually a differential heat of adsorption and can be described as the energy necessary to remove an adsorbed molecule from its adsorbed state, including the attractive forces of its adsorbed neighbors, to an infinite distance from the surface, plus energy equivalent to the degrees of freedom of the "free" molecule in excess of those in the adsorbed state (55). At a surface coverage of 2.0×10^{-3} moles of phenol per gram of carbon, q_{st} is calculated as 1.8 kcal./mole-^{O}K for the data shown in Figure IV-7.

The heat of adsorption, Q, can also be calculated from the Langmuir equations by first determining the Langmuir equation parameters for the low concentration range of the experimental data and then by using the b values in Equation IV-4.
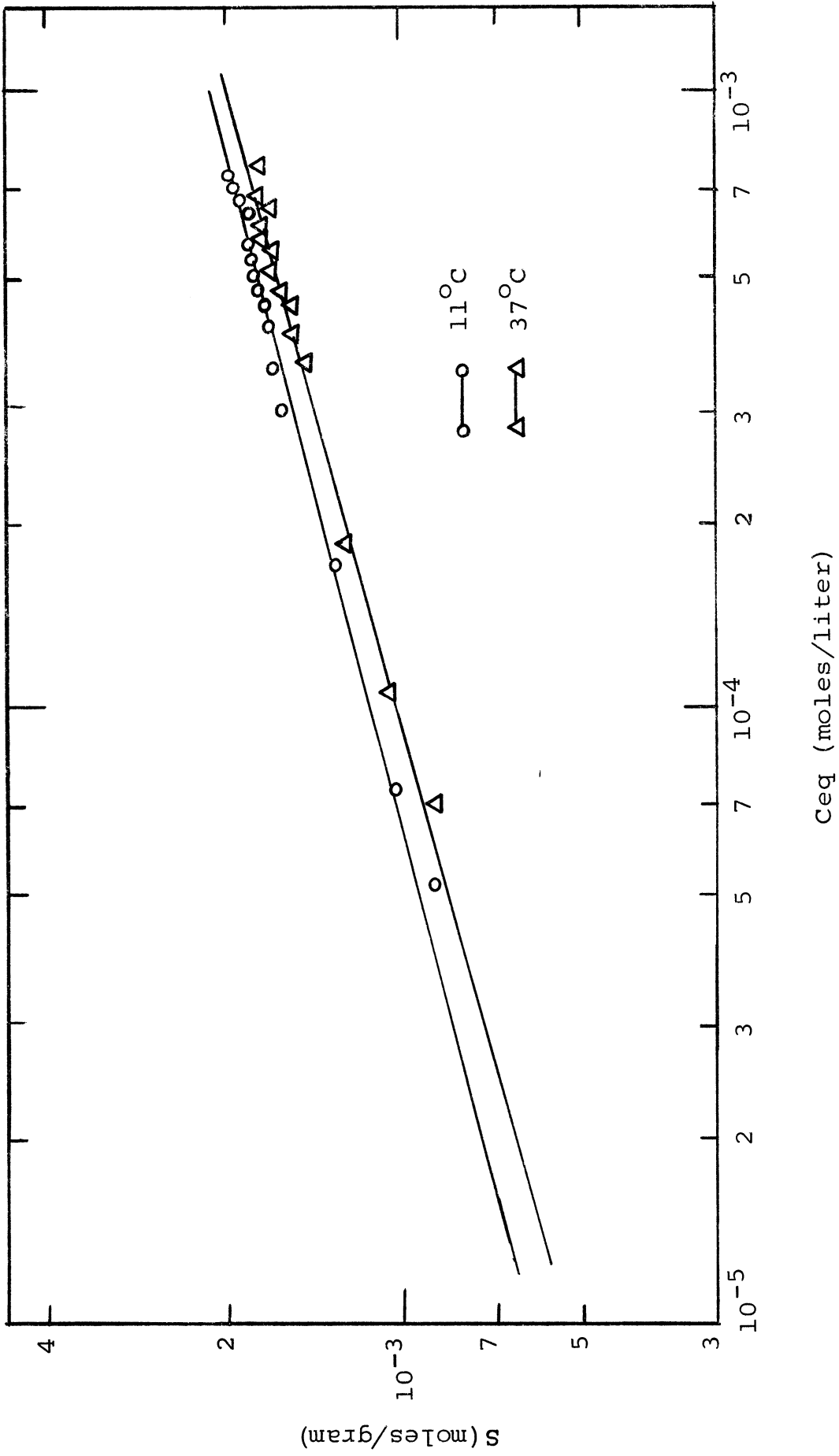
Figure IV-7. Phenol Equilibria at Different Temperatures

The Langmuir equation constants are given in Table IV-1. The heat of adsorption, Q, using only the b values for 11° and 37° C. is 0.8 kcal./mole-^{O}K.

TABLE IV-1

Langmuir Parameters for Phenol and 4-Nitrophenol
Adsorption at Different Temperatures

Temperature ^{O}C.	Langmuir Parameters		Solute
	$S_m x10^3$	$bx10^{-3}$	
11	1.75	22.7	phenol
25	1.70	21.0	phenol
37	1.65	20.2	phenol
11	3.07	26.3	4-nitrophenol
25	2.89	24.7	4-nitrophenol
37	2.76	21.3	4-nitrophenol

The Langmuir adsorption model is based on the assumption that Q is constant throughout the adsorption process, and thus there is no valid point of comparison between Q and q_{st}. It is interesting to note, though, the values which the data predict for each, especially since the Langmuir equations are so often used.

Equilibrium studies were performed at the same temperatures for the 4-nitrophenol-distilled water-carbon system, and the data for 11° and 37^OC is given in Figure IV-8 along with the Freundlich equations for the data. The isosteric heat of adsorption, calculated this time at S = 2.0 x 10^{-3} moles per
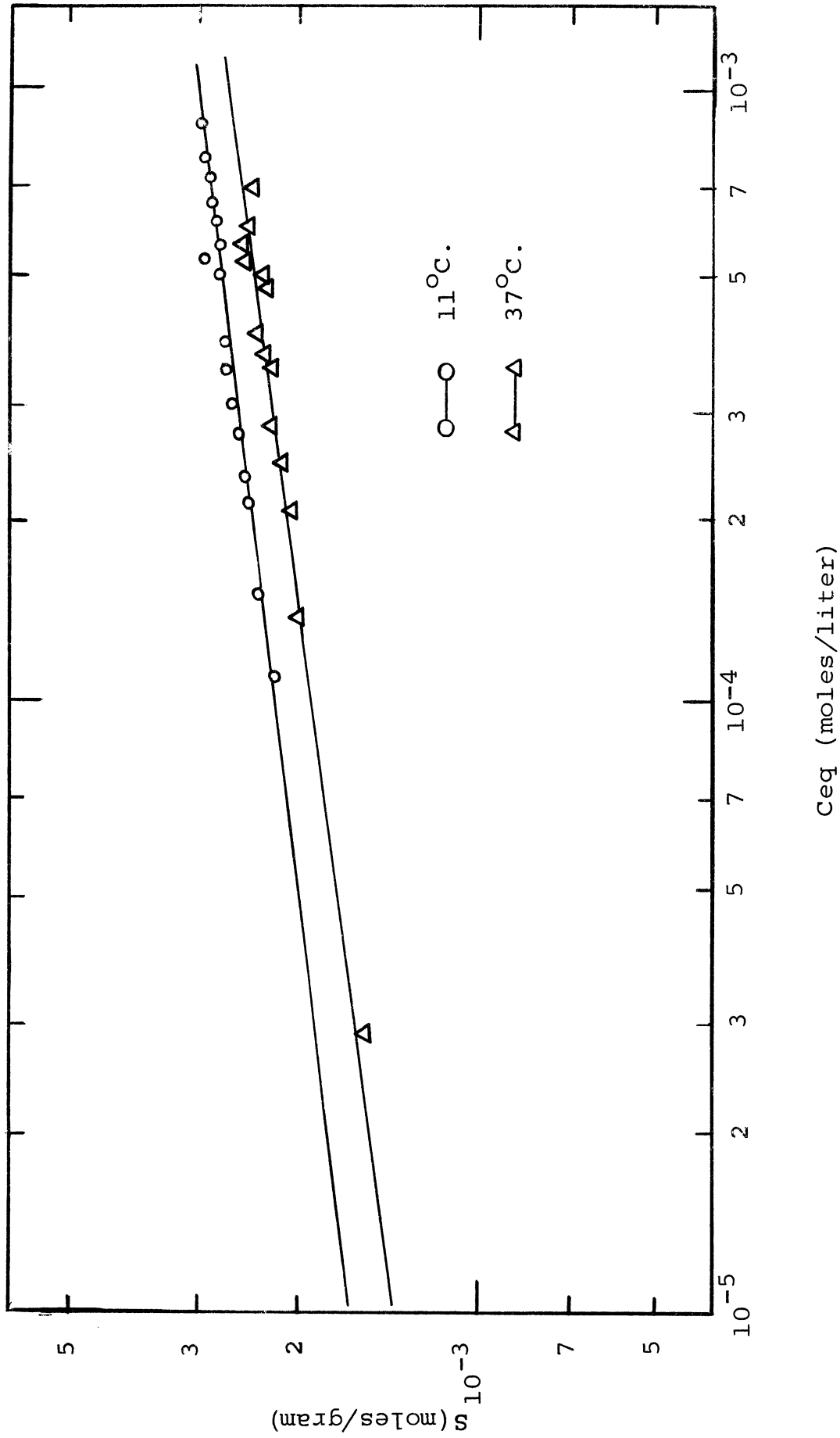
Figure IV-8. 4-Nitrophenol Equilibria at Different Temperatures

gram, is q_{st} = 5.6 kcal/mole-^OK. For comparison, the Langmuir

equations were again determined, and the constants are shown

in Table IV-1. Q, as calculated from these constants, is 1.5

kcal/mole-^OK. By comparing the values of Q and q_{st} for both

phenol and 4-nitrophenol, it can be seen that the heat of

adsorption for 4-nitrophenol is about twice as large as that

for phenol regardless of whether Q or q_{st} is used for the com-

parison. These heats of adsorption all fall within the range

indicative of physical adsorption (75).

PHENOL AND 4-NITROPHENOL ADSORPTION RATES

The rate-limiting step for adsorption of phenol and 4-

nitrophenol was assumed to be intraparticle pore diffusion

as it was for the acid adsorption study reported in Chapter III.

The batch systems used for the rate studies were well mixed

and the carbon was kept in suspension at all times. The stir-

ring rate was well above the 500 RPM Weber (66) found was

necessary to make the rate of adsorption independent of the

rate of stirring. Based on the assumption that pore diffusion

is limiting, the diffusion model described and used in Chapter

III is applicable. It should be noted, however, that in this

case, concentration and activity are equivalent. The computer

program is also the same and is given in Appendix I. The equili-

brium equation used for all rate curve calculations was the

Freundlich question, which fit the experimental data best for

equilibrium concentrations less than the initial concentration

of the rate study. The carbon dosage used for all phenol studies

was 0.135 grams per liter and the initial concentration, C_o, was 6.9×10^{-5} $\underline{M}$ unless otherwise noted. The carbon dosage for the 4-nitrophenol system was 0.320 grams per liter and the initial concentration was 1×10^{-4} $\underline{M}$ unless otherwise noted. The carbon dosage of 0.135 grams per liter corresponds to an "A", or volume served per particle, of 0.0593 cm^3, and 0.320 grams per liter to an "A" of 0.025 cm^3.

The calculated rate curves and experimental data for phenol and 4-nitrophenol are shown in Figures IV-9 and IV-10, respectively. In each case, the experimental data shown are a composite of two or more experiments. The ordinate for these plots is C/Co, or the solute concentration at any time, t, divided by the initial concentration and the abcissa is the dimensionless time parameter, $\mathcal{T}$, which is given by D^t/a^2. D in this case is the pore diffusion coefficient and a is the particle radius, 0.01365 cm. The D used to plot the experimental data was arbitrarily selected as the one which made the data correspond to the calculated curve at the time and C/Co corresponding to one-half completion of the adsorption process. The system parameters and the calculated diffusion coefficients are given in Table IV-2. Included also in this table is the range of diffusion coefficients which would make all data correspond to the calculated curve.
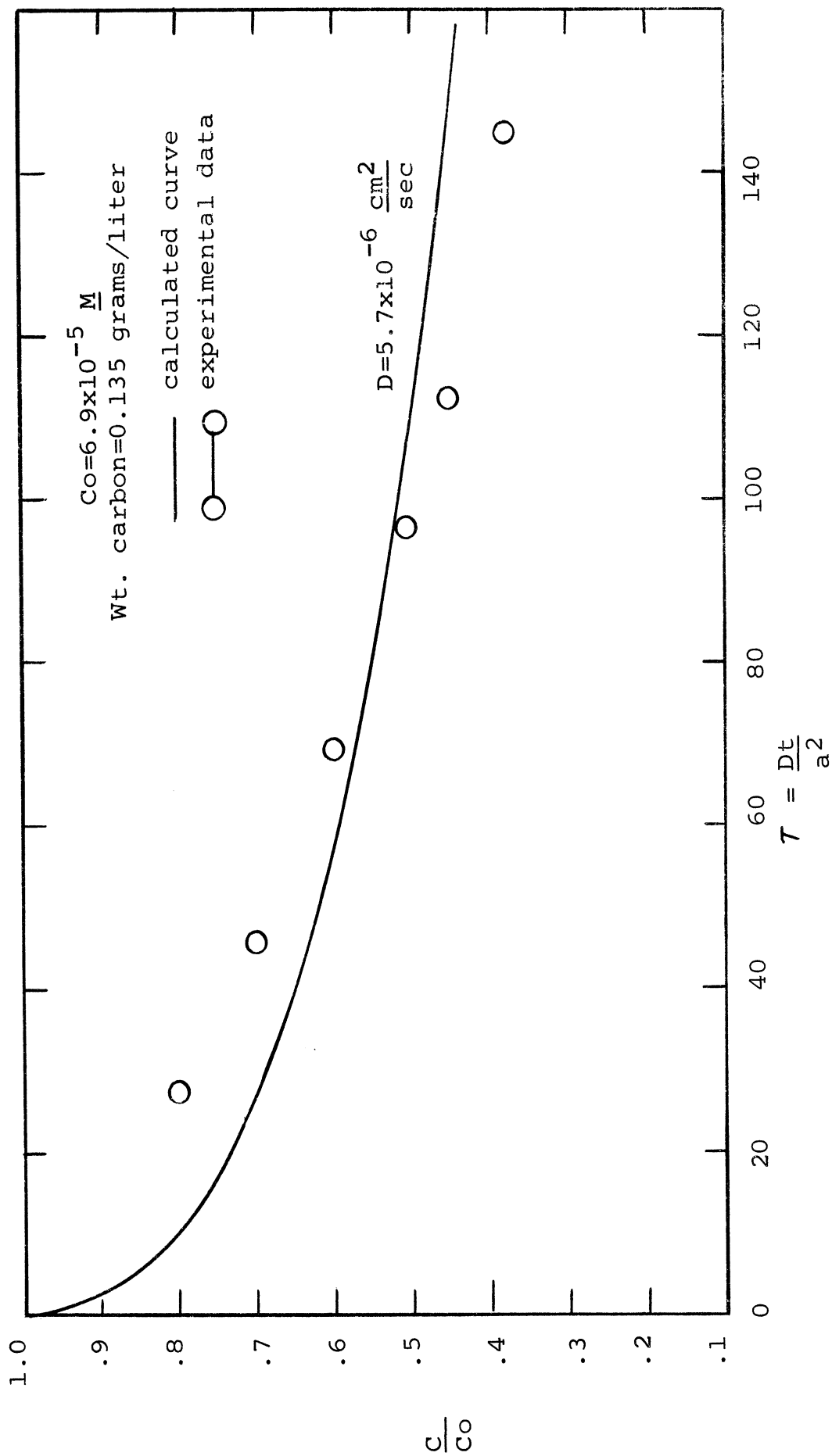
Figure IV-9. Phenol Rate of Adsorption
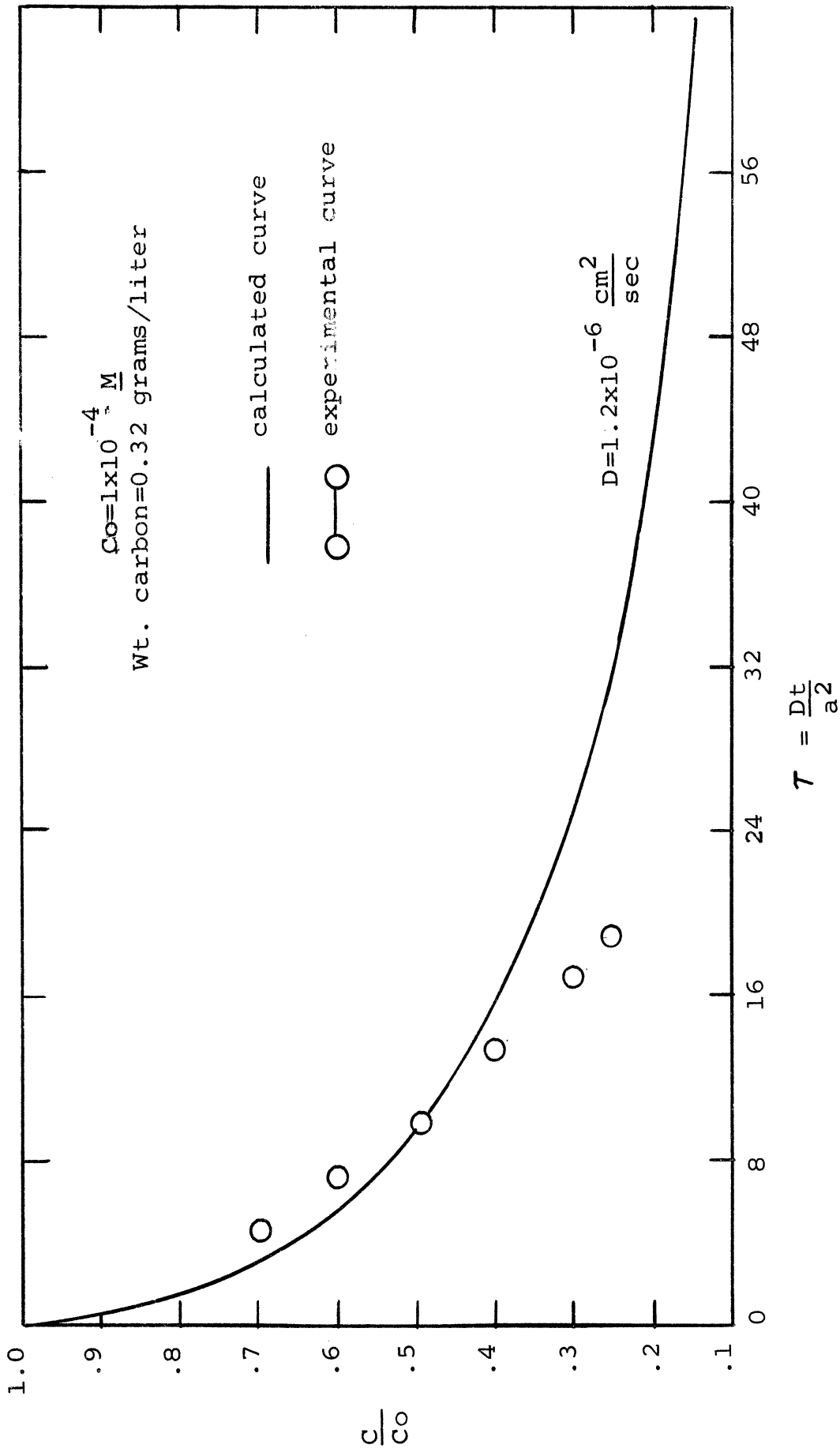
Figure IV-10. 4-Nitrophenol Rate of Adsorption

95

TABLE IV-2

Diffusion Coefficients for Phenol and 4-Nitrophenol

Solute	Freundlich Parameters		D $(cm^2/sec) \times 10^6$
	F	N	
Phenol	.046	.40	5.7 (2.0 - 10.6)
4-Nitrophenol	.0175	.223	1.2 (0.8 - 2.0)

As can be noted from Figures IV-9 and IV-10, the calculated rate curves do not correspond very well with the experimental data. The diffusion coefficient range calculated by making all data correspond to the theoretical curve increases with increasing time of reaction, with the effect being much more significant for the phenol system than for the 4-nitrophenol system. The fact that a constant diffusion coefficient was not found is contrary to the assumption made in developing the model, and is also contrary to the results obtained in Chapter III for acid adsorption rates.

The effect of surface diffusion on the walls of the pores was examined in an attempt to determine the reason for the differences between experimental and calculated curves. This was done by first assuming that only surface diffusion was important and that the mass transfer contribution from pore diffusion was negligible. This could easily be done by replacing the dimensionless concentration term "x" in Equation III-4 by the dimensionless surface concentration term "s" to yield,

$$\frac{\partial c}{\partial T} = \frac{1}{\rho^2} \frac{\partial}{\partial \rho}\left(\rho^2 \frac{\partial s}{\partial \rho}\right) - \frac{\partial s}{\partial T} \qquad\qquad \text{IV-11}$$

This equation could then be solved by the computer in the same manner as before, subject to the same boundary conditions as before. A curve similar to that shown in Figure IV-9 was calculated for the phenol system and from it the surface diffusion coefficient could be calculated. D_s for the same experimental data shown in Figure IV-9 was determined to be 5 to 15 x 10^{-10} cm^2/sec. Because this variation is about the same as the variation in the pore diffusion coefficient calculated above, it was decided that this procedure was not a good alternative to calculating the pore diffusion coefficient.

Another alternative was to combine the effects of both pore diffusion and surface diffusion in one model. This has been done by others (7), but the solution arrived at for the phenol system following their procedure did not yield a unique set of diffusion coefficients. This alternative can not be discarded, however, until a more extensive study is undertaken.

Other possibilities which could be causing the observed discrepancies in addition to surface diffusion include the possibility that D is a function of concentration, or that adsorption from solution significantly affects the rates in addition to diffusion. The possibility that the variation is due to equilibrium curve equations predicting too high a value for surface concentration at very low solution concentrations is not likely. Wide changes in the isotherms equation for low concentration were found to make very little difference

in the calculated curve. The best possibility at present

seems to be that surface diffusion is playing a significant

role. This is especially indicated by heat of adsorption data

which will be presented below.

Since a constant D could not be determined for these

systems, it was decided to use the D calculated at the time

the adsorption process for the system was one-half completed

for comparison. For phenol, this corresponds to a value of

5.7×10^{-6} cm^2/sec, which is a reasonable value. This value

for D can be compared to an aqueous solution value of 8.9 to

9.6×10^{-6} cm^2/sec (18). The value for pore diffusion should

be somewhat lower because both porosity and tortuosity of path

effects which are not included in the diffusion model would

tend to make the diffusion coefficient smaller. The value

of D for 4-nitrophenol calculated in the same manner is 1.2

$\times 10^{-6}$ cm^2/sec. This coefficient is expected to be somewhat

less than that for phenol because of the larger molecular size.

It should also be noted that the variation in D for these two

solutes is much greater for phenol than for 4-nitrophenol.

If surface diffusion of the solute is an important effect, it

does not appear to be as important for 4-nitrophenol as for

phenol. This observation is in keeping with the fact that

the heat of adsorption for phenol is one-third that for 4-

nitrophenol. The phenol molecules would not be held as tightly

on the surface, and surface diffusion could thus play a larger

role.

TEMPERATURE DEPENDENCE OF ADSORPTION RATES

The rates of adsorption of phenol and 4-nitrophenol (PNP) have been studied as a function of temperature. The system in each case consisted of solute, distilled water and carbon, except that the pH of the 4-nitrophenol system was adjusted slightly to 4.0 with HCl. The calculated rate curves together with the experimental data are shown in Figures IV-11 and IV-12 for temperatures of 11° and $37^{\circ}C$. The calculated diffusion coefficients together with the parameters used for the calculations are shown in Table IV-3. The activation energy can then be calculated by means of Equation III-8. Using only the 11° and $37^{\circ}C$ diffusion coefficients, the activation energy for phenol can be calculated as -5.3 kcal/mole-$^{\circ}$K and as -5.8 kcal/mole-$^{\circ}$K for 4-nitrophenol.

TABLE IV-3

Diffusion Coefficients for Phenol and
4-Nitrophenol at Different Temperatures

Solute	Temperature $^{\circ}C$	Freundlich Parameters		D $(cm^2/sec) \times 10^6$
		F	N	
Phenol	11°	.014	.273	2.8 (1.1 - 4.2)
Phenol	25°	.014	.28	4.7 (2.6 - 7.3)
Phenol	37°	.014	.29	6.2 (2.3 - 9.0)
PNP	11°	.0073	.127	1.0 (0.5 - 1.5)
PNP	25°	.0175	.223	1.2 (0.8 - 2.0)
PNP	37°	.0068	.136	2.4 (1.3 - 3.8)
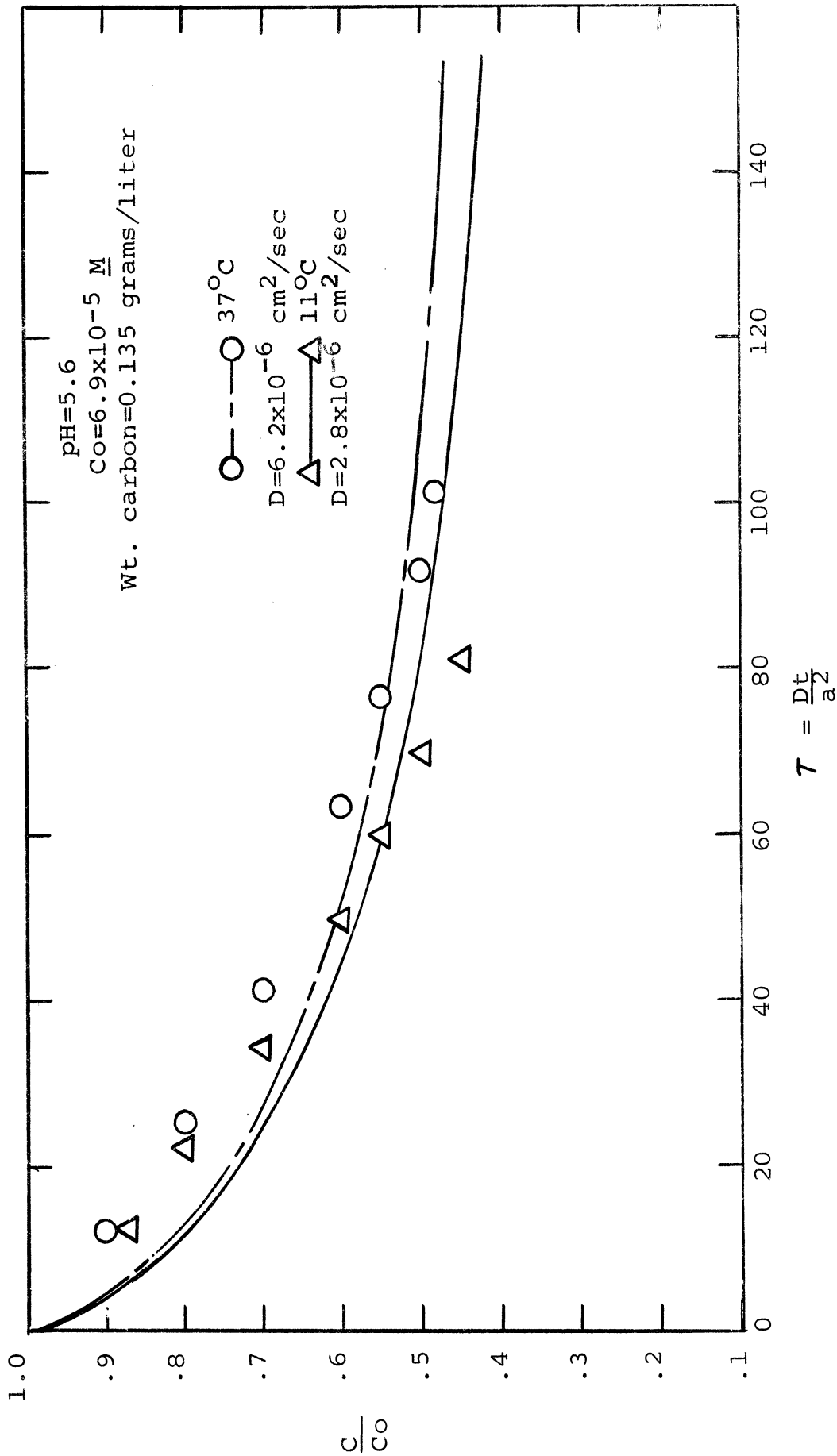
Figure IV-11. Phenol Rate of Adsorption at Different Temperatures
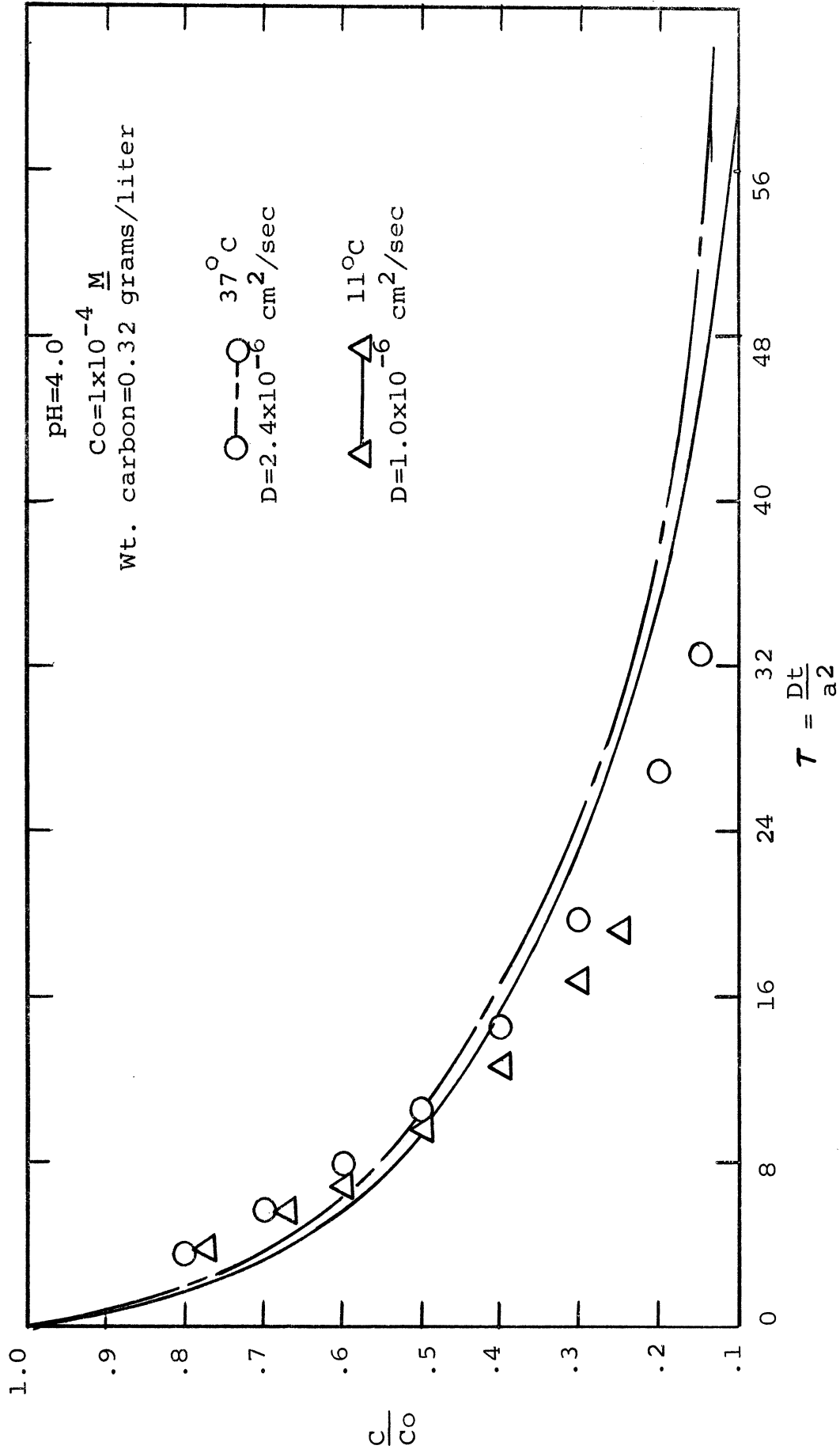
Figure IV-12. 4-Nitrophenol Adsorption at Different Temperatures

An alternative means for calculating the activation energy involves the use of the slope, k, of the S_t vs. t plots of the rate data. This methods yields activation energies which compare favorably with those calculated from the diffusion coefficients. Such a plot is shown for the phenol system in Figure IV-13 and for the 4-nitrophenol in Figure IV-14.

These plots show that the straight line portion of the curve intercepts the abcissa of a positive value of $t^{\frac{1}{2}}$. This same intercept has been noted for all rate studies of strong acid adsorption, and phenol and 4-nitrophenol adsorption. The possibility that this intercept was due to the time required to "wet" the carbon at the beginning of a rate study was checked by wetting the carbon thoroughly with distilled water before adding it to the system. The rate curve obtained using the wetted carbon did not differ at all from the rate curves obtained using the dry carbon. Some other phenomenon which is not readily apparent to the author is evidently causing this intercept. Regardless of the intercept, however, the slope of the straight line portion of this plot, k, can be used to good advantage. Weber and Gould (68) found that by using the square of this slope, k^2, as a relative rate constant, that Equation III-8 gives reasonable values for the activation energy of intraparticle diffusion. A plot of Equation III-8 for the phenol system at temperatures of 2°, 11°. 25°, 37° and 50°C is shown in Figure IV-15 and for 4-nitrophenol at the same temperatures in Figure IV-16. E_a as calculated from the slopes of these plots is -3.6 kcal/mole-$^\circ$K for phenol and -3.9 kcal/mole-$^\circ$K for
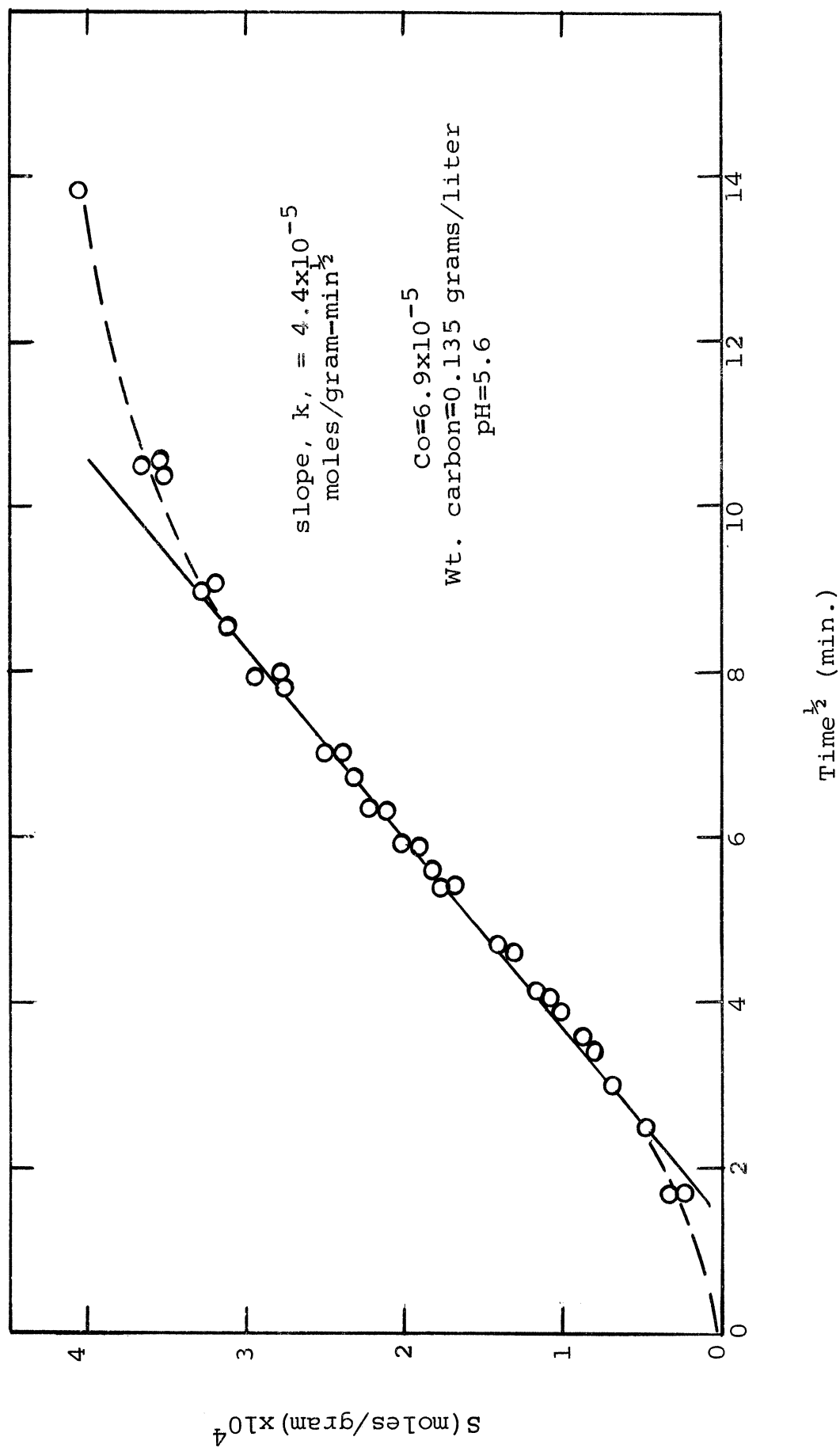
Figure IV-13. Phenol Rate of Adsorption
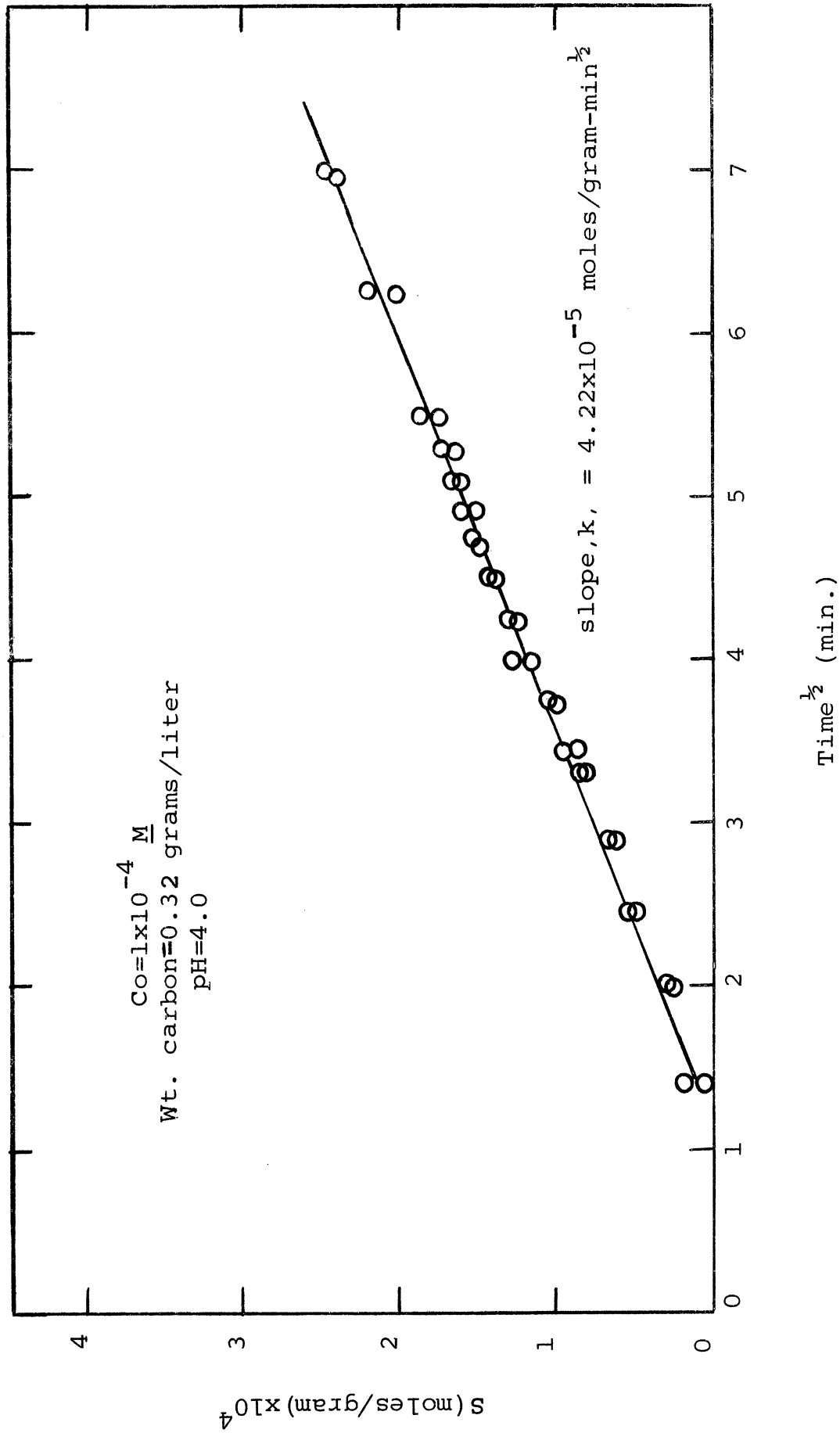
Figure IV-14. 4-Nitrophenol Rate of Adsorption
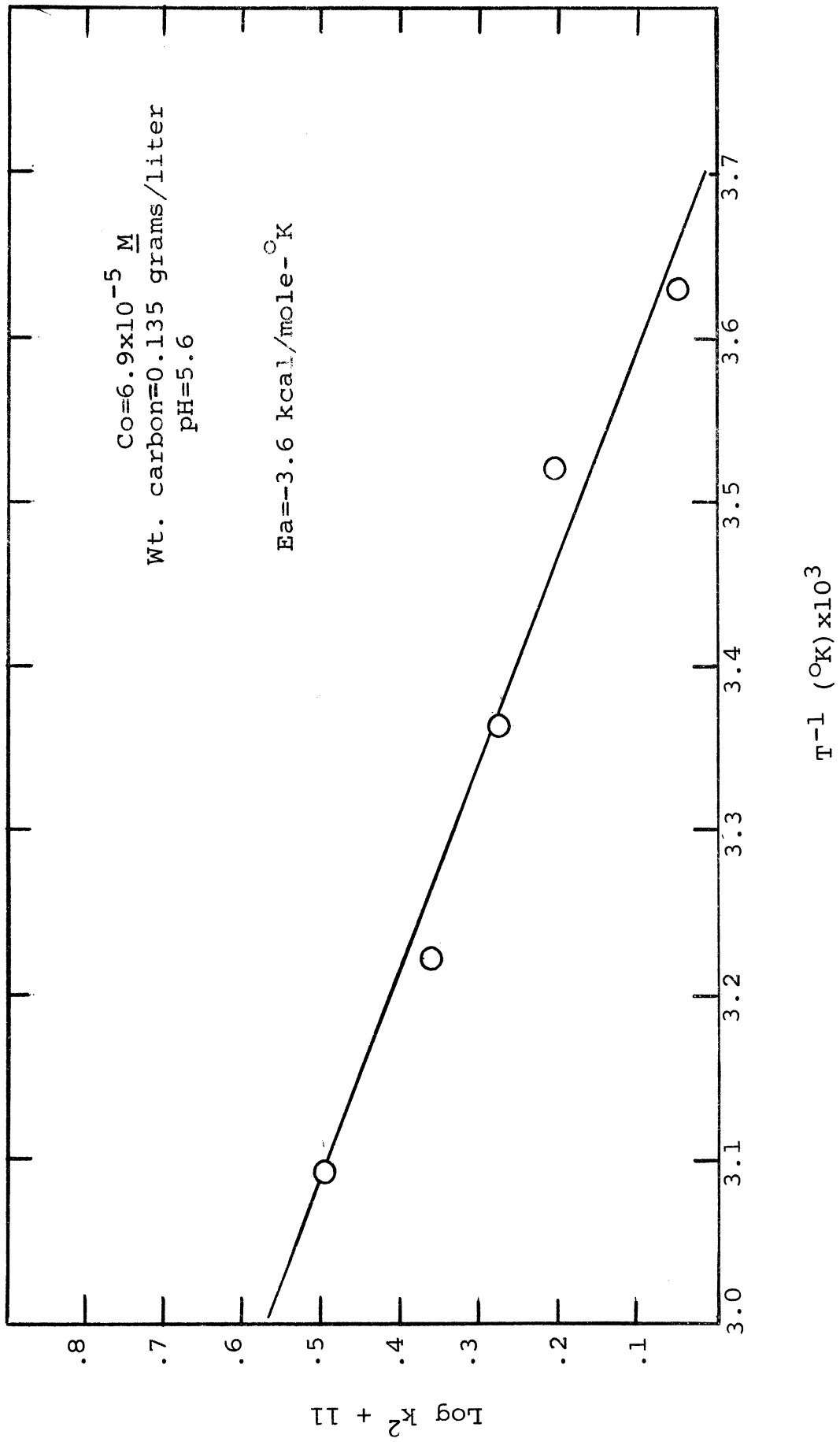
Figure IV-15. Temperature Dependence of Phenol Rate of Adsorption
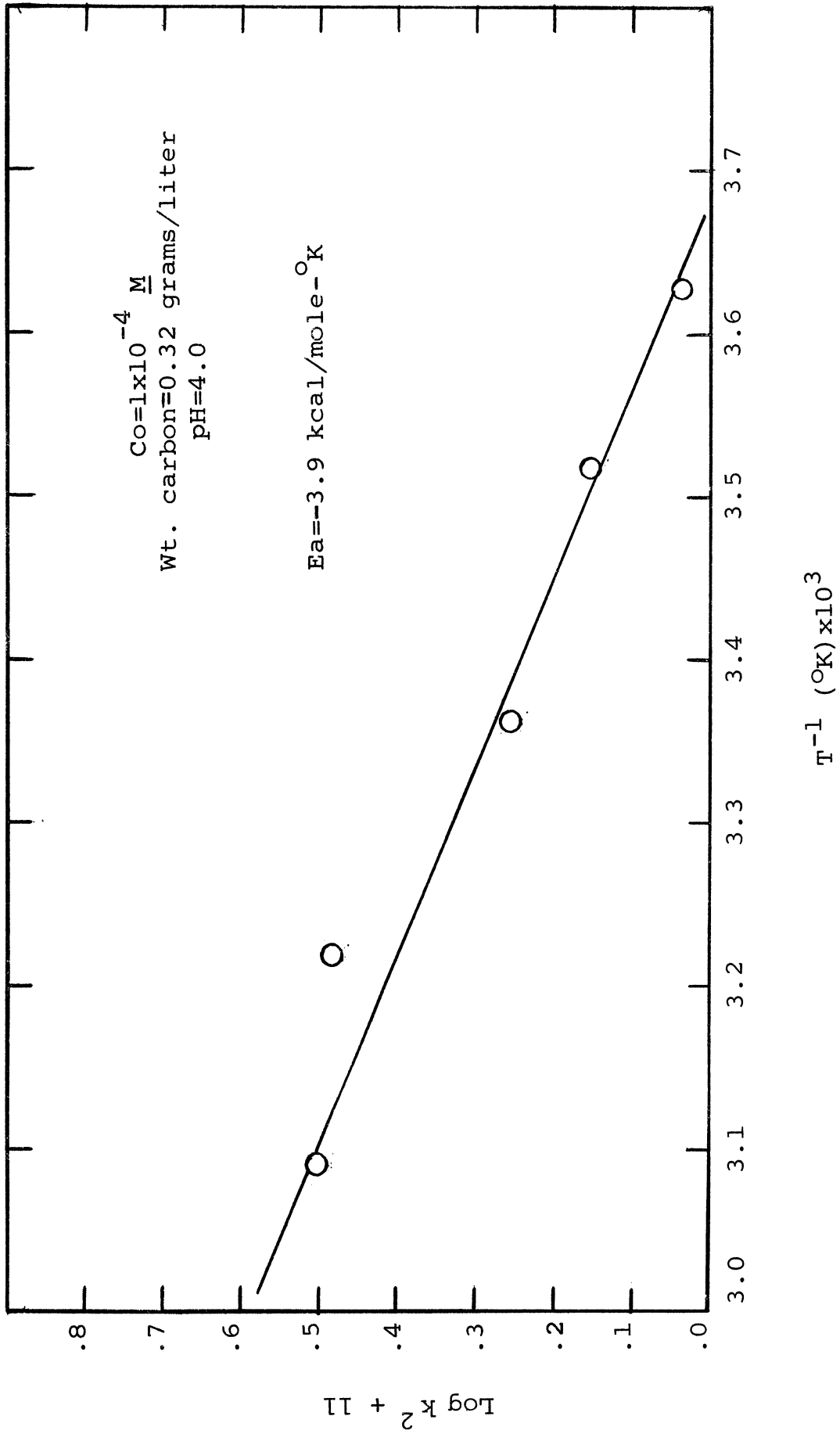
Figure IV-16. Temperature Dependence of 4-Nitrophenol
Rate of Adsorption

4-nitrophenol.

The value of E_a = -3.9 kcal/mole-$^{\circ}$K for 4-nitrophenol can be compared with a value of -8.9 kcal/mole-$^{\circ}$K found by Weber and Gould (68). This difference is apparently due to the different systems which were used--Co = 1x10^{-4}M and 0.32 grams per liter of carbon in this case, and Co = 1x10^{-5}M and 0.025 grams per liter used by Weber and Gould. The values of k^2 used for these plots are tabulated in Table IV-4. The fact that the S vs. $t^{\frac{1}{2}}$ is linear for some time after the carbon is added to the system also supports the assumption that diffusion is rate controlling. Crank (14) illustrates many processes for which this occurs.

TABLE IV-4

The Relative Rate Constant at Different Temperatures

Temperature $^{\circ}$C	Phenol		4-Nitrophenol	
	$k \times 10^5$ $\frac{moles}{gm-min}$.5	$k^2 \times 10^{10}$	$k \times 10^5$ $\frac{moles}{gm-min}$.5	$k^2 \times 10^{10}$
2	3.5	11.2	3.29	10.8
11	4.0	16.0	3.78	14.2
25	4.4	19.4	4.22	17.8
37	4.8	23.0	5.55	30.8
50	5.6	31.3	5.66	32.0

DEPENDENCE OF ADSORPTION RATE ON CARBON DOSAGE

The effect of carbon dosage on the rate of adsorption of 4-nitrophenol. The system chosen for the study was the distilled water 4-nitrophenol system at pH = 4.0. The carbon dosages studies were 0.032, 0.064, 0.16 and 0.32 grams per liter. The results are shown in Figure IV-17 in an S_t vs. $t^{\frac{1}{2}}$ plot. The slopes of these rate curves vary from 4.2×10^{-5} moles/gm-min$^{\frac{1}{2}}$ for a dosage of 0.32 grams per liter to 11.8×10^{-5} moles/gm-min$^{\frac{1}{2}}$ for a dosage of 0.032 grams per liter. Thus, decreasing carbon dosage causes the rate of adsorption to increase significantly. The difference in rate seems to be due to a more rapid decrease in driving force in the systems with the higher dosage. For example, at a surface coverage of 2.5×10^{-4} moles per gram, the solution concentration in the 0.032 grams per liter system is 9.2×10^{-5} $\underline{M}$, while for the 0.32 grams per liter system the solution concentration is $2.5 \times 10^{-5}\underline{M}$. As the carbon dosage approaches zero, the infinite bath case would be approached, and the rate of removal would no longer be a function of carbon dosage.

In spite of the fact that the rate of uptake as indicated by the S_t vs. $t^{\frac{1}{2}}$ plot would be expected to change with carbon dosage, the diffusion coefficient should not change if the assumptions included in the model are valid. However, D was found to increase with decreasing carbon dosage, contrary to the assumptions in the model, and contrary to the results of the acid adsorption data. The problem again seems to be that the model inadequately describes the data as discussed
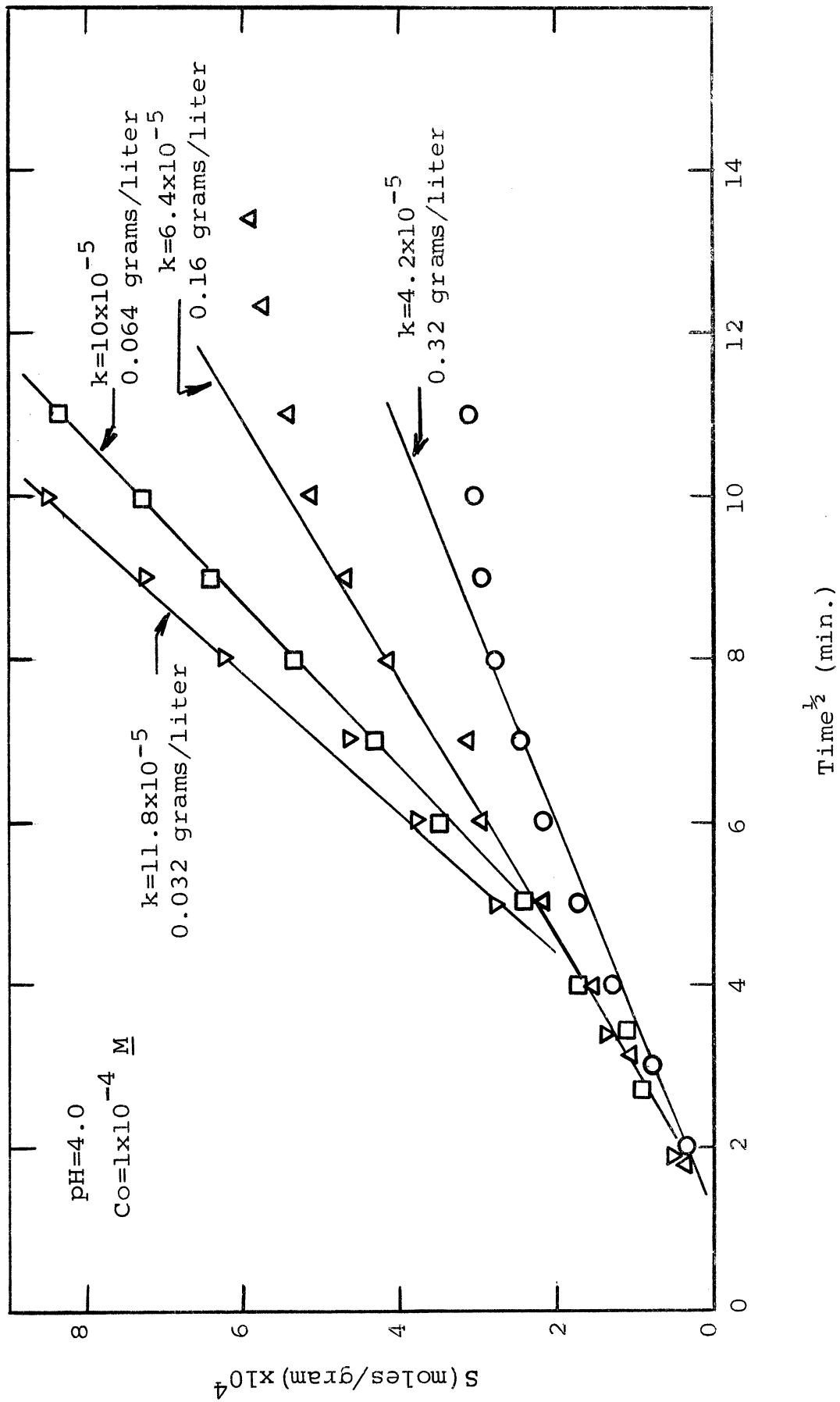
Figure IV-17. 4-Nitrophenol Rate of Adsorption at
Different Carbon Dosages

before, and a model which describes the data better is now being sought. The D chosen for comparison was arbitrarily selected as the one for which the data and calculated curve corresponded when the adsorption process was one-third completed. The results of this calculation are given in Table IV-5. It should be noted, however, that D increases not only with decreasing carbon dosage, but also with increasing surface coverage. This point supports the hypothesis that surface diffusion is a significant part of the rate phenomenon.

TABLE IV-5

Diffusion Coefficients at
Different Carbon Dosages

4 Nitrophenol , $S = .0175C^{.223}$, $Co = 1 \times 10^{-4} \underline{M}$		
Carbon Dosage (gms/liter)	A cm^3	D $(cm^2/sec) \times 10^6$
0.032	0.25	5.4
0.064	0.125	4.1
0.160	0.05	1.5
0.320	0.025	0.8

DEPENDENCE OF ADSORPTION RATE ON INITIAL CONCENTRATION OF SOLUTE

Rate studies were performed on the phenol-distilled water-carbon systems at initial phenol concentrations of 6.9×10^{-5} and $1 \times 10^{-3} \underline{M}$. The calculated rate curves together with experimental data are shown in Figure IV-18. The diffusion coefficient calculated at the point at which the adsorption

110
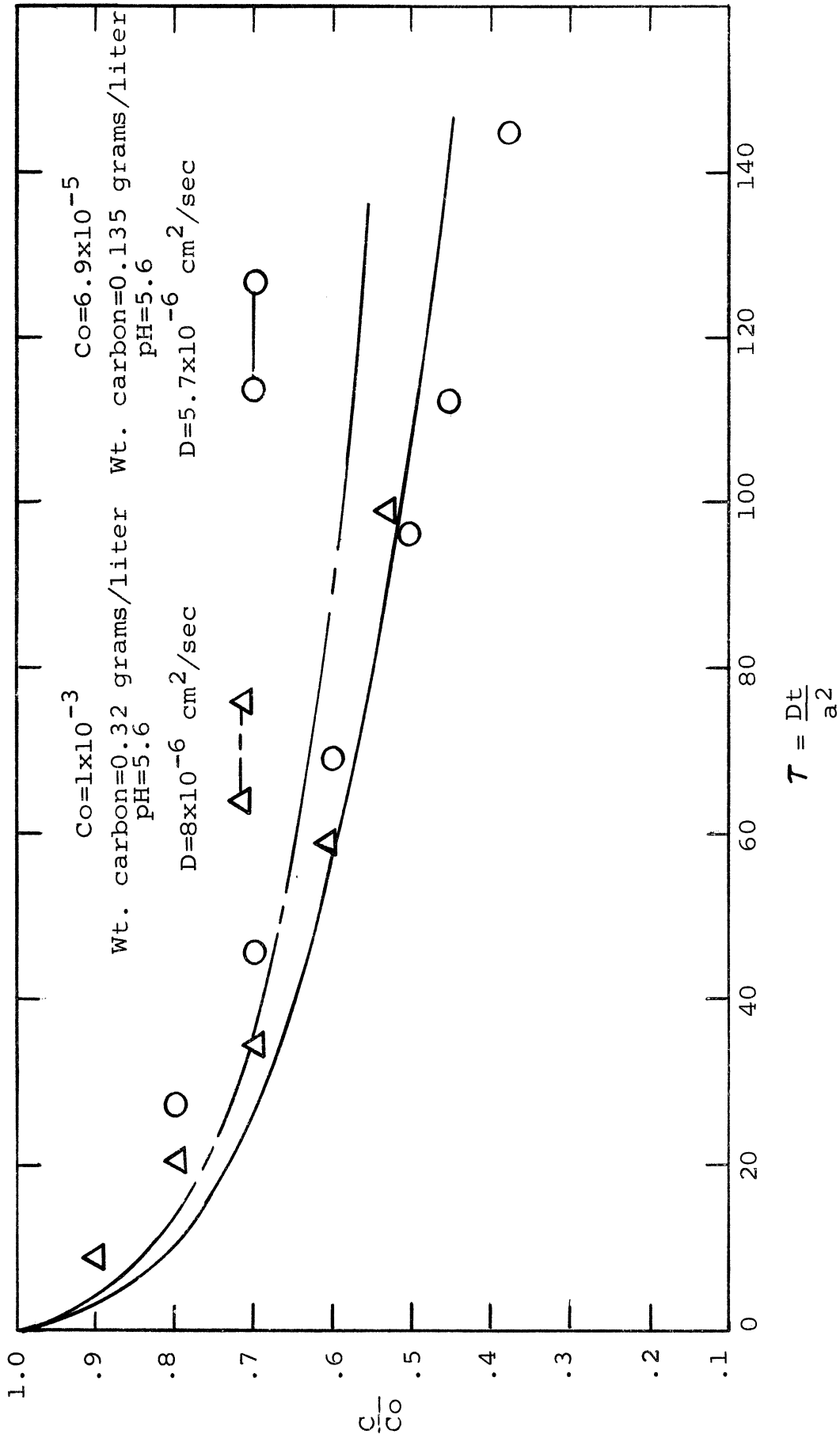
Figure IV-18. Phenol Rate of Adsorption at
Different Initial Concentrations

process is 50% completed is 5.7×10^{-6} cm^2/sec for Co = 6.9 $\times 10^{-5}$ M, and 8.0×10^{-6} cm^2/sec for Co = 1×10^{-3} M. The fact that the diffusion coefficient changes with initial concentration again is not in accord with the assumption of a constant diffusion coefficient which is inherent in the model, but the fact that the diffusion coefficient increases with surface coverage again indicates that surface diffusion could be an important consideration.

It is also interesting to look at the S_t vs. $t^{1/2}$ plot of this rate data in Figure IV-19. The slope of this plot, k, is 4.7×10^{-4} moles/gm-min for Co = 1×10^{-3} M and 4.4×10^{-5} moles/gm-min for Co = 6.9×10^{-5} M. Assuming a straight line relationship for dependence of k^2 on Co after Weber and Gould (68), k^2 is increasing at the rate of 2.34×10^{-4} moles-liter/gm^2-min. This compares with a value of 1.97×10^{-5} moles-liter/gm^2-min found for 2, 4-dinitro-o-sec-butylphenol (68)

EFFECT OF ASH REDUCTION

The effect of reduction of ash content of the carbon on adsorption of phenol was also studied. The carbon was the same as that described in Chapter III which was treated with 1+1 HCl to reduce the ash content from 0.7% to 0.3%. Both rate and equilibrium studies were performed on the phenol-distilled water-carbon system at pH = 5.6. No significant effect was noted either on the equilibrium isotherm or on the rate of phenol adsorption.
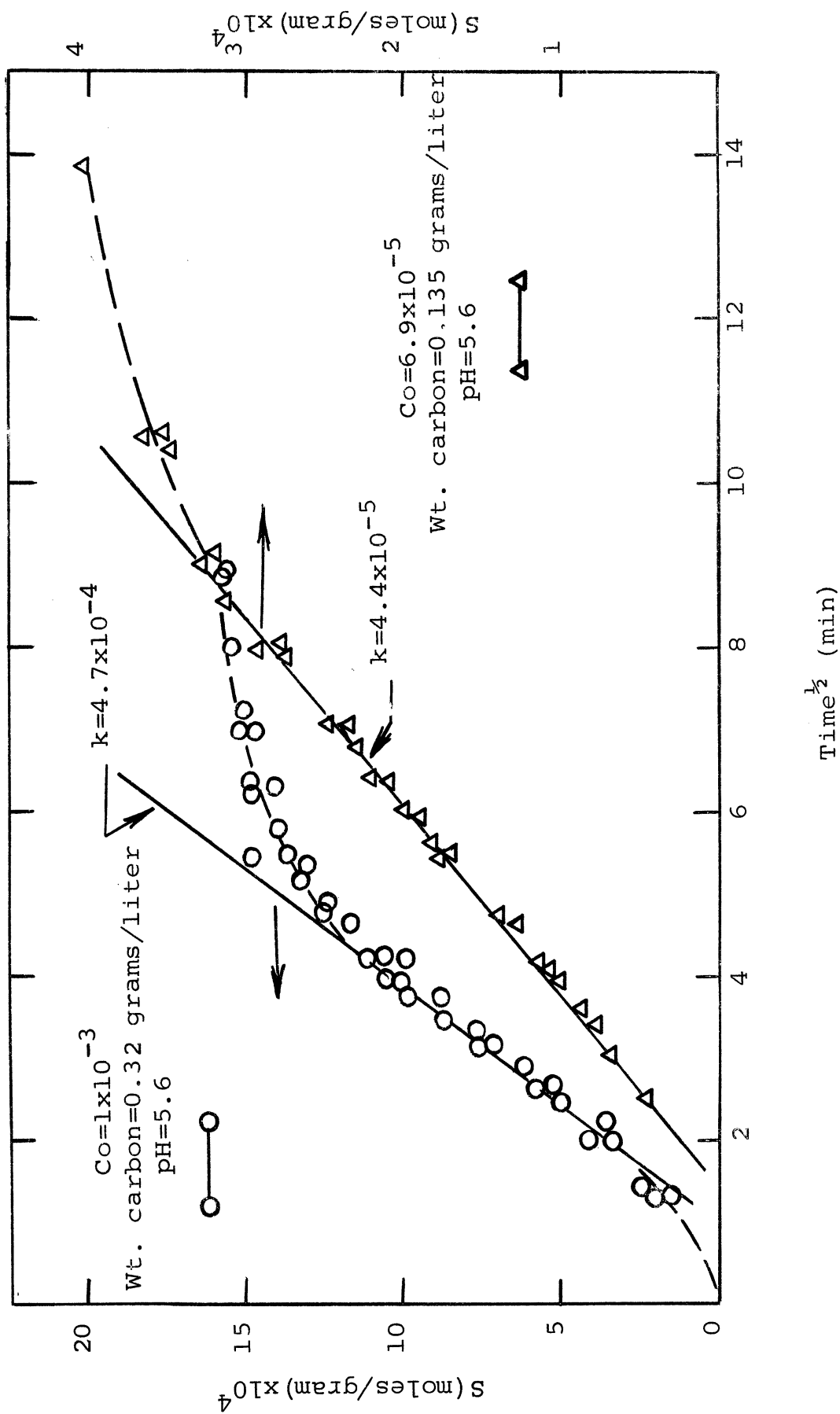
Figure IV-19. Phenol Rate of Adsorption at Different
Initial Concentrations

The reason that no effect of treatment of the carbon for reduction of ash content was noticed probably was due to the fact that the original ash content was small. If the ash content had been larger, the effect on adsorption could well have been more significant, and this should be further studied using carbons of high ash content.

EFFECT OF pH ON ADSORPTION

The effect of solution pH on adsorption of phenol and 4-nitrophenol was also studied extensively. The pH effect on adsorption can be attributed, in general, to either effects on the sorbate molecule or on the sorbent surface. The adsorption characteristics of the sorbate in its neutral form will be different than those for the anion, at least because the anionic species is more soluble and thus does not tend to be adsorbed as readily from solution. However, repulsive forces between the anionic sorbate and the sorbent could also become more significant, especially if the surface has a net negative charge. The effect of different pH on the adsorbent surface could take place in the form of a destruction or alteration of surface sites, or in the alteration of the surface potential so that attractive and repulsive forces are affected. In order to examine these effects more closely, rate and equilibrium studies were performed on both phenol and 4-nitrophenol over a range of pH's.

Effect of pH on Equilibria

Phenol equilibria studies were performed on the

phenol-distilled water system at different pH with only HCl or NaOH used for pH adjustment. The results of these studies are shown in Figure IV-20, and the Freundlich constants for these curves are shown in Table IV-7. It should be kept in mind that the pK_a of phenol is 9.9 so that the principal adsorbing species above this pH is most likely anionic. A summary plot of these isotherms is shown in Figure IV-21. A significant result is the reduction in amount adsorbed with pH decreased from 7.5. The solubility of phenol is constant at 0.8 $\underline{M}$ in the pH range 2.0 to 5.6 as determined experimentally and it is assumed that no change in solubility occurs between pH = 5.6 and 7.5. Apparently the nature of the surface is being altered in some manner by the acid used to adjust the pH. The mechanism of phenol adsorption on oxide surfaces such as activated Alumina has been determined as adsorption with the -OH group forming a bond with the surface oxide (36). Assuming that at least some of the phenol is being adsorbed in this manner on the carbon oxide groups, then some of these sites would be altered as acids react with the chromene functional groups. Also, if acid is being adsorbed on the microcrystallite basal planes inside the carbon pores (6), the phenol which would adsorb "flat" on these basal planes would have to compete with the acid.

Equilibrium capacity also decreases with increasing pH above 7.5. (Capacity measurements were made at only one pH above the pK because crystals appeared in the solution at higher pH. Apparently, the carbon was catalyzing some reaction which produced the crystals since phenol solutions at
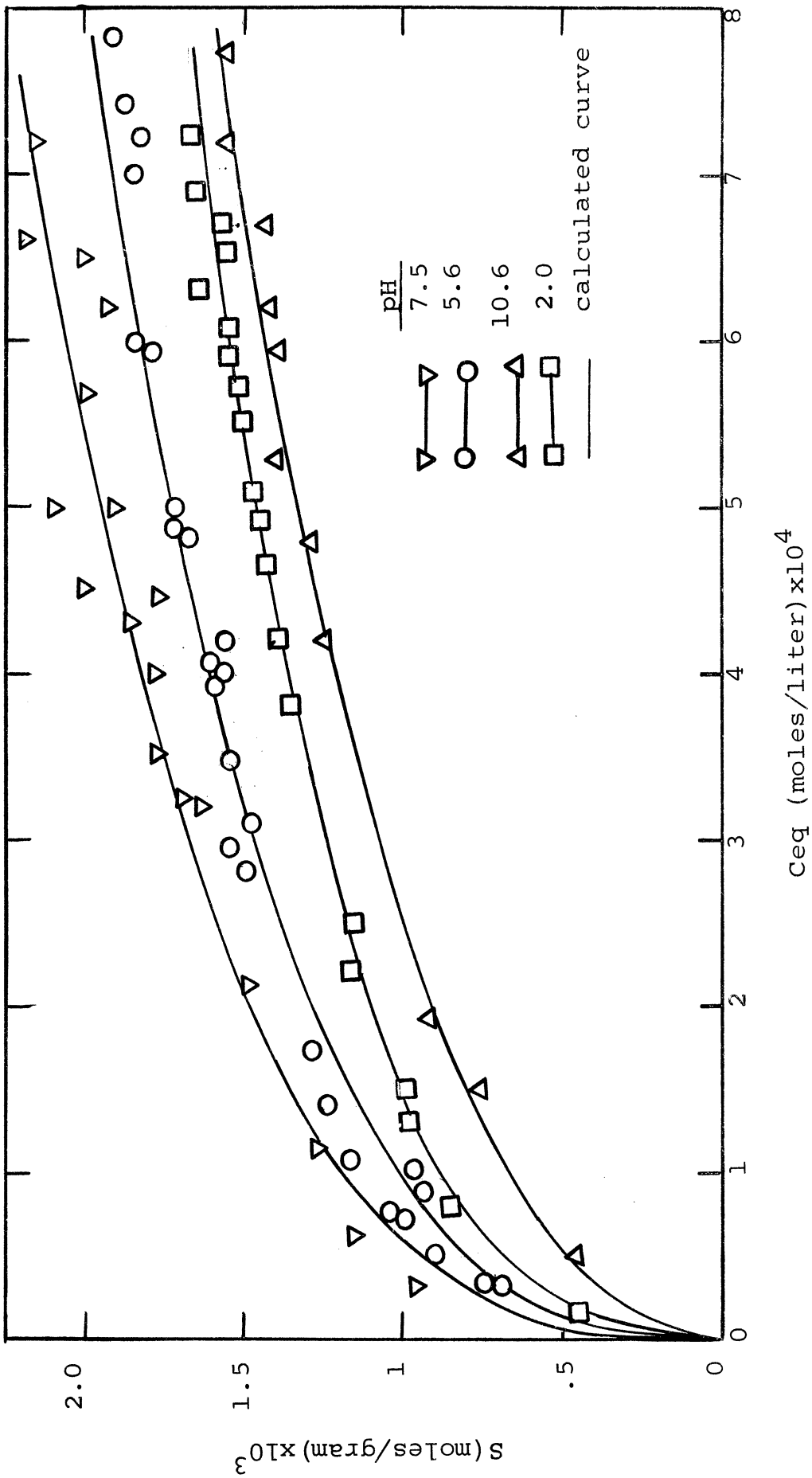
Figure IV-20. Phenol Equilibria at Different pH
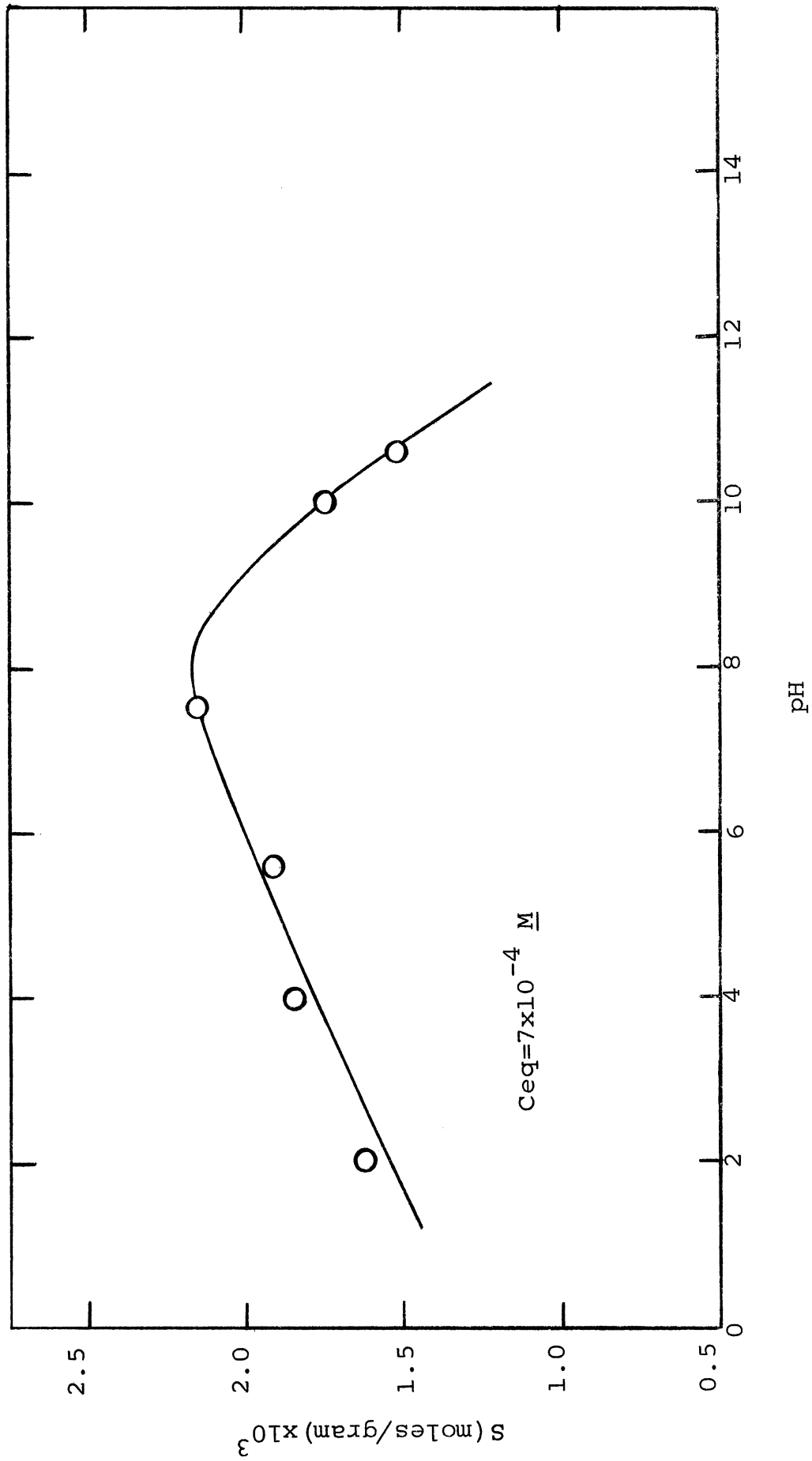
Figure IV-21. Phenol Equilibria at Different pH

high pH are usually quite stable. Further research will be required to find out more about this reaction.) Sodium phenolate is very soluble in solution and as a consequence the extent to which it is soluble was not determined. Experiments with 4-nitrophenol indicate, however, that the high pH is affecting the surface of the carbon in addition to increasing the solubility of the sorbate (see Figure IV-23). The Langmuir parameters were calculated for the same phenol concentration range for the pH = 7.5 data and the pH = 10.6 data, and it was found that the b value for the neutral species was about 75% larger than for the anionic species, (34,000 <u>vs</u>. 19,000 liters/mole), thus indicating a lower heat of adsorption for the anionic species.

Equilibrium studies were made to determine the effect of pH on 4-nitrophenol adsorption in the same manner as for phenol. The results of these studies are shown in Figure IV-22, and the Freundlich equation parameters for these curves are shown in Table IV-8. The equilibrium capacities in this case did not decrease with decreasing pH from the pK = 7.0. This would indicate that some of the sites at which phenol and 4-nitrophenol are adsorbed are not the same, at least for low concentration. It was shown previously (see Figure IV-5) that at high equilibrium concentration, the surface concentrations are the same for both phenol and 4-nitrophenol, and in this case it is likely that the same sites are covered with sorbate. Specifically, in the lower equilibrium concentration region, 4-nitrophenol is apparently not adsorbed at the specific surface
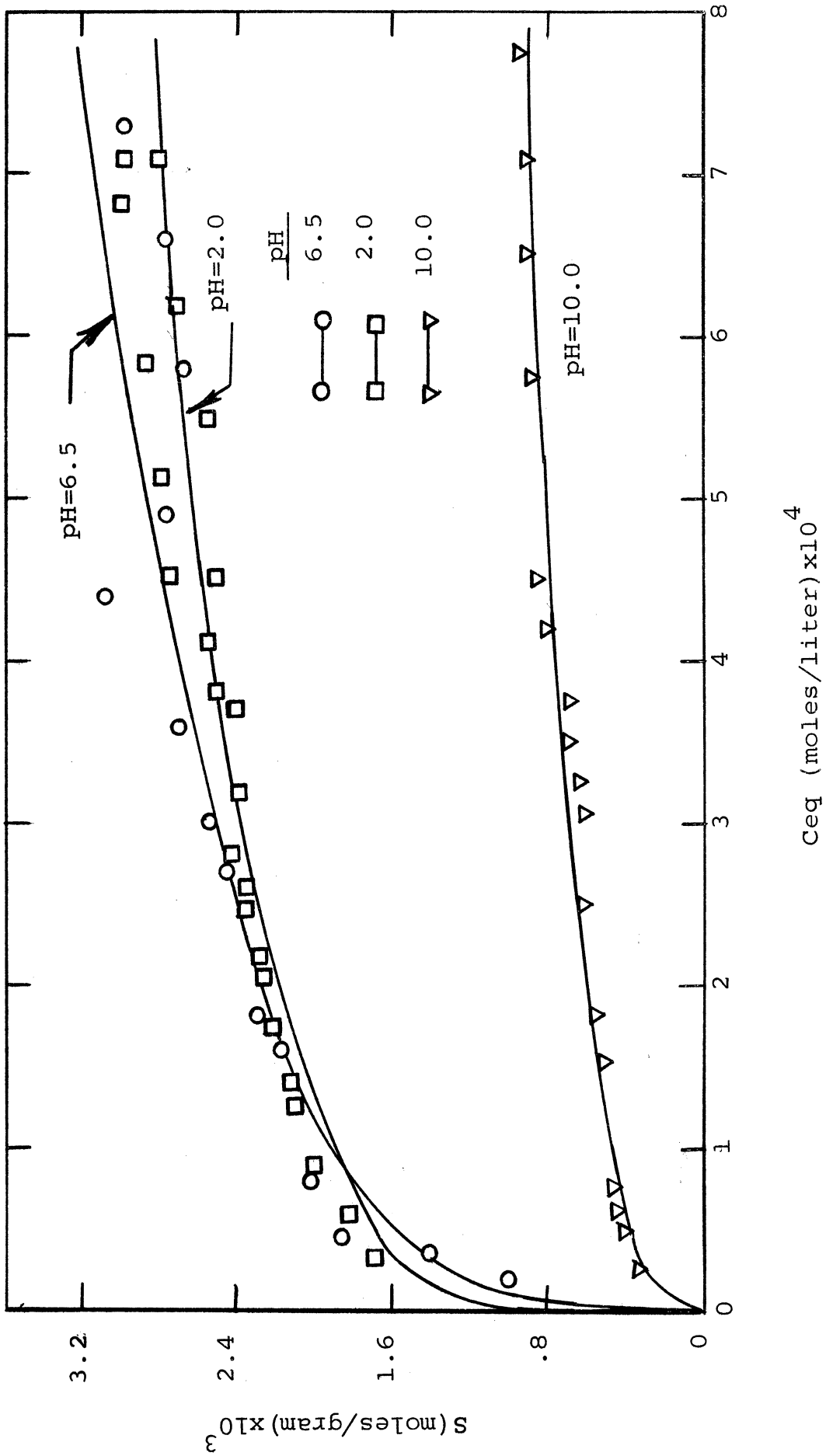
Figure IV-22. 4-Nitrophenol Equilibria at Different pH

oxides which are affected by pH and at which phenol absorbs.

Alternatively, 4-nitrophenol may displace the physically adsorbed acid more easily than phenol. The latter mechanism is indicated by the fact that the heat of adsorption of 4-nitrophenol is about three times that of phenol (q_{st}, phenol = 1.8 kcal/mole-^{O}K; q_{st}, 4-nitrophenol = 5.6 kcal/mole-^{O}K).

The capacity of carbon for 4-nitrophenol decreases with increasing pH above 7.0 as it did for phenol. In order to determine if the solubility differences between the neutral and anionic species were the principal cause of this decrease in capacity, a plot of reduced concentration (C/C_s) was made as a function of S for the pH = 4 and pH = 10 data. This plot is shown in Figure IV-23; only the normalized data curves are shown. The solubility limit of the anion was experimentally determined as 0.2 M while that for the neutral species was 0.1 M. It can be seen from this plot that solubility does not play a major role, but that the effect of high pH on the carbon surface is more significant. Calculation of the Langmuir parameters revealed b for the pH = 10 data was 14,000 liters/mole compared with 50,000 liters/mole for the pH = 4 data. This indicates a lower heat of adsorption for the anionic species, and therefore it is possible that increased repulsive forces between the negative molecule and the negative surface are causing the lower capacity. The negative surface charge of the carbon is possibly being increased by physical adsorption of OH$^-$ ions on the surface, or by ionization of very weak, acidic functional groups on the surface such as the phenolic functional group.
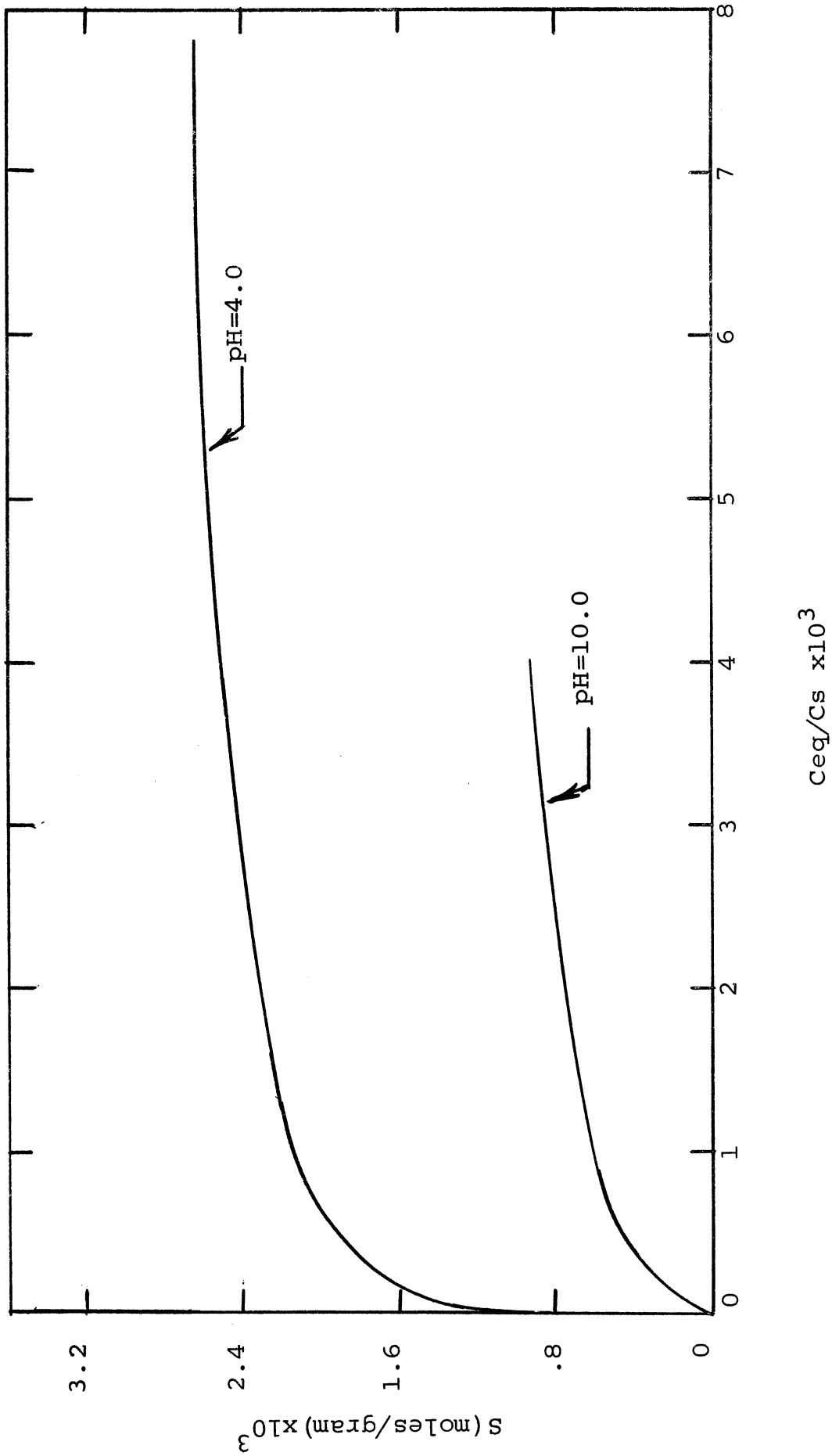
Figure IV-23. 4-Nitrophenol Equilibria as a Function
of Reduced Concentration

Equilibrium data at different temperatures were taken for both phenol and 4-nitrophenol. The data for the 4-nitrophenol system at pH = 10 are shown in Figure IV-24 for temperatures of 11° and $37^{\circ}C$. The isosteric heat of adsorption, q_{st}, calculated for this data at $S = 6 \times 10^{-4}$ moles/gram is 0.75 kcal/mole-$^{\circ}K$ as compared with 6 kcal/mole-$^{\circ}K$ for the neutral species at $S = 2.5$ kcal/mole-$^{\circ}K$. The implications of this low heat of adsorption are that the anionic species will not be bound as tightly at the surface and that surface diffusion could be more prevalent for the anionic species than for the neutral species.

The temperature dependence of the 4-nitrophenol adsorption process at pH = 2 was found to be essentially the same as at pH = 4.0. No difference in temperature dependence was expected because the capacity for 4-nitrophenol is the same at these two pH's.

The temperature dependence of phenol adsorption at pH = 2 was found to be quite different than that at pH = 5.6, however, in keeping with the effect of pH on capacity for the neutral species. The data for pH = 2 at temperatures of 11° and $37^{\circ}C$ are shown in Figure IV-25. The systems used for this study contained 1×10^{-2} $\underline{M}$ NaCl, but it should be noted that at all pH's studied, there was no effect on the capacity of carbon for either phenol or 4-nitrophenol due to the presence of 1×10^{-2} $\underline{M}$ NaCl as compared with no NaCl. The temperature effect for phenol adsorption at pH = 2 was also found to vary more extensively with surface concentration than was previously
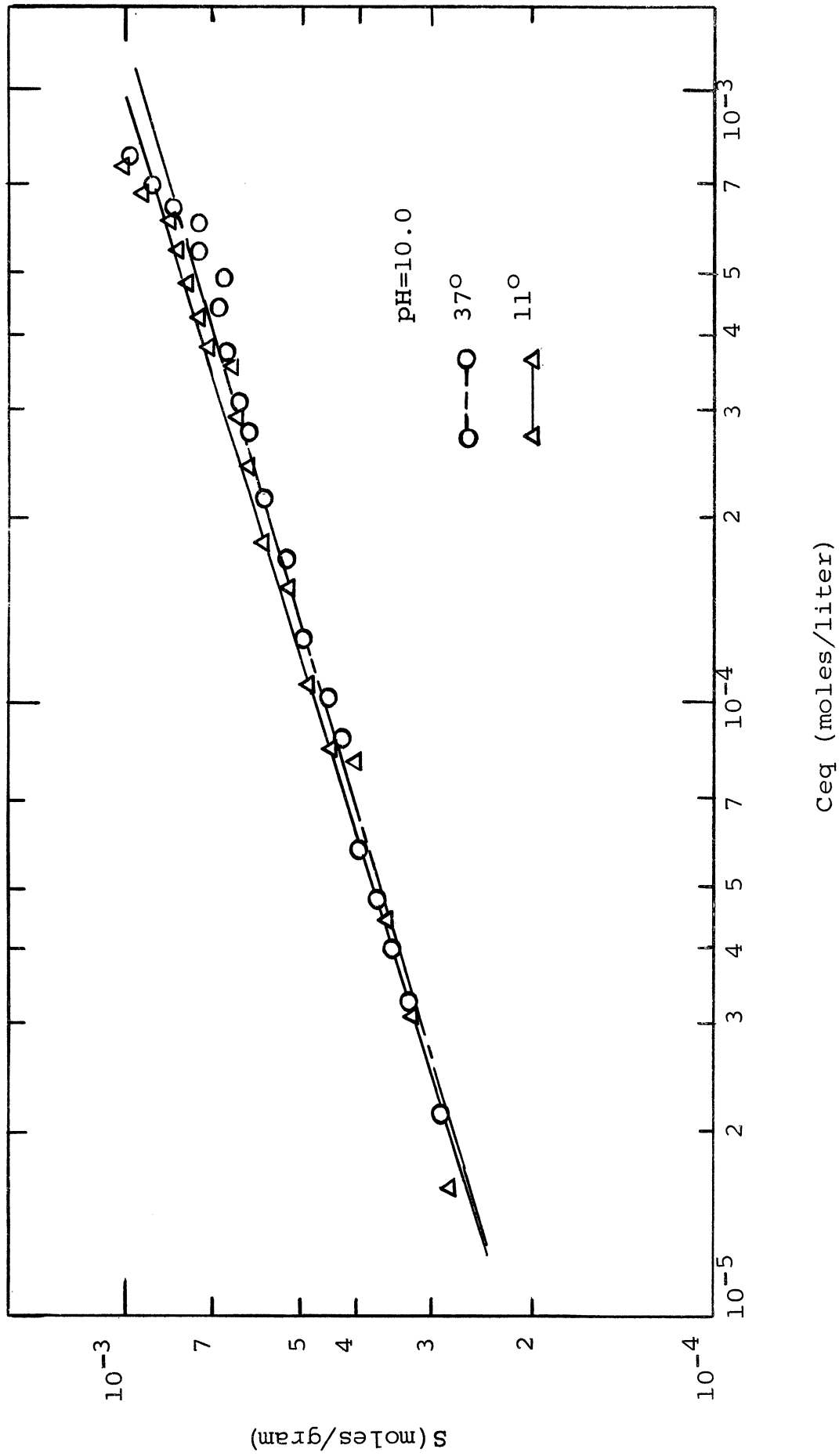
Figure IV-24. 4-Nitrophenol Anion Equilibria at
Different Temperatures

123
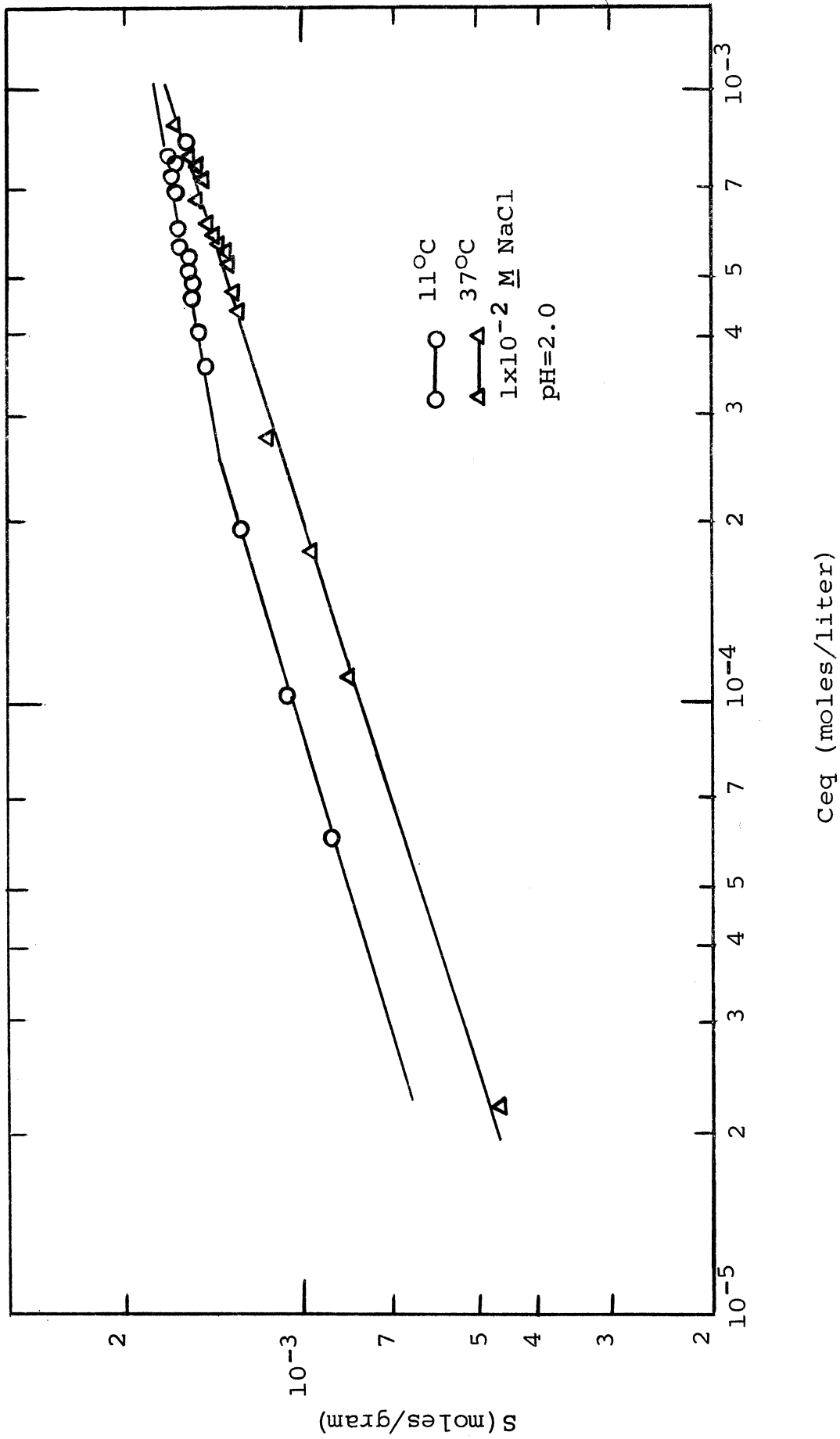
Figure IV-25. Phenol Equilibria at Different Temperatures

observed at pH = 5.6. In order to express this effect quanti-
tatively, the isosteric heat of adsorption, q_{st} was calculated
for pH = 2 and pH = 5.6 at different surface coverages. The
data for the pH = 5.6 calculations was taken from Figure IV-7.
The results are tabulated in Table IV-6.

TABLE IV-6

Isosteric Heats of Adsorption at Different
Phenol Surface Coverages

S (mole/gram) x 10^3	1.0	1.25	1.50	1.75	2.0
q_{st}, pH = 2.0 (kcal/mole-$^{\circ}$K)	5.4	4.8	3.7	0.7	
q_{st}, pH = 5.6 (kcal/mole-$^{\circ}$K)	2.7	2.2	2.0	2.5	1.8

The greater effect of temperature on phenol adsorption
at pH = 2 is quite possibly related to the effect of tempera-
ture on the quantity of acid adsorbed. Although there is
much scatter in the data, the acid adsorption isotherms shown
in Figure III-13 indicate that the process is endothermic at
high acid concentrations. Since the phenol adsorption process
is exothermic, an increase in temperature would cause less
phenol to be adsorbed. In addition, however, the increase in
temperature at the same time would cause more acid to be ad-
sorbed on the carbon surface, the presence of which would
further decrease the amount of phenol which could be adsorbed.
The acid, then, would tend to magnify the effect of temperature.

125

Effect of pH on Rate

Kinetic studies were performed to determine the effect of pH on rate of phenol and 4-nitrophenol adsorption. The theoretical rate curves were again calculated and the diffusion coefficients were determined. The diffusion coefficients for phenol together with parameters used to calculate the rate curves are given in Table IV-7, and for 4-nitrophenol in Table IV-8. Typical calculated rate curves and experimental data are shown in Figure IV-26 for phenol at pH = 7.5 and pH = 10.6, and in Figure IV-27 for 4-nitrophenol at pH = 4.0 and pH = 10.0.

TABLE IV-7

Diffusion Coefficients for Phenol at Different pH

pH	Freundlich Parameters		D $(Cm^2/sec) \times 10^6$
	F	N	
2.0	.016	.316	5.7 (1.4 - 7.4)
4.0	.012	.260	3.5 (0.9 - 5.1)
5.6	.046	.40	5.7 (2.0 - 10.6)
7.5	.020	.306	4.0 (1.6 - 5.7)
10.6	.041	.453	2.2 (1.5 - 2.4)

Figure IV-26. Phenol Rate of Adsorption at Different pH
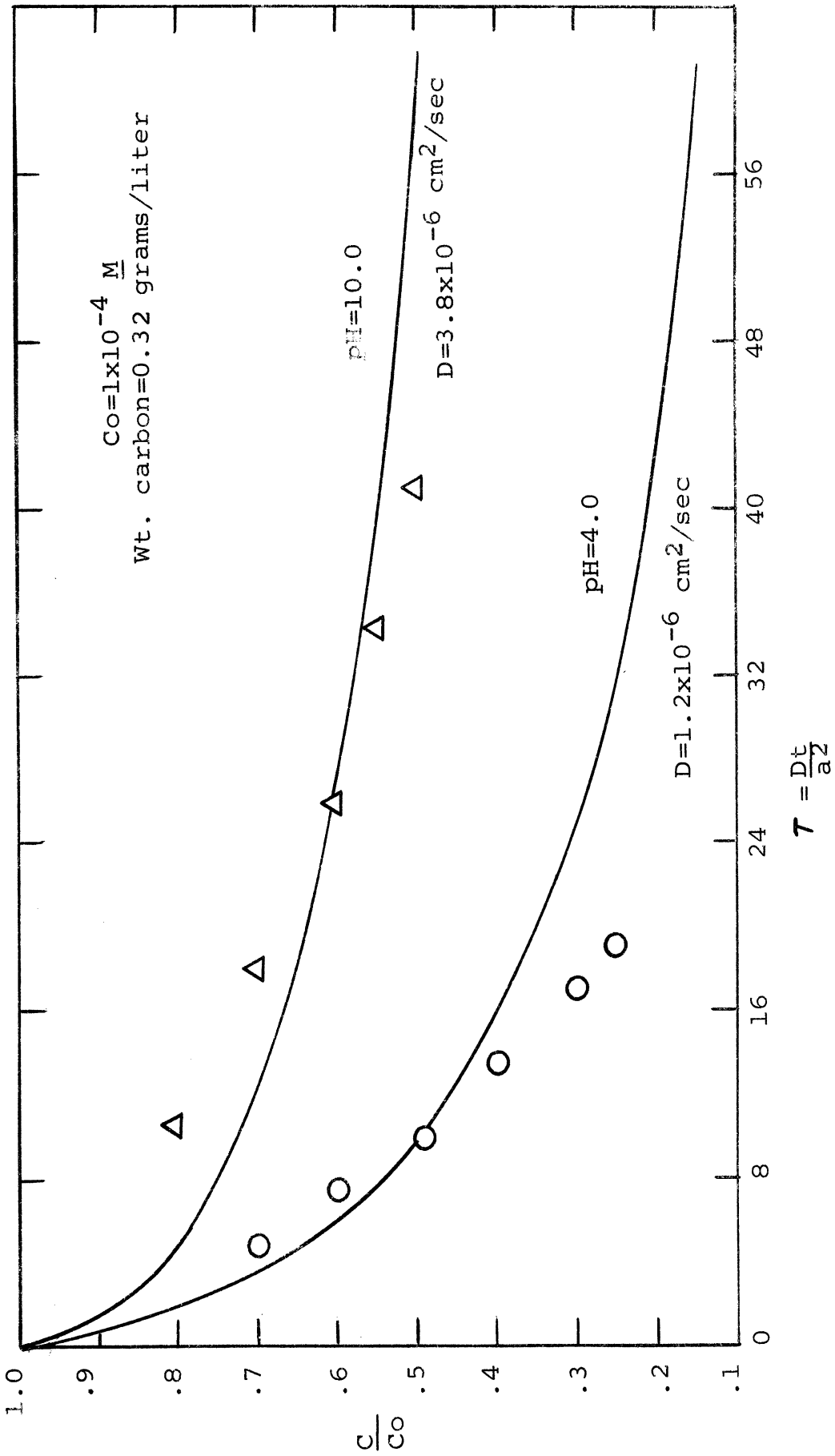
Figure IV-27. 4-Nitrophenol Rate of Adsorption at Different pH

128

TABLE IV-8

Diffusion Coefficients for 4-Nitrophenol at Different pH

pH	Freundlich Parameters		D $(cm^2/sec) \times 10^6$
	F	N	
2.0	.0088	.160	1.1 (0.6 - 1.6)
4.0	.0175	.223	1.2 (0.8 - 1.75)
6.5	.019	.230	1.3 (0.5 - 2.0)
10.0	.011	.333	3.8 (1.6 - 5.3)
12.0	.0045	.27	3.2 (1.4 - 4.8)

The diffusion coefficients for phenol appear relatively constant for the neutral species. The coefficient used for comparison again was arbitrarily selected as the one for which the calculated curve and experimental data correspond when the adsorption process is 50% completed. The diffusion coefficient is smaller, though, for the anionic species. A smaller coefficient is expected because of the additional repulsive forces as the negative molecule passes by the negative surface, but it is difficult to place any real significance on the difference noted because of the arbitrary means of selecting the particular value of the coefficient for comparison. The range of diffusion coefficients, however, also indicate that the diffusion coefficient for the anionic species is smaller than the neutral species.

The 4-nitrophenol diffusion coefficient is also relatively constant over the pH range corresponding to the neutral species. The higher diffusion coefficient for the anion

is unexpected, however. One possible explanation is that
because the heat of adsorption is lower than for the neutral
species (q_{st} = 0.75 vs. 6.0 kcal/mole-$^{\circ}$K at S = 2.5 x 10^{-3}
moles/gram) surface diffusion plays a more prominent role
making the diffusion coefficient larger. This effect would
not be as great for phenol since the heat of adsorption of
the neutral phenol species is much less than that for the
neutral nitrophenol species. However, this can not be asserted
with any degree of certainty until a better model is developed
to interpret the rate data.

Summary plots of the relative rate constant, k, as a
function of pH are given in Figure IV-28 for phenol and Figure
IV-29 for 4-nitrophenol. These constants, too, are quite uni-
form over the pH range of the neutral species, but drop off
sharply for the anionic species. The decrease in k is probably
due to the fact that the capacity of the carbon for the anion
has decreased, and to the increased resistance to movement
inside the pore due to repulsive forces.

It is important to note that the relative rate constants
for both phenol and nitrophenol decrease significantly for
anionic species as compared with the neutral species, while D
for the nitrophenol anion increased and D for phenol decreases
slightly. The reason for this occurrence is that the relative
rate constant includes the effect of pH on capacity, while the
model used to calculate D separates out the capacity effect.

The temperature effect on the rate of 4-nitrophenol
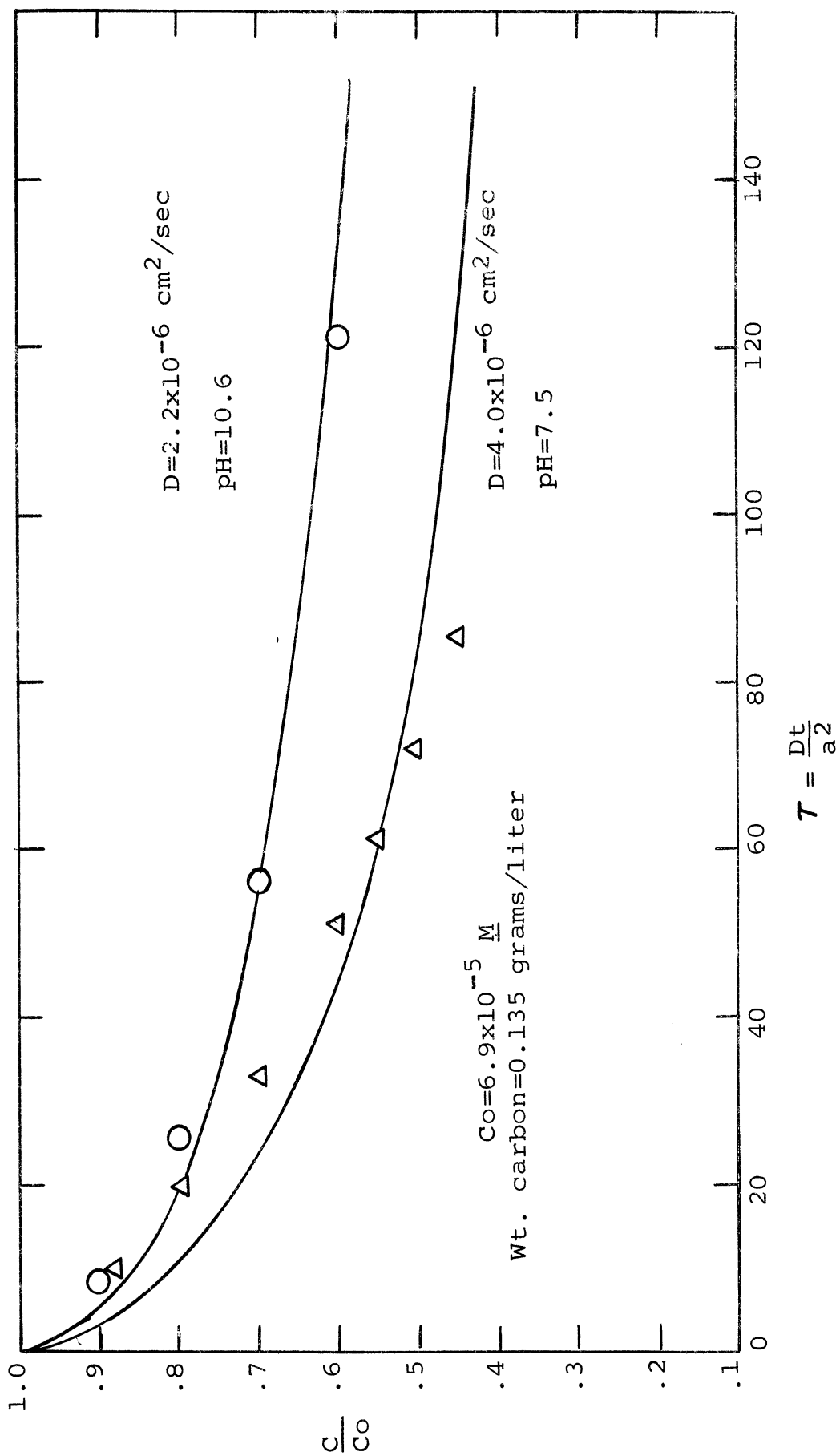anion adsorption was studied at pH = 10.0. The calculated
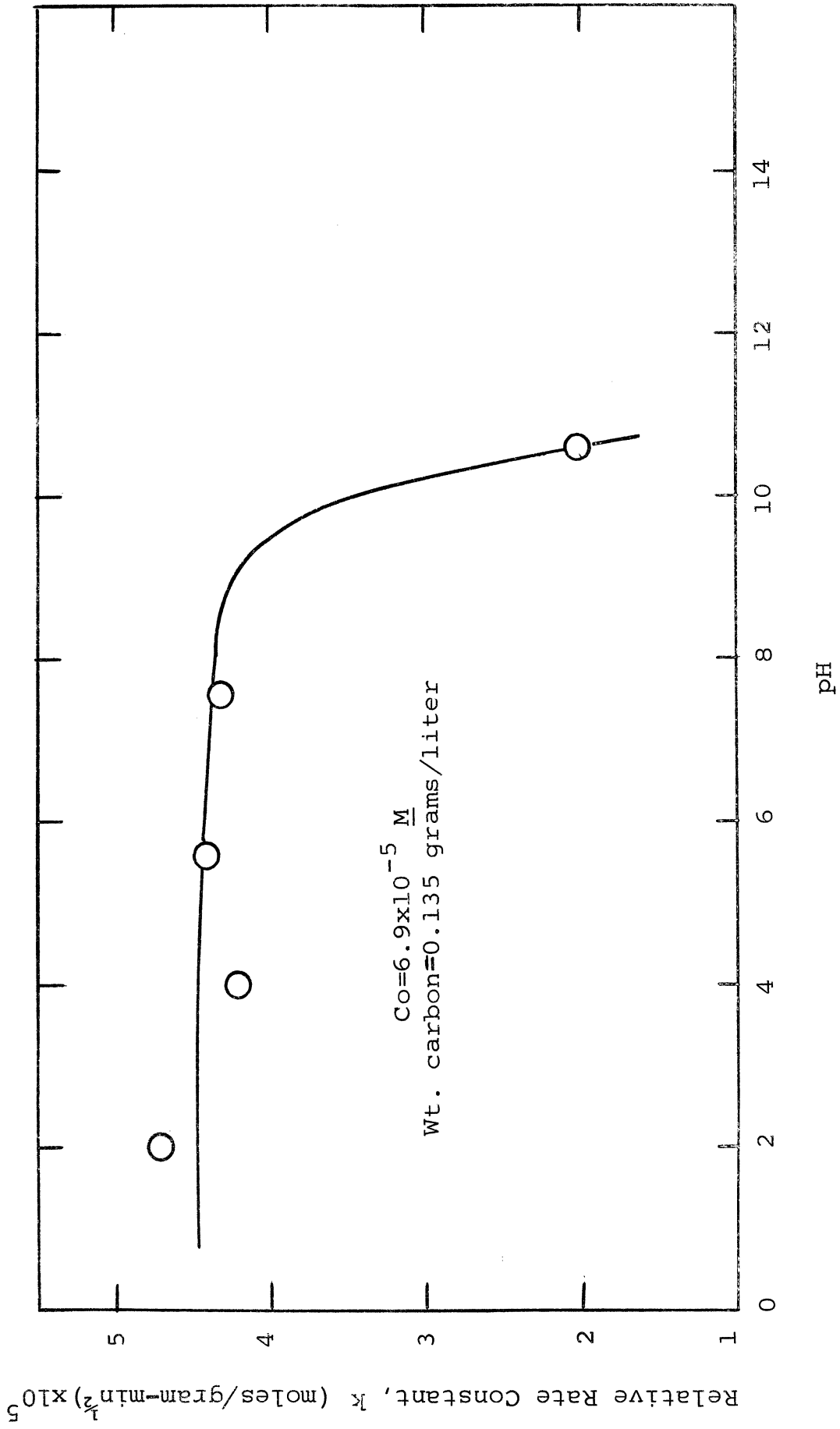
Figure IV-28. Phenol Rate of Adsorption at Different pH
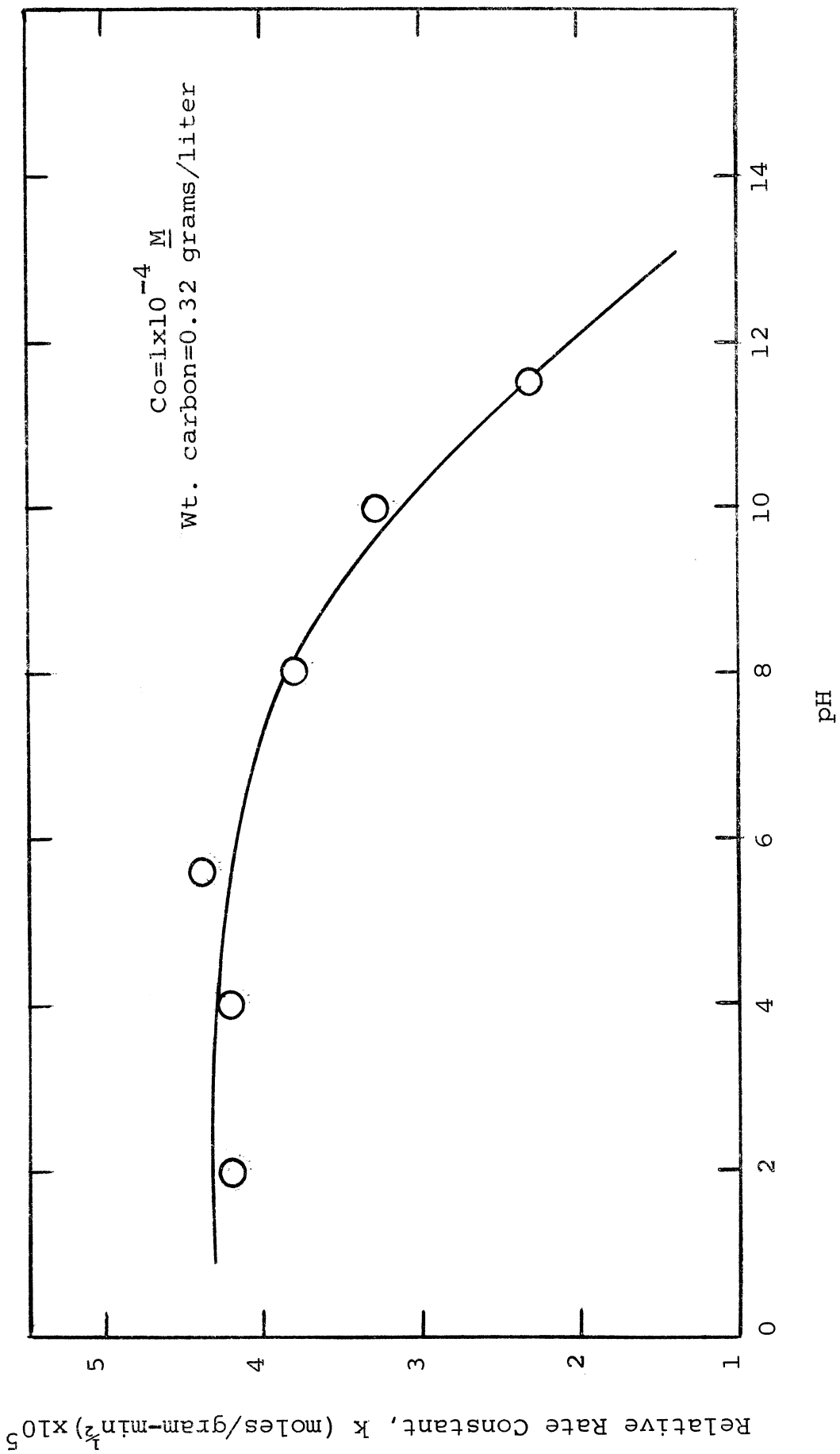
Figure IV-29. 4-Nitrophenol Rate of Adsorption at Different pH

rate curve and experimental data are shown in Figure IV-30 for temperatures of 11° and 37° C. Only one calculated rate curve is shown because the curves calculated for the two temperatures are nearly identical, in keeping with the very small temperature effect on equilibrium at this pH. The parameters used for the calculation in addition to the calculated diffusion coefficients are shown in Table IV-9. The activation energy calculated from the 11° and 37° C diffusion coefficients is -3.8 kcal/mole-$^\circ$K. This value can be compared with a value of Ea = -2.2 kcal/mole-$^\circ$K calculated previously by Weber and Gould (68) using the relative rate constant, k. It should be noted that again, as for the neutral species, different initial concentrations and different carbon dosages were used which could cause the difference in activation energies.

TABLE IV-9

Diffusion Coefficients at Different
Temperatures for 4-Nitrophenol Anion

Temperatures $^\circ$C	Freundlich Parameters		D $(cm^2 sec) x10^6$
	F	N	
11	.0094	.330	3.2 (0.7-3.7)
25	.0110	.333	3.8 (1.6-5.3)
37	.0080	.313	5.7 (1.5-6.7)

EFFECT OF NaCl ON ADSORPTION

Effect of NaCl on Equilibria

Equilibrium studies were performed for phenol and
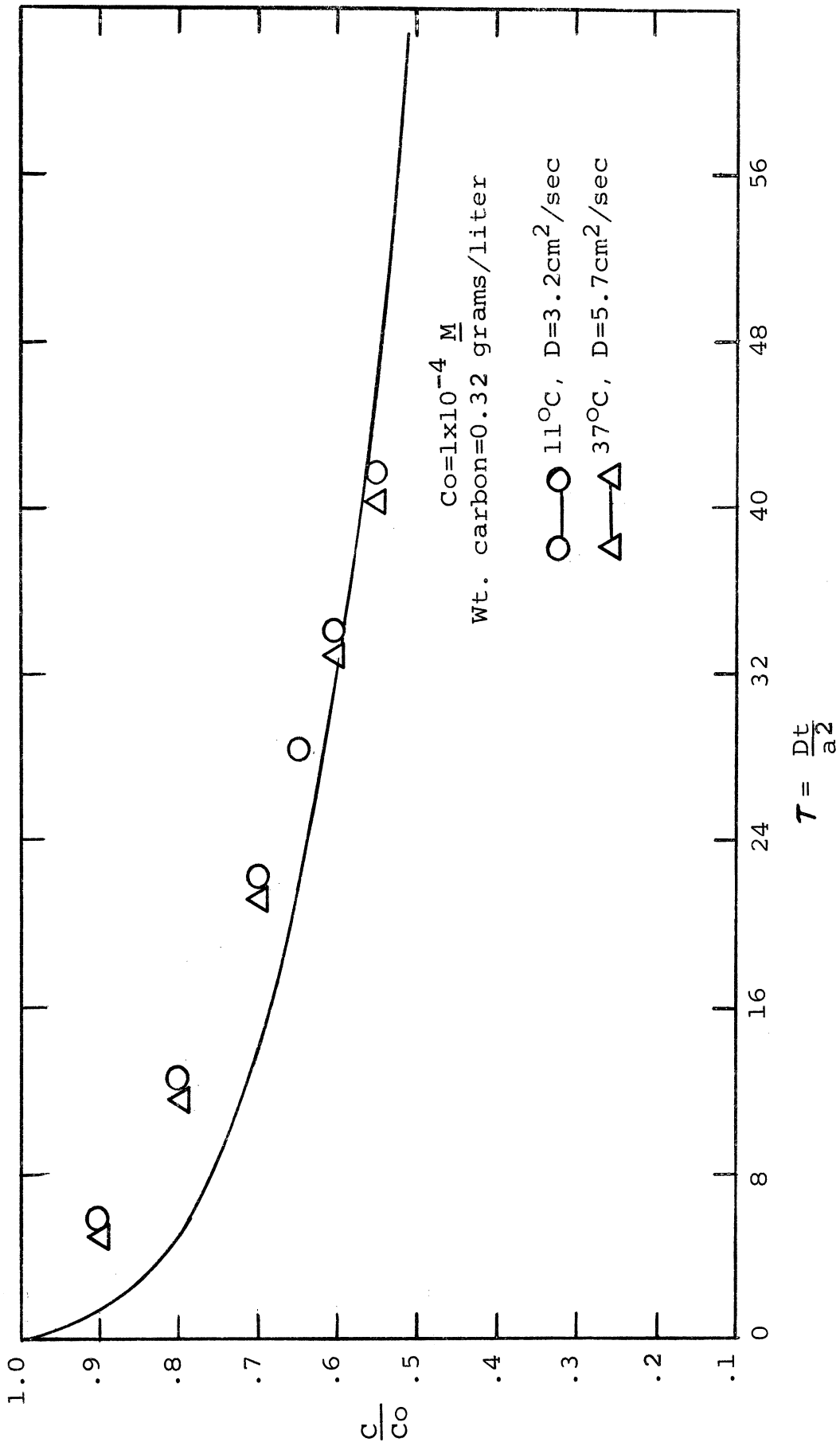
Figure IV-30. 4-Nitrophenol Anion Rate of Adsorption at Different Temperatures

4-nitrophenol systems at pH = 2.0 and NaCl concentrations of 0, $1x10^{-2}$ and 1 $\underline{M}$. No significant effects of NaCl on capacity were noted for any of these systems.

Studies on the 4-nitrophenol system at pH = 10.0, however, show that the effect of 1 $\underline{M}$ NaCl on the isotherm is quite significant when compared with the isotherms for systems containing 0 and $1x10^{-2}$ $\underline{M}$ NaCl. This comparison is shown in Figure IV-31. The data for $1x10^{-2}$ $\underline{M}$ NaCl is not shown because it is essentially the same as the 0 $\underline{M}$ NaCl isotherm. The concentration measurements made on the 1 $\underline{M}$ NaCl - 4-nitrophenol system were changed to activity, X, by means of an activity coefficient of γ = .75 given by Harned (31). Comparison of the Langmuir equation b values calculated for the lower concentration regions of the two isotherms indicate that the heat of adsorption is greater for the 1 $\underline{M}$ system than for the 0 $\underline{M}$ system. A b value of 36,000 liters/mole was calculated for the 1 $\underline{M}$ system compared with 15,000 liters/mole for the 0 $\underline{M}$ system. A distinct possibility for the cause of the difference between the two isotherms is the high salt concentration is compressing the electrical double layer, thereby reducing the repulsive forces between the organic anion and the surface and allowing more adsorption to occur at lower equilibrium concentrations. No change would be expected in the amount of sorbate which would be taken up at high equilibrium concentration since new adsorption sites are not being created, and this is verified by the fact that the isotherms are rapidly converging to the same surface coverage.
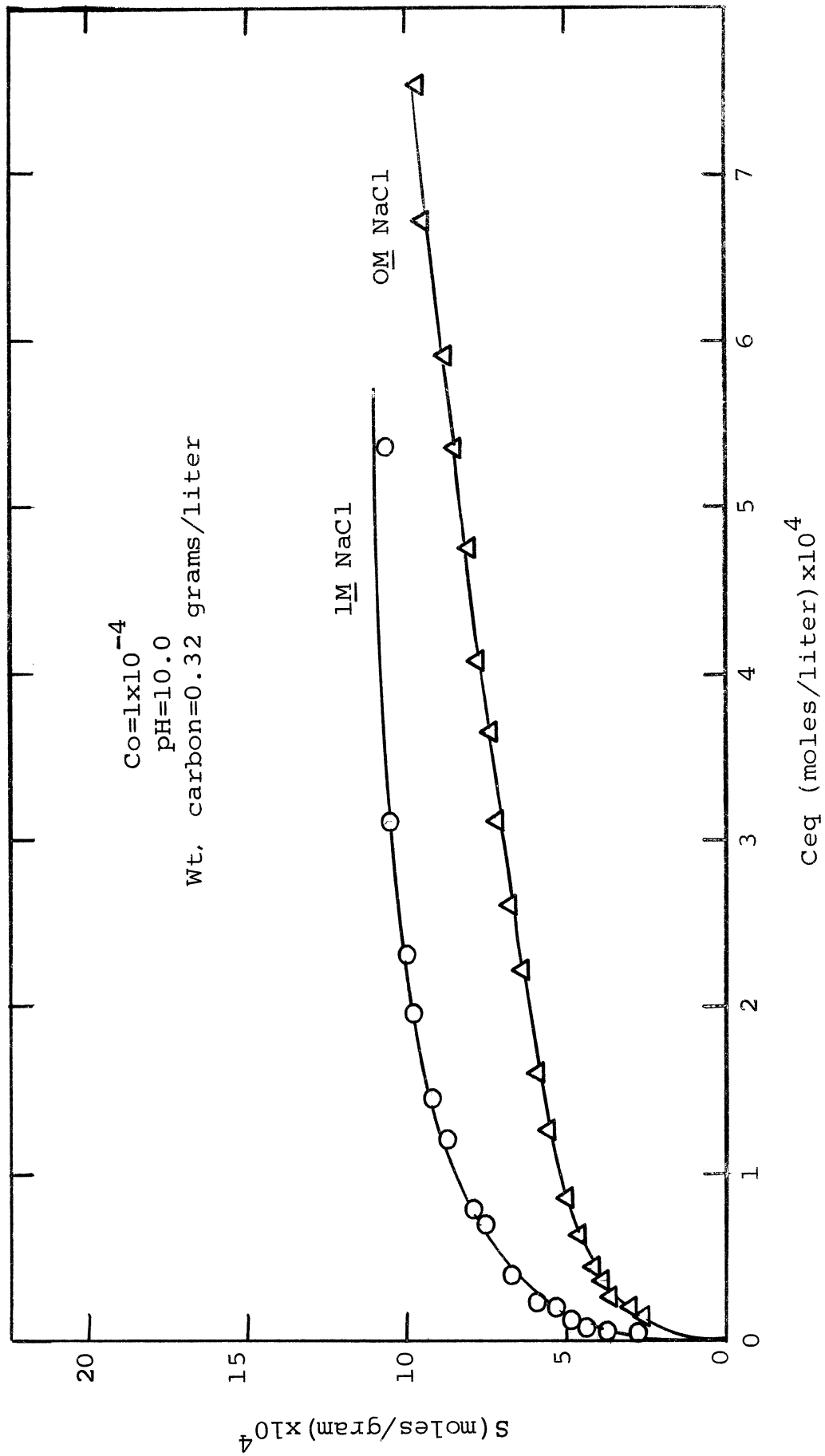
Figure IV-31. 4-Nitrophenol Anion Equilibria at
Different Salt Concentration

Effect of NaCl on Rate

A study of the rate of adsorption as a function of salt concentration showed that salt has little effect on the kinetics of adsorption of the neutral species of both phenol and 4-nitrophenol, as expected.

Also, at pH = 10.0, the 4-nitrophenol anion has essentially the same diffusion coefficient in the 1 $\underline{M}$ NaCl system as in the 0 $\underline{M}$ NaCl system. The high salt concentration apparently does not reduce the repulsive forces in the pore enough to allow the anion to pass more easily.

EFFECT OF TYPE OF STRONG ACID ON ADSORPTION

Kinetic and equilibrium studies were made for both phenol and 4-nitrophenol at pH = 2.0 using $HClO_4$, H_3PO_4, H_2SO_4 and HNO_3 for pH adjustment. The results, however, differed very little from those reported above for HCl. It is felt that some differences would occur if the study were performed at much lower surface coverages, but their effect appears to be too small to be observed for the surface coverages used in these studies.

V. CONCLUSIONS

ACID ADSORPTION

Strong acids were found to react extensively with both the coconut-shell and coal-base carbons studied, and this reaction apparently has significant effect on the adsorption of specific organic molecules from solution by active carbon. Specific information was found about the strong acid-carbon interaction which proved useful in interpreting the results of phenol and nitrophenol adsorption on carbon and should prove useful in interpreting results of adsorption of other organic molecules on carbon.

The kinetic data for this reaction, for example, was found to conform to an intraparticle diffusion model with the rate of conjugate anion movement in the pore appearing to limit the rate of diffusion of the acid. Diffusion coefficients were calculated which compared favorably with those found for anions in ion-exchange resins.

Physical and chemical interactions between the diffusing species and the pore wall apparently act to reduce the rate of diffusion as shown by studies on carbons with different ash content and different pore size.

The rate of pore diffusion of acids was found to increase significantly with increasing salt concentration in keeping

137

with higher anion activity gradients in the pore.

The temperature dependence of acid diffusion is cha-racterized by an activation energy of -2 to -3 kcal/mole-^{o}K, in keeping with values for electrolyte diffusion.

The isotherm for acid sorption is best described by the Fruendlich equation, thus indicating a heterogeneous surface with respectto site energy.

The capacity of carbon for strong acids increases sig-nificantly with increasing salt concentration.

The capacity of carbon for different types of acids varies; the coconut-shell carbon capacity for $HClO_4$ is twice that for HCl for example.

The capacity of carbon for acid depends upon the type of carbon as shown by the fact that the coal-base carbon has twice the capacity for HCl as coconut-shell carbon per unit weight of adsorbent and per unit surface area since the coconut-shell carbon has a surface area of 800 sq. meters per gram (71), while that for the coal-base carbon is about 1000 sq. meters per gram (51).

The reduction of the ash content of the coconut-shell carbon had no effect on its capacity for adsorbing acid. This was probably due to the fact that the original ash content was very low and the conclusion may not be valid for carbons of higher ash content.

The mechanism of acid adsorption was not uniquely defined, but the data obtained can be explained in terms of both physical adsorption and chemical reaction with the chromene functional

group.

PHENOL AND 4-NITROPHENOL ADSORPTION

Phenol and 4-nitrophenol adsorption was studied both in the absence and presence of strong acids and salts in order to learn more about the nature of the active carbon surface and the mechanism of adsorption on the surface.

A study of phenol and 4-nitrophenol adsorption in distilled water in the absence of inorganic acids and salts strongly indicates that the active carbon surface is very heterogeneous with respect to the energy of the sites at which adsorption occurs. Heterogeneity is indicated by the fact that the adsorption isotherms for both phenol and 4-nitrophenol can best be described by the Freundlich equation.

Reversibility studies on phenol, also in the absence of inorganic acids and salts, indicate that a large percentage of adsorption occurs in "ink bottle" pores for the coconut-base carbon thus making it difficult to desbrb the phenol. This finding is important because it could mean that the oxidizing agents used in the regeneration process would not be able to easily remove the adsorbed organic molecules from the carbon surface.

4-Nitrophenol was found to be adsorbed more extensively, and with a greater heat of adsorption, than phenol in the lower, reduced equilibrium concentration range. Adsorption evidently becomes non-specific at higher surface coverages, however, since the ultimate capacity for both solutes appears to be about the

same at 4×10^{-3} moles per gram. This is also shown by the fact
that heats of adsorption decrease with increasing surface
coverage.

A percentage of the sites at which phenol adsorption takes
place are evidently different than those at which 4-nitrophenol
adsorption occurs. The capacity of carbon for phenol is re-
duced by 25% when adsorption takes place in a pH = 2 system
as compared with a pH = 5.6 system, while the capacity for
4-nitrophenol is approximately constant over the same pH
range. This occurs even though the two solutes have similar
acid-base characteristics. The acid is apparently destroying,
or competing with phenol for, some of the sites at which
phenol adsorption occurs. This finding illustrates the im-
portance of adjusting to near neutrality the pH of solutions
from which phenol is to be adsorbed on carbon.

The capacity of carbon for phenol is also decreased by
30 to 50% over the equilibrium concentration range of 1 to
10×10^{-4} $\underline{M}$ as the solution pH changes from 7.5 to 10.6, while
the capacity for 4-nitrophenol is reduced by about 67% for the
pH change from 4.0 to 10.0. This decrease in capacity can
best be attributed to an increase in repulsive forces between
the anionic sorbate and the negative carbon surface. The isos-
teric heat of adsorption decreases from 6 kcal/mole-$^{\circ}$K for the
neutral species to 1 kcal/mole-$^{\circ}$K for the anionic species,
thus indicating the size of these repulsive forces.

A 1 $\underline{M}$ NaCl concentration at pH = 10 appears to compress
the electrical double layer, thereby reducing repulsive forces

and allowing the 4-nitrophenol anion to adsorb more easily.
This NaCl concentration had no significant effect on the
neutral species of either solute.

Reduction in ash content of the coconut-shell carbon
from 0.7% to 0.3% did not affect the carbon's capacity for
phenol. This again is probably due to the fact that the orig-
inal ash content is very small.

The kinetic data for both solutes did not conform well
to the pore diffusion model used for strong acid diffusion.
Surface diffusion is strongly indicated as being of importance
in addition to pore diffusion because 1) A larger variation
in the diffusion coefficient calculated from the pore diffu-
sion model occurs for the neutral phenol molecule than for
the neutral 4-nitrophenol species in keeping with the lower
heat of adsorption for phenol. The phenol molecule would thus
be more likely to diffuse on the surface. 2) The variation
in the 4-nitrophenol diffusion coefficient increases with in-
creasing surface coverage as shown in the effect of carbon dos-
age study. Surface diffusion would be more prevalent at higher
surface coverages again because of the lower heat of adsorption.
3) The diffusion coefficient for the 4-nitrophenol anion is
larger and varies more than that for the neutral species, again
in keeping with the lower heat of adsorption for the anion.

The temperature effect on rate of adsorption is in keep-
ing with the assumption of diffusion since the activation
energy is in the range of -3 to -6 kcal/mole-$^{\circ}$K.

The rate of solute removal from solution per unit weight

of adsorbent increases with decreasing carbon dosage for a
given initial concentration. Thus, more efficient use is
made of carbon at smaller dosages.

For a given carbon dosage, the rate of solute removal
from solution per unit weight of adsorbent increases with
increasing initial concentration.

FURTHER RESEARCH

A logical extension of this research would involve
the development of a diffusion model which would include the
effects of surface diffusion and/or the actual adsorption
step as well as pore diffusion. Such a model could be tested
with the data presented in this study.

Further studies should also be performed on the effect
of the ash content of carbon on adsorption. For this study,
carbons with a much higher ash content than the coconut-shell
carbon should be used. Included could be carbons which have
been through one or more regeneration cycles and which have
a significant ash build-up.

The results obtained in this study on the effect of
pH and salt concentration on adsorption should be extended to
other carbons and other solutes. Especially, the effect of
pH in systems which have a low solute concentration should
be examined since the effect could well be more important than
in the concentration range examined in this study.

```
$COMPILE, MAD, EXECUTE, DUMP, PRINT OBJECT, PUNCH OBJECT

          DIMENSION C(50), S(50), CNEW(50, SNEW(50),
        1 CC(50), CTEMP(50), STEMP(50)
          INTEGER I,P,M,IP
START     READ AND PRINT DATA P,A,RADIUS,DELT,ERR,TEND,
        1 CO, RHO, COUNT
          DELR=1./P
          IP=P+1
          EXECUTE ZERO. (CC(1)...CC(IP,C(1)...C(IP),
        1 CNEW(1)...CNEW(IP),S(1)...S(IP), SNEW(1)...
        1 SNEW(IP),T,Q)
          ARR=4.*3.14159*(RADIUS.P.3.)/A
          R=R*RHO*(CO).P.(N-1)
NEW       INDEX=0
          THROUGH DIFF, FOR M=P, -1,M.L.2.
          EM=M-1
          COEF=DELT/(2.*EM*DELR*DELR)
          TERM=(EM-1.)*(C(M-1)+CNEW(M-1))
          TERMS=(EM+1)*(C(M+1)+CNEW(M+1))
        1 *2.*EM*(C(M)+CNEW(M))+    TERM
          WHENEVER .CNEW(M).G.    SNEW(M)
          CC(M)=C(M) + COEF*TERMS - (SNEW(M)-S(M))
          CC(M)=.ABS.CC(M)
          WHENEVER .ABS.(CC(M)-CNEW(M)).G.ERR*CNEW(M),
        1 INDEX=1
          CNEW(M)=CC(M)
          SNEW(M)=R*(CNEW(M).P.N)
          OTHERWISE
          SS=S(M)+COEF*TERMS-(CNEW(M)-C(M))
          SNEW(M)=.ABS.SS
          WHENEVER SNEW(M).L.TEST
          CC(M)=0.
          OTHERWISE
          CC(M)=(SNEW(M)/R).P.(1./N)
          END OF CONDITIONAL
          WHENEVER.ABS.(CC(M)-CNEW(M).G.ERR*CNEW(M)
          CNEW(M)-CC(M)
DIFF      END OF CONDITIONAL
          WHENEVER CNEW(1).G.SNEW(1)
          CC(1)=C(1) + (3.*DELT/(DELR*DELR))*((CNEW
        1 (2)+C(2))-(CNEW(1)+C(1)))-(SNEW(1)-S(1))
          CC(1)=.ABS.CC(1)
          WHENEVER .ABS.(CC(1)-CNEW(1)).G.ERR*CNEW(1),
        1 INDEX=1
          CNEW(1)=CC(1)
          SNEW(1)=R*(CNEW(1).P.N)
```

```
      OTHERWISE
      SS=S(1)+(3.*DELT/(DELR*DELR))*((CNEW(2) C(2))
1 -(CNEW)(1)+C(1)))  -(CNEW(1)-C(1))
      SNEW(1)=.ABS.SS
      WHENEVER SNEW(1).L.TEST
      CC(1)=0
      OTHERWISE
      CC(1)=(SNEW(1)/R).P.(1./N)
      END OF CONDITIONAL
      END OF CONDITIONAL
      WHENEVER .ABS.(CC(1)-CNEW(1)).G.ERR*CNEW(1),
1 INDEX=1
      CNEW(1)=CC(1)
      SUM1=0
      SUM2=0
      THROUGH SUM, FOR I=P,-2,I.L.2
      SUM1 = SUM1 + (I-1).P.2.* (CNEW(I)+SNEW(I))
      SUM2 = SUM2 + (I-2).P.2.*(CNEW(I-1)+SNEW(I-1))
      PROD1=4*SUM1
      PROD2=2*SUM2
      COE=DELR.P.3./3
      GRAL=COE*(P*P*(CNEW(IP)+SNEW(IP))+PROD1+PROD2)
      CC(IP)=1.-GRAL*ARR
      CC(IP)=.ABS.CC(IP)
      WHENEVER .ABS(CC(IP)-CNEW(IP)).G.ERR*CNEW(IP),
1 INDEX=1
      CNEW(IP)=CC(IP)
      SNEW(IP)=R*(CNEW(IP).P.N)
      WHENEVER INDEX .E.1.,TRANSFER TO NEW
      T=T+DELT
      Q=Q+1
      WHENEVER Q.GE.COUNT
      PRINT RESULTS T, CNEW (IP)
      Q=0.
      END OF CONDITIONAL
      WHENEVER T.G. TEND-PROF
      PRINT RESULTS T,CNEW(IP), SNEW(1)...SNEW(IP)
      END OF CONDITIONAL
      WHENEVER T.G.SUB
      DELT=NEXT
      COUNT=CHANG
      SUB=SUB1
      SUB1=SUB2
      SUB2=SUB3
      NEXT=NEXT1
      NEXT1=NEXT2
      NEXT2=NEXT3
      END OF CONDITIONAL
      WHENEVER T.G. TEND, TRANSFER TO START
      THROUGH NEWVR, FOR I=1,1,I.G.IP
      CTEMP(I)=C(I)
      STEMP(I)=S(I)
```

```
          C(I)=CNEW(I)
          S(I)=SNEW(I)
          CNEW(I)=CNEW(I)+(CNEW(I)-CTEMP(I))
NEWVR     SNEW(I)=SNEW(I)+(SNEW(I) -STEMP(I))
          TRANSFER TO NEW
          END OF PROGRAM
```

REFERENCES

(1)   Adamson, A. W., Physical Chemistry of Surfaces,
        pp. 400-402, 548; Interscience Publishers, New
        York, London, 1967.

(2)   Adamson, A. W., Ling, I., "Effect of Radiation on
        the Surfaces of Solids. I. Analysis of Adsorption
        Isotherms to Obtain Site Energy Distributions," in
        Solid Surfaces and the Gas-Solid Interface, Advances
        in Chemistry Series #33, R. F. Gould, Ed., Am. Chem.
        Soc. Publications, 1961.

(3)   Allen, J. B., Joyce, R. S., "Column Calculations for
        Intraparticle Diffusion Controlled Adsorption,"
        Proc. Fifty-Ninth Annual Meeting, American Institute
        of Chemical Engineers, Detroit, December 4-8, 1966.

(4)   Barrer, R. M., "Specificity in Physical Sorption,"
        J. Colloid Interface Sci. 21 (4), 415 (1966).

(5)   Blackburn, S., Kipling, J. J., "Adsorption from
        Binary Liquid Mixtures: Some Effects of Ash in
        Commercial Charcoal," J. Chem. Soc., London, 1955,
        4103.

(6)   Boehm, H. P., "Chemical Identification of Surface
        Groups" in Advances in Catalysis, D. D. Eley, H.
        Pines, P. B. Weisz, Eds., Vol. 16, Academic Press,
        New York and London, 1966.

(7)   Brecher, L. E., Kostecki, J. A., Camp, D. T.,
        "Combined Diffusion in Batch Adsorption Systems
        Displaying B. E. T. Isotherms: Part I," in Chemical
        Engineering Progress, Symposium Series 74, Vol. 63,
        1967.

(8)   Brewster, R. Q., Organic Chemistry, p. 622. Prentice-
        Hall, Inc., Englewood Cliffs, New Jersey, 1953.

(9)   Brunauer, S., "Solid Surfaces and the Gas-Solid
        Interface," in Solid Surfaces and the Gas-Solid
        Interface, Advances in Chemistry Series #33, R. F.
        Gould, Ed., Am. Chem. Soc. Publications, 1961.

(10)   Brunauer, S., Emmett, P. H., Teller, E., "Adsorption
        of Gases in Multimolecular Layers," J. Am. Chem.
        Soc. 60, 309 (1938).

(11)   Carr, C. W., Fruendlich, H., Sollner, K., "The
       Influence of Salts on Adsorption of Strong Acids,"
       J. Am. Chem. Soc. 63, 693 (1941).

(12)   Chu, B., Whitney, D. C., Diamond, R. M., "On Ion-
       Exchanges Resin Selectivities," J. Inorg. Nucl. Chem.
       24, 1405 (1962).

(13)   "Columbia Activated Carbon," circular, National Carbon
       Co., New York, 962.

(14)   Crank, J., The Mathematics of Diffusion, Clarendon
       Press, London, 1965.

(15)   Dostal, K. A., Harrington, J. J., Robeck G. G.,
       Clark, R. M., "Development of Optimization Models
       for Carbon Bed Design," J. Am. Water Works Assoc.
       58 (9), 1170 (1966).

(16)   Dubinin, M. M., "Porous Structure and Adsorption
       Properties of Active Carbon," in Chemistry and
       Physics of Carbon, Vol. 2, P. L. Walker, Ed., Marcel
       Dekker, Inc., New York, 1966.

(17)   Dubinin, M. M., Plavnik, G. M., Zaverina, E. D.,
       "Integrated Study of the Porous Structure of Active
       Carbons from Carbonized Sucrose," Carbon 2, 261 (1964).

(18)   Edeskuty, F. J., Amundson, N. R., "Effect of Intra-
       particle Diffusion: I. Agitated Non-Flow Adsorption
       Systems," Ind. Eng. Chem. 44, 1698 (1952).

(19)   Garten, V. A., Weiss, D. E., "The Quinone-Hydro-
       quinone Character of Activated Carbon and Carbon Black,"
       Australian J. Chem. 8, 68 (1955).

(20)   Garten, V. A., Weiss, D. E., "A New Interpretation of
       the Acidic and Basic Structures in Carbons II. The
       Chromene-Carbonium Ion Couple in Carbon," Australian
       J. Chem. 10, 309 (1957).

(21)   Garten, V. A., Weiss, D. E., "The Reaction of Carbon
       Blacks with Sodium Borohydride," Australian J. Chem.
       14, 155 (1961).

(22)   Garten, V. A., Weiss, D. E., "The Ion-and Electron-
       Exchange Properties of Activated Carbon in Relation to
       its Behavior as a Catalyst and Adsorbent," Rev. Pure
       Appl. Chem. 7, 69, (1957).

148

(23) Garten, V. A., Weiss, D. E., Willis, J. B., "A New Interpretation of the Acidic and Basic Structures in Carbon I. Lactone Groups of the Ordinary and Fluorescein Types in Carbons," Australian J. Chem. 10, 295 (1957).

(24) Gasser, C. G., Kipling, J. J., "The Effect of Surface Complexes on Adsorption from the Liquid Phase by Carbon Black," Proc. Conf. Carbon, 4th, Buffalo, N. Y., 1959, pp. 55-61, Pergamon Press, New York, 1960.

(25) Gould, J. P., "The Influence of Structure and pH on the Kinetics of Adsorption of Substituted Phenols from Aqueous Solution by Active Carbon," Masters Thesis, Univ. of Mich., 1967.

(26) Hallum, J. V., Drushel, H. V., "The Organic Nature of Carbon Black Surfaces," J. Phys. Chem. 62, 110 (1958).

(27) Halsey, G., "Physical Adsorption on Non-Uniform Surfaces," J. Chem. Phys. 16 (10), 931 (1948).

(28) Halsey, G., Taylor, H. S., "The Adsorption of Hydrogen on Tungsten Powders," J. Chem. Phys. 15 (9), 624 (1947).

(29) Hansen, R. S., Craig, R. P., "The Adsorption of Aliphatic Alcohols From Aqueous Solutions by Non-Porous Carbons," J. Phys. Chem. 58, 211 (1954).

(30) Harker, H., Jackson, C., Wynne-Jones, W. F. K., "Electron Spin Resonance in Carbon," Proc. Roy. Soc., London A262, 328 (1961).

(31) Harned, H. S., Owen, B. B., The Physical Chemistry of Electrolyte Solutions, p. 593, Reinhold Publishing Corp., New York, 1958.

(32) Hassler, J. W., Activated Carbon, Chemical Publishing Co., New York, 1963.

(33) Heckman, F. A., "Microstructure of Carbon Black," Rubber Chem. Technol. 37, 1245 (1964).

(34) Helfferich, F., Ion Exchange, pp. 234-309, McGraw-Hill Book Co., Inc., New York, 1962.

(35) Hennig, G. R., "Surface Oxides on Graphite Single Crystals," Proc. Conf. Carbon, 5th, Penn State Univ., Pa., 1961, 1 pp. 143-146, Pergamon Press, New York, 1962.

(36) Higgins, B., Richards, J. H., "The Effect of Aprotic Solvents on the Adsorption of Phenol by Alumina," J. Pharm. Parhmacol. 19 (10), 641 (1967).

(37)   Ingram, D. J. E., "Electron Resonance Studies of Heat-Treated Organic Compounds," Proc. Conf. Carbon, 3rd, Buffalo, N. Y., 1957, pp. 93-102, Pergamon Press, New York, 1959.

(38)   Johnson, R. L., Lowes, F. J., Jr., Smith, R. M., Powers, T. J., "Evaluation of the Use of Activated Carbons and Chemical Regenerants in Treatment of Waste Water," Public Health Service Publication No. 999-WP-13, May 1964.

(39)   Joyce, R. S., Sukenik, V. A., "Feasibility of Granular Activated Carbon Adsorption for Waste Water Renovation," Public Health Service Publication No. 999-WP-12, May 1964.

(40)   Keinath, T. M., Weber, W. J., Jr., "A Predictive Model for the Design of Fluid-Bed Adsorbers," presented at 40th Annual Conference of the Water Pollution Control Federation, New York, October 8-13, 1967.

(41)   Kipling, J. J., "Adsorption on Solids from Binary Liquid Mixtures--The Importance of the Surface Structure of the Adsorbent," Proc. Intern. Congr. Surface Activity, 2nd, London III, p. 462 (1957).

(42)   Kipling, J. J., Shooter, P. V., "The Adsorption of Iodine Vapor by Graphon and Spheron 6," J. Colloid Interface Sci. 21 (2), 238 (1966).

(43)   Kitchner, J. A., "Physical Chemistry of Ion-Exchange Resins," in Modern Aspects of Electrochemistry, J. Bockris, Ed., Butterworths Scientific Publications, London, 1959.

(44)   Kolthoff, I. M., "Properties of Activated Charcoal Reactiviated in Oxygen at 400 °C.," J. Am. Chem. Soc. 54, 4473 (1923).

(45)   McNeil, R., Weiss, D. E., "Some Novel Carbonaceous Polymers," Proc. Conf. Carbon, 4th, 1958, pp. 281-290, Pergamon Press, New York, 1960.

(46)   Miller, E. J., "Adsorption by Activated Charcoal. I. Proof of Hydrolytic Adsorption," J. Am. Chem. Soc. 46, 1150 (1924).

(47)   Miller, E. J., "Adsorption by Activated Sugar Charcoal. Adsorbability of Hydrogen and Hydroxyl Ions," J. Am. Chem. Soc. 47, 1270 (1925).

(48)   Miller, E. J., "The Adsorption of Electrolytes by Ash-Free Charcoal," J. Phys. Chem. 36, 2967 (1932).

(49)   Nemerow, N. L., Theories and Practices of Industrial Waste Treatment, Addison Wesley Publishing Co. Inc., Reading, Mass., 1963.

(50)   Parks, L. R., Bartlett, P. G., "The Effect of Inorganic Salts on the Adsorption of Inorganic Acids and Bases," J. Am. Chem. Soc. 49, 1698 (1927).

(51)   "Pittsburg Activated Carbon," circular #AC7-556, Pittsburg Coke and Chemical Co., Pittsburg, Pa.

(52)   Puri, B. R., Mahajan, O. P., Singh, D. D., "Interaction of Carbon with Chlorine Water. II.," J. Indian Chem. Soc. 37, 171 (1960).

(53)   Puri, B. R., Mahajan, O. P., Singh, D. D., "Chemisorption of Oxygen by Charcoal on Treatment with Some Mild Oxidizing Agents," J. Indian Chem. Soc. 38, 135 (1961).

(54)   Puri, B. R., Singh, D. D., Nath, J., Sharma, L. R., "Chemisorption of Oxygen on Charcoal and Sorption of Acids and Bases," Ind. Eng. Chem. 50, 1071 (1958).

(55)   Ross, S., Olivier, J. P., On Physical Adsorption, Ch. 4 and 5, Interscience Publishers, New York, 1964.

(56)   Snow, C. W., Wallace, D. R., Lyon, L. L., Crocker, G. R., "Reaction of Carbon Blacks with Oxygen," Proc. Conf. Carbon, 3rd., Buffalo, N. Y., 1957, pp. 279-87, Pergamon Press, New York, 1959.

(57)   Soldano, B. A., Boyd, G. E., "Self-Diffusion of Anions in Strong-Base Anion Exchangers," J. Am. Chem. Soc. 75, 6099 (1953).

(58)   Sondheimer, E., "On the Relation Between Spectral Changes and pH of the Anthocyanin Pelargonidin 3-Monoglucoside," J. Am. Chem. Soc. 75, 1507 (1953).

(59)   Standard Methods, 11th edition, p. 79, American Public Health Association, Inc., New York, 1960.

(60)   Stern, K. H., Amis, E. S., "Ionic Size," Chem. Rev's. 59, 1 (1959).

(61)   Stokes, R. H. "The Diffusion Coefficients of Eight Uni-univalent Electrolytes in Aqueous Solution at 25°," J. Am. Chem. Soc. 72, 2243 (1950).

(62)   Studebaker, M. L., "Direct Titration of Carbon Blacks," Proc. Conf. Carbon, 5th, Penn State Univ., Pa., 1961, 2, pp. 189-97, Pergamon Press, New York, 1963.

(63)   Walker, P. L., Jr. "Carbon--An Old but New Material,"
         Am. Scientist 50, 259 (1962).

(64)   Walker, P. L., Jr., Austin, L. G., Nandi, S. P.,
         "Activated Diffusion of Gases in Molecular-Sieve Mater-
         ials," in Chemistry and Physics of Carbon, Vol. 2,
         P. L. Walker, Jr., Ed., Marcel Dekker, Inc., New York,
         1966.

(65)   Wawzonek, S., "Coumarins," in Heterocyclic Compounds,
         R. C. Elderfield, Ed., Vol. 2, Wiley, New York, 1950.

(66)   Weber, W. J., Jr., "Adsorption of Alkylbenzenesulfonates
         on Carbon," Ph.D. Thesis, Harvard Univ., 1962.

(67)   Weber, W. J., Jr., "Fluid-Carbon Columns for Sorption
         of Persistent Organic Pollutants," Paper I-12, Proc.
         Intern. Conf. Water Pollution Res. 3rd, Munich, Germany,
         1966.

(68)   Weber, W. J.,Jr., Gould, J. P., "Sorption of Organic
         Pesticides from Aqueous Solution," Advances in Chemistry
         Series, No. 60. Chem. Soc. Publications, 1966.

(69)   Weber, W. J. Jr., Morris, J. C., "Kinetics of Adsorption
         on Carbon from Solution," J. Sanit. Eng. Div. Am. Soc.
         Civil Engrs. 89, SA2, 31 (1963).

(70)   Weber, W. J., Jr., Rumer, R. R., Jr., "Intraparticle
         Transport of Sulfonated Alkylbenzenes in a Porous Solid:
         Diffusion with nonlinear Adsorption," Water Resources
         Research 1 (3), 361 (1965).

(71)   Weber, W. J., Jr., Morris, J. C., "Equilibria and Ca-
         pacities for Adsorption on Carbon," J. Sanit. Eng. Div.
         Am. Soc. Civil Engrs. 90, SA3, 79 (1964).

(72)   Weller, S., Young, T. F., "Oxygen Complexes on Charcoal,"
         J. Am. Chem. Soc. 70, 4155 (1948).

(73)   Wolff, W. F., "The Structure of Gas-Adsorbent Carbons,"
         J. Phys. Chem. 62, 829 (1958).

(74)   Wolff, W. F., "A Model of Active Carbon," J. Phys. Chem.
         63, 653 (1959).

(75)   Zettlemoyer, A. C., "Modern Techniques for Investigating
         Interactions with Surfaces," Chem. Rev's. 59, 937 (1959).

(76)   Zettlemoyer, A. C., Narayan, K. S., "Adsorption from
         Solution on Graphite Surfaces," in Physics and Chemistry
         of Carbon, Vol. 2, P. L. Walker, Jr. Ed., Marcel Dekker,
         Inc., New York, 1966.